FACULTEIT TOEGEPASTE WETENSCHAPPEN
DEPARTEMENT BURGERLIJKE BOUWKUNDE
AFDELING MIJNBOUW
W. DE CROYLAAN 2
B-3001 HEVERLEE (BELGIUM)

KATHOLIEKE
UNIVERSITEIT
LEUVEN

"MINE DESIGN IN CLAY"

CORA-PROJECT TRUCK-I

[FAS No 63218]

B. Van de Steen, A. Vervoort

August 1998

DRAFT VERSION

CORA 98-46
[Werkdocument]

PREFACE

This report forms part of the CORA research programme, investigating the radioactive waste disposal in the Netherlands taking into account the constraints imposed by the required retrievability. A first mine design has been made for the retrievable disposal of the estimated volume of high, middle and low radioactive waste in a clay formation at a depth of 500 m. The research was mainly oriented towards a stability analysis of the underground excavations at this depth and the effect of the presence of the heat generating waste on the temperature distribution in the surrounding rock mass. For the proposed mine design a time planning has been made for excavating the shafts and all the tunnels, for storing the waste and for filling the voids in successive steps. For each operating phase, the minimum required air volumes in the various sections of the mine have been calculated. Finally, some further thought was given to the implications of ensuring the retrievability of the waste.

SUMMARY

Within the CORA research programme, the aim of the TRUCK-I project can be summarized as follows:

(i) For the total volume of high, middle and low radioactive waste in the Netherlands, a mine design in a clay formation has to be made, taking into account the prerequisites of retrievability for the high radioactive waste. The mine is situated at a depth of 500 m.
(ii) For the proposed mine design, hydromechanical simulations have to be carried out to analyse the stability of the excavations.
(iii) For the heat generating high level radioactive waste, the effect of the heat sources on the temperature distribution in the clay mass and on the stresses has to be quantified.
(iv) A time schedule has to be proposed for the excavating phase, the phase of waste storage and subsequent filling of the voids in successive steps, taking into account the prerequisites of retrievability.
(v) The minimum required quantity of air flow in the various mining zones has to be estimated.

(i) Mine design

The mine consists of one level only, in the middle of a thick clay layer. Apart from two vertical shafts, only circular horizontal tunnels are excavated, in a square or rectangular pattern. The centre distances between the tunnels are either 40 m or 50 m. The three types of waste (high level heat generating, high level not generating heat and middle/low level radioactive waste) are stored in three different zones, separated by a barrier of at least 50 m wide. The high level waste is stored in such a way that the canisters are individually retrievable. The total surface extent of the entire mine is about 4 km^2. The total volume of rock which has to be excavated is about 1,3 million m^3. Nearly 500 thousand m^3 filling material is required to fill up all the voids and galleries. Part of this filling material can be formed by the excavated clay.

(ii) Hydromechanical simulations

Hydromechanical simulations are carried out using the finite difference code FLAC. The immediate reaction of the rock mass following the excavations is studied, as well as the longterm behaviour for permeable and impermeable lining. The clay characteristics, known for the Boom clay at a depth of 225 m, are used as input. These values should be a conservative approach for the same clay formation at a depth of 500 m. Based on these simulations, a centre distance of 40 m to 50 m between adjacent tunnels seems to be safe. If one would decrease the centre distance to 30 m or less, the remaining elastic zone in the clay mass between tunnels becomes small. When the clay mass around the tunnels is drained, in addition to the increased load, specific attention should be given to the differential radial loading of the support when designing the lining. When the lining would on the other hand be impermeable, precautions should also have to be taken against the relatively high total radial stress against the lining. A combination of a permeable lining and a saturated backfill creates around the shroud conditions comparable to the situation in which the lining is impermeable. The situation is probably not hazardous for the lining, as the backfill counteracts the loading.

A sensitivity analyses of the input parameters indicates that the friction angle of the clay is so far the most critical parameter.

(iii) Heat generating sources

The effect of storing the heat generating high level radioactive waste in the underground is evaluated using the three-dimensional boundary element code MAP3D combined with some analytical calculations. Although the exact temperature variation in function of the time of the combination heat generating waste - canister - backfill material - lining is not known, some useful conclusions are derived.

In the vicinity of the tunnel, the temperature increases fast. For example 10 m above the repository the temperature increases by about 30° during the first 10 years. This temperature increase has an effect on the behaviour of the clay: on the one hand, the material characteristics change, and on the other hand, the pore water pressure and the effective stresses change.

If one would use as prerequisite a maximum increase of 4° at the top of the clay layer (50 m above the storage level), all simulations indicate that it is unlikely to satisfy this condition with a 50 m x 50 m pattern. A larger spatial distribution of the heat generating canisters could be a solution, but making the centre distance between galleries larger has not only a direct effect on the economics, but also on the mining and storing operations. Another solution would be combining both types of high level radioactive waste (heat generating and not heat generating waste) in the same mining zone (e.g. alternatively, placing a warm and cold canister). The mining operation would remain similar, but the number of heat sources per area decreases. An important disadvantage, however, is that both zones are not segregrated anymore, which is one of the ways suggested to make the waste more easily retrievable. Therefore, in the planning the basic grid size of 50 m x 50 m is kept for the storage of the heat generating waste. It is suggested that the problem of the high temperature in the rock mass is solved by storing the waste for a longer time period at the surface. This solution could fit in the global strategy of retrievability without too many consequences. The various types of waste remain separated and the canisters of the high level waste remain individually retrievable.

(iv) Time schedule for mining operations

The total time required for excavating the entire mine is estimated to be 10 to 13 years. The storage time for the middle and low level radioactive waste requires just below 5 years. The storage time for the two types of high level radioactive waste is less: 302 working days for the heat generating waste and 632 working days for the high level waste that does not generate heat. The final filling of the secondary and primary galleries would require maximum 3,5 years. This could be reduced if one works at the same time in the various zones.

(v) Ventilation requirements

During excavation the maximum required flow rate of the downcast air is 50,7 m^3/s, resulting in a maximum air velocity close to the shaft of 3,2 m/s. In comparison to conventional mining operations, both figures are acceptable and should not cause any practical problem. However, for the auxiliary ventilation a problem could arise to find fans which are small enough to fit easily in the envisaged diameters. Best would be to use axial flow fans, but the required pressure are difficult to attain with this type of fans. The auxiliary fans should be able to handle 4,15 m^3/s at up to 10,4 kPa.

The project TRUCK-I will be followed by the TRUCK-II project. Some of the additional goals of TRUCK-II is to translate the constraints of the retrievability in practical concepts, to look at alternative scenarios for storing the radioactive waste and to formulate requirements for a monitoring programme.

Contents

1 Introduction

1.1 Research, part of the CORA programme

The main objective of the CORA research programme is the development of a safe retrievable disposal technique for the Dutch radioactive waste. This could be at the surface (e.g. for a period of 300 years) or underground in either salt or clay formations. One of the requirements for the underground disposal is the prerequisite that the waste remains retrievable, at least the first 50 to 300 years. After that, a definitive geological sealing could be considered.

The TRUCK-I project, 'Mine design in clay', forms an integral part of the CORA research programme. It looks specifically at the option of the waste storage in clay formations and its main aim is to make a first mine design based on the total volumes of high, middle and low radioactive waste to be stored. The main factors influencing the mine design are the demands posed on the stability and the problems posed by the temperature rise as a consequence of the storage of the heat generating high radioactive waste. The design takes also the retrievability into account. An additional factor having a direct bearing on the mine design is that in the Netherlands a minimum depth of 500 m is imposed for the storage of radioactive waste. This minimum cover is related to the observed depth of glacial erosion channels. The CAR-project [Rijksgeologische Dienst, 1996], another CORA-project, has shown that within the territory of the Netherlands clay, formations are present at a depth of500 m and with a minimum thickness of two times 50 m as a vertical barrier (another constraint).
The results of this project are also the input for other CORA-projects like for example the safety analyses in METRO and a more detailed design in TRUCK-II.

1.2 Objectives of the research project TRUCK-I

In making a first mine design in a clay formation, taking into account the constraints imposed by the Netherlands, the project aims at evaluating the feasibility of such a mining operation. More specifically, this project gives answers to the following questions:

- Based on the current knowledge of clay characteristics, could stable excavations be made in clay at a depth of 500 m and could the zone of plastic deformation around the excavations be considered acceptable? [*Positive answer based on numerical simulations*]*
- For such stable excavations, what would be a realistic estimate of the distance between tunnels? [*Answer: 40 to 50 m*]*
- What is the temperature effect of placing sources with a constant temperature (drums of heat generating high radioactive waste) on the temperature increase in the surrounding rock mass and in which way does this affect the spatial distribution of the drums (e.g. minimum distance between drums)? [*Answer: the temperature effect is non-negligeable and a three dimensional approach is necessary; the spatial distribution is function of the temperature considered acceptable at e.g. the top of the clay formation*]*

---

* Here, only a general answer is given. The detailed results are presented in the next chapters.

- What is to the total surface area required for the entire mine, if each drum of high radioactive waste is individually accessible from the adjacent tunnel and taking into account the answers on the questions above? The individual accessibility of the drums is a requirement to ensure that the high radioactive waste is easily retrievable. [*Answer: an area of about 4 km*^{2}]*

For the various calculations, sensitivity analyses are also conducted, by varying the clay characteristics and the heat source within realistic limits. The effect of increasing the cover depth from about 200 m (current Belgian concept) to 500 m (Dutch constraint) is quantified.

Once the mine layout is made, calculations related to the planning and the actual implementation of the mine design are conducted. E.g. a time schedule is developed for excavating the shafts and all the tunnels, for storing the waste and for filling the voids in successive steps. The total length of tunnels and the total volume of excavated rock are also calculated. The volume of air required for a safe ventilation of the various mine sections during the successive mining and storage steps is calculated as well.

Within this project, a global mine design is made for the disposal of the radioactive waste in a clay formation, taking the constraints into consideration which are specific for the situation in the Netherlands. The aim of the project is certainly not to solve all practical problems or to design each aspect of the entire mining complex. Before one could start designing the 'details' of such a mining operation, like for example the support or the excavation equipment, more information on the clay characteristics and on specific local conditions is required. Collecting this information is certainly useful, but it should probably be preceded by an economic and safety comparison of the proposed mine layout with the other alternatives. This should give a good indication of the suitability of clay at a depth of 500 m as a host material for radioactive waste.

1.3 Constraints imposed for the waste disposal

1.3.1 Waste to be stored

The waste is generated by nuclear power plants, industrial activities, the medical sector and research institutions. The list of waste being generated used in the OPLA study, A strategy [J. Grupa, 1998], has been the basis for calculating the required storage capacity. To develop a waste storage strategy, the waste has been subdivided into three categories:

- High level heat generating waste: highly radioactive vitrified waste, that generates heat.
- High level waste not generating heat: highly radioactive waste, that does not generate heat.
- Middle and low level radioactive waste.

The volumes to be stored, as well as the size of the drums and the number of drums to be used are given in Table 1.1. Where the size of the waste containers or the volume of waste to be expected were not provided, estimates have been made.

	Total # of drums	Total volume (m^3)	# 0,175 m^3 drums	# 0,20 m^3 drums	# 0,21 m^3 drums	# 1,18 m^3 drums	# 1,46 m^3 drums	# 2,43 m^3 drums*
HLW heat gen.	300	52	300	-	-	-	-	-
HLW not gen. heat	1260	514	20	-	1040	-	200	-
MLW	56288	19173	-	52508	-	400	-	3380
Total	57848	19739	320	52508	1040	400	200	3380

Table 1.1: Waste to be stored (OPLA, A strategy [J. Grupa, 1998])

The dimensions of the drums and containers are as follows:

0,175 m^3 canisters	diameter = 0,43 m	length = 1,335 m
0,20 m^3 drums**	diameter = 0,59 m	length = 0,87 m
0,21 m^3 drums**	diameter = 0,59 m	length = 0,87 m
1,18 m^3 containers**	diameter = 0,50 m	length = 1,65 m
1,46 m^3 containers	diameter = 1,15 m	length = 1,65 m
2,43 m^3 containers**	diameter = 1,40 m	length = 1,65 m

The 0,175 m^3 canisters are of the Cogema type design. They contain about 150 *l* of vitrified waste, which corresponds with the waste generated by 1,33 tonnes heavy metal (U) [R.J. Heijboer et al., 1998]. The expressions used to describe the power generated by the heat sources take account of both the fission products and the actinides.

1.3.2 Retrievability

The mine design has to be such that the high level radioactive waste could be retrieved. There are two main reasons for this condition:

- Firstly, it would give future generations the possibility to retrieve valuable elements or to re-process the waste with the aim of realizing more stable and safer elements.
- Secondly, if an unforeseeable event would occur in the future, creating a hazardous situation, one could still recuperate the waste for further processing.

---

* Estimated container volume

** Estimated diameter and length

To provide the possibility to take actions in case a hazardous situation occurs, it is also necessary to monitor the environment around the disposal.

In this study, it is assumed that the high level waste got to be individually retrievable. This means that the possibility must exist to remove each canister or each drum containing high level radioactive waste without having to remove or displace any other canister or drum. As such, the same starting conditions are taken as in the studies where salt is the host material. The evaluation of improvement in safety and the increase in cost associated with the principle of individual retrievability falls outside the scope of this study. The retrievable storage of the middle and low radioactive waste is not a constraint imposed by the CORA-programme.

1.3.3 Layout

The underground laboratory in Mol, SCK-CEN, is used as basic concept for designing the mine layout. The mine consists of 1 level only, in the middle of a thick clay layer. Apart from two vertical shafts, only circular horizontal tunnels are excavated. The three types of waste (high level heat generating, high level not generating heat and middle/low level radioactive waste) are stored in three different zones of the mine.

For safety reasons, the option is taken that first all openings are excavated and only once the entire mine is finished the storage of the waste starts.

1.3.4 Geological conditions

From a geological point of view, the host material should be a horizontal or sub-horizontal clay formation at a depth of 500 m with a minimum vertical thickness of 2 times 50 m (mine level in the middle of the formation). The horizontal extension of the layer should be several times the required surface area. The mine should be located in a geological stable area and no faults should be running through the concession.

All calculations and the mine design are done in a generic way and are not site specific. The CAR-project has shown however that these geological conditions are common in the Netherlands [Rijksgeologische Dienst, 1996].

2 Mine design

2.1 General layout principles

The following principles were applied for the mine design:

(i) The three types of waste are stored in three separated zones (see Figure 2.1.a). It allows to take different actions for each waste type (e.g. sealing off, keeping open or retrieving waste).
(ii) Each zone is surrounded by a barrier of clay with a horizontal distance of about 50 m. The barriers not only allow to delineate clearly the different parts of the mine, but it also allows to isolate the highly radioactive parts from the rest of the repository. The use of more barrier pillars within each zone to enable the isolation of certain parts of the mine within each zone could be considered. The number of tunnels intersecting these barriers is as much as possible limited (only two intersections per zone). It results in the additional advantage that sealing off an entire zone can be done relatively quickly and easily.
(iii) Within each zone, a regular mesh of tunnels is excavated, resulting in square or rectangular blocks of clay between the tunnels. In one direction tunnels are excavated, allowing access to the storage galleries (in the perpendicular direction). The blocks of un-excavated clay between galleries is required for supporting the mass above the excavation level (see further).

In Figure 2.1, the successive steps in mining the underground facility is presented, as well as the proposed final layout. This layout allows at any time to excavate a new zone next to the existing ones with a limited additional investment in the main infrastructure.

The following different types of tunnels can be distinguished:

- Primary galleries: these are the main arteries of the mine and the galleries connecting them (Figure 2.1.b). The primary galleries are the main transport roads enabling access to the various parts of the mine. The primary galleries have to remain open, at least as long as a particular part of the mine has to remain accessible.
- Secondary galleries: they are parallel to the shaft-shaft connection (Figure 2.1.c). They give access to the waste storage galleries. After waste has been stored in all the waste storage galleries being accessed by a secondary gallery, the secondary gallery can remain open to allow easy access to the waste storage galleries for retrieval purposes. If desired, they can at a later stage be totally sealed off.
- Tertiary galleries or waste storage galleries, are smaller diameter galleries (see also 2.2), in which the radioactive canisters, drums or containers are stored (see Figure 2.1.d). They are constructed perpendicular to the secondary galleries. These galleries are sealed off as soon as the waste has been brought in place.

To make the High Level Waste (= HLW) individually retrievable, each canister got to be accessible without having to move any other container. This implies that in both the HLW heat generating zone and the HLW zone in which no heat is generated, a maximum of two containers can be stored in any tertiary gallery in between two secondary galleries. As the requirement of retrievability does not appertain to the Middle and low Level Waste (= MLW), the containers holding the MLW, can be stacked in the tertiary galleries over their entire height and length.

2.2 Gallery and shaft dimensions

Two shafts with an inner diameter of 5 m are foreseen. The outer diameter is tentatively set at 6,2 m. The downcast shaft is during the development phase used for the transport of personnel and material. The upcast shaft serves as emergency exit, and is used for the transport of the mined clay. During the emplacement phase, personnel, material and backfill material is to be transported through the downcast shaft, while the waste containers are ridden down through the upcast shaft. The reason for transporting the radioactive waste in the upcast shaft is related to safety: the contaminated air does not pass through the whole of the workings in case one of the containers leaks during transportation. The ventilation is ensured by exhaust fans, situated on surface.

The internal diameter of the primary and secondary galleries is 3,5 m; the external diameter, i.e. the diameter to be cut, is in the first stage taken to be 4,6 m, which leaves 0,55 m for the thickness of the initial convergence, the lining and the overcut (see Figure 2.2). The internal diameter of the tertiary or storage galleries is equal to 2,2 m, with the external diameter being 3,2 m, leaving 0,5 m for lining, the initial convergence and overcut. The horizontal plane in which the axes of the secondary and the tertiary galleries are situated do not coincide, but are 0,56 m apart. This to ensure that the width at the floor level of both galleries can be wide enough without having to ramp down or up. Constructing the floor level at 0,525 m from the bottom of the lining in the primary and the secondary galleries provides a floor width of 2,5 m, and a maximum height of 2,975 m in these galleries. Constructing the floor level in the tertiary galleries at the same level as in the secondary, taking the offset of the axes of 0,56 m into consideration requires to construct the floor level at 0,45 m from the bottom of the lining, leaving a maximum height of 1,766 m, and a floor width of 1,75 m. An alternative to the above concept as proposed by SCK, will be worked out in the TRUCK-II project. In this so-called PRETEL-concept, use is made of a new technology still under development by SCK for placing the lining.

The tertiary galleries in the HLW section do not extend from secondary gallery to secondary gallery. The tertiary galleries are excavated to a distance of 15 m from the centre of the secondary galleries. Taking account of a 0,5 m concrete plug at the end and the 2,3 m outer diameter of the secondary gallery, results in an effective tunnel length of 12,2 m. A buffer of 1 m filling material is foreseen in between the plug and the container. The containers are placed in a bed of filling material, such that their axis coincides with the axis of the tertiary tunnels (Figure 2.3).

The MLW has not to be stored individually, the waste disposal galleries are therefore filled with drums and containers. While the 200 l drums are stacked on top of each other (see Figure 2.4), with 6 drums per stack, the containers larger than 1 m^3 are not stacked, but are only placed behind each other. The different stacks of drums, are of course also stored the one behind the other in the disposal galleries. With a container length of 1,65 m, and a 3,5 m backfill between the last container and the gallery entrance, 23 big containers can be stored per tertiary gallery. If six 200 l drums can be stacked on top of each other, 40 stacks of 6 drums can be placed behind each other in the 45,4 m long tertiary galleries, providing for a 5 m backfill at both entrances.

2.3 Distance between galleries (hydromechanical response)

2.3.1 Design approach

While for the selected diameters of the various galleries (see 2.2) mainly the experience of SCK, Mol, is used, no experience exists of the centre distances between galleries in a clay mass (in two directions), certainly not at a depth of 500 m. Therefore, a first estimate is made, which is checked by different numerical simulations.

The basic pattern (centre distances) is 50 m x 50 m for the zone containing the heat generating waste and 40 m x 50 m for the two other zones with the cold waste. These centre distances are used as input for non-linear numerical simulations in two dimensions. These simulations should indicate if this choice is realistic. The choice is deemed realistic if the remaining clay mass between the galleries is large enough to support the above-lying rock mass. The plastic deformation around the galleries should hereby remain acceptable and the extent of the zone between the galleries in which the clay mass remains elastic should not be excessive. This would render the proposal uneconomic.

It will only be possible after knowing the clay characteristics of a particular site more accurately and after gaining some in situ experience at the depth of 500 m that these distances can be further optimized.

2.3.2 Methodology

To quantify the hydromechanical response of the clay, following the excavation, use is made of the two-dimensional finite difference software package FLAC [Itasca Consulting Group Inc., 1995]. FLAC calculates over the entire model the various stress components, the pore pressure, the deformation, the displacement and the plastic-elastic behaviour. FLAC also simulates the support and the interaction between support and rock mass. For all these calculations FLAC takes the plastic deformation into account. The groundwater flow can be modelled, and coupled hydromechanical calculations belong to the possibilities of the code as well. The elastic and plastic deformations are instantaneous, while the groundwater flow is a time dependant problem.
Of the numerous data generated by FLAC, the interpretation of the results mainly concentrates on the total and effective stresses in the vicinity of the tunnels, on the convergence (radial displacement) of the tunnels and on the extent of the plastic zone around the tunnels. A check on the deformation of the tunnel support and on the stresses within the lining has to ensure that they remain acceptable for the envisaged concrete lining.

A thorough stability analysis has to consider the excavation period, as well as the longterm behaviour of the tunnel:

(i) Excavation period
When digging a tunnel, some time elapses between the moment the clay is removed and the moment the support is installed (directly at the face). This time period should be as short as possible. For the tunnels in this study, the final support is immediately installed and no temporary support is required as is often the case for conventional tunnels. During the period the

clay remains unsupported, the convergence is largest. The rock mass in the 'unsupported' zone is only indirectly supported by the rock mass ahead of the face and by the support elements further back.
The behaviour of clay is complex, partly due to the presence of pore water coupled with a very low hydraulic conductivity (10^{-10} m/s). It is just because of this low conductivity that one can assume realistically that no drainage occurs within the clay mass during the excavation period. This period can range from a few hours to a maximum of a few days (e.g. a long weekend).

(ii) Longterm behaviour (without heat generating waste)
Once the interaction rock mass vs. support has reached an equilibrium, one would expect no or very small variations in stresses and displacements. However, in the longterm, the flow of the pore water cannot be neglected. This means that while for the excavation period the condition of no drainage is realistic, in the longterm one has to consider the possibility of drainage of the rock mass. Two situation are considered, namely permeable and impermeable lining. Even though they are entirely opposite, they could both occur with time. Before the waste material is stored and the voids around the canisters are filled (e.g. with a bentonite type material), the permeable situation is most likely valid, except if one takes specific precautions to ensure an impermeable lining. Once the filling material is saturated, a state simular to the impermeable situation is created around the shroud. A stress distribution characteristic for an impervious tunnel lining then arises around the shroud.

All the above-mentioned situations are simulated using the FLAC software. However, before any of these simulations can be conducted the so called 'convergence-confinement' curves have to be established (for some more background reading on this topic, see e.g. M. Panet, 1995). The 'convergence-confinement' curves represent the interaction between support and rock mass around the tunnel. On the one hand, the variation in radial pressure applied on the tunnel wall is plotted in function of the radial displacement of the tunnel wall (convergence curve), and, on the other hand, the variation of the pressure applied on the support elements in function of the radial displacement (confinement or loading curve) is depicted. Equilibrium is reached between the support and the rock mass, where both curves intersect. These curves have been established for the situation of a single tunnel, at a depth of 500 m, with a diameter of 2,3 m and clay surrounding the tunnel (see 2.3.4).
As discussed above the support is installed with a delay, namely at a certain distance from the face. Hence, convergence has already occurred when the support is installed. The support selected is a simple concrete lining, which is a typical passive type of support. This means that no initial supporting pressure is applied and that none of the initial convergence is reversed; the support pressure is only induced by additional convergence. To determine the amount of convergence which occurs till the support is installed, an axisymmetric (around the tunnel axis) model is developed and the succession of excavation - support installation has been repeated 35 times to get an estimate of the initial convergence.
This value is taken as the start of the loading curve for the support on the 'convergence-confinement' graphs. It is only now that the equilibrium point support-rock mass for a single tunnel can be determined, which is the input for further simulations.
In practice, the initial convergence is taken into account to determine the required overexcavation gap, so that the concrete lining fits well.

All simulations so far can be considered as preparation for the simulations, needed to evaluate the proposed centre distance between the galleries (50 m). As indicated above, three different phases are considered:

(i) Excavation period
An infinite number of adjacent tunnels are simulated with centre distances equal to 50 m. The undrained situation is considered. The support is simulated by a constant radial pressure (null stiffness), equal to the equilibrium point determined in the 'convergence-confinement' analyses (see above). These calculations aim in first instance to show the immediate effect on the rock mass behaviour of excavating adjacent tunnels.

(ii) Longterm behaviour, impermeable lining, but possibility of flow within clay mass
Again an infinite number of adjacent tunnels are simulated with centre distances equal to 50 m. Within the clay mass, the pore water can flow and the pressure in all pores can evolve to an equilibrium. Due to the stress redistribution, caused by the excavations (see (i)), a pressure build-up in the pores can be created, which in the longterm should evolve to an equilibrium as water flows from one zone to the other. At the tunnel wall the pore pressure is allowed to increase. In comparison to the previous case, the support is simulated by an imposed radial displacement (infinite stiffness), equal to the equilibrium point determined in the 'convergence-confinement' analyses. These calculations aim in first instance to show the longterm stability effect in a clay mass in which the water is free to flow.
The main reason for choosing a support with an infinite stiffness in these simulations, while a null stiffness is used for the simulations of the excavation period (i), is to evaluate the effect of the two extreme 'theoretical' behaviours of the support. In reality the support behaviour is somewhere between both extremes. As will be shown further, the effect of the choice of the support stiffness is small for the given model.

(iii) Longterm behaviour, permeable lining, drained situation
Again an infinite number of adjacent tunnels are simulated with centre distances equal to 50 m. Within the clay mass, the pore water is free to flow. The tunnel wall is now assumed to be a free surface, which means that the pore pressure has to be 0 MPa. The support is also simulated by an imposed radial displacement (infinite stiffness), equal to the equilibrium point determined in the 'convergence-confinement' analyses. These calculations aim in first instance to show the effect of drainage of the rock mass via the excavated tunnels.

2.3.3 Input parameters for model

The mechanical response of the soil is composed of two components, firstly the reaction of the grain matrix and secondly the pore water contained in the void spaces. This distinction is also made for the stresses: the effective stresses are acting on the grain matrix, while the pore pressure represents the water pressure in the voids. The sum of both is called the total stress. The values of the characteristics are also different, if one applies the effective or total stress definition. In Table 2.1, the effective stress parameters are given (see ').

Most of the parameter values are obtained from SCK in Mol, while others are obtained from the literature, or from the CAR II study. The last column in Table 2 gives an indication of the source.
As no information is directly available on the Boom clay characteristics at a depth of 500 m, the characteristics of the Boom clay at a depth of 225 m are mainly used in Table 2.1. It is expected that the greater depth, from a mechanical point of view, will have a beneficial effect on the clay characteristics [R.H.B. Rijkers et al., 1998], meaning that the values used should be a conservative approach. The porosity and the hydraulic conductivity are likely to decrease, while other values, such as the Young's modulus and the cohesion may increase. It should further be stressed that the soil is assumed to be fully saturated at all times, and that the pore water does not contain dissolved air or gasses (K_w = 2000 MPa). The three-dimensional stress state is assumed to be isotropic, meaning that the two horizontal stress components are equal to the vertical stress component [SCK, 1994]. In function of the depth, the stress increases with the weight of the overburden.

The Mohr-Coulomb failure criterion was used to determine the yield surface, while the clay is assumed to behave linear-elastic before yielding, and perfectly plastic upon yielding. The dilatation angle is fixed at 0 degrees, which implies that no compression or dilatation of the clay is assumed to take place as a consequence of the plastic deformation.

The geometric and support parameters used, are given in Table 2.2. The reasons to carry out the simulations on a tunnel with the dimensions of the primary and the secondary galleries are twofold. The primary and secondary tunnels have the largest diameters, which gives rise to the most critical situation (see sensitivity analyses, 2.3.8). Secondly, the tertiary galleries in which the heat generating high level waste has to be stored will be backfilled as soon as the vitrified waste has been brought into place. The backfill material is expected to have a beneficial effect on the mechanical behaviour of these tunnels by exerting an internal pressure against the tunnel wall.

The values presented in Tables 2.1 and 2.2 are considered to be the basic values of the various characteristics. However, a sensitivity analyses has also been conducted, whereby in successive simulations the value of one characteristics is changed while the others remain at their basic value.

The selected parameters for the sensitivity analyses as well as their base values and the different alternatives are listed in Table 2.3. The influence of the parameters was evaluated for the excavation period only. The extensive calculation time (27 hours to simulate a 31 year period), makes routine calculations for the drained response almost unachievable.

2.3.4 Convergence-confinement curves (single tunnel)

In Figure 2.5, the results of the radial displacement around the tunnel face for the axisymmetric model is presented. It can be seen that before the tunnel lining is installed an initial convergence (*) of 142,7 mm occurs.

(*) In this report, convergence is defined as the absolute radial displacement of the tunnel wall and not as the relative displacement (shortening) of two opposite points on the tunnel wall. Apart for the axisymmetric model, the convergence can be different for each point of the tunnel wall.

Description	Symbol	Unit	Value	Source
Specific weight clay (dry)	γ_d	kN/m^3	16,60	calculated
Specific weight clay (wet)	γ_n	kN/m^3	20,5	SCK
Coefficient of Poisson	ν' (*)	-	0,125	SCK
Young's modulus	E' (*)	MPa	300	SCK
Friction angle	ϕ' (*)	degrees	18	SCK
Dilatation angle	ψ	degrees	0	assumption
Cohesion	c' (*)	kPa	300	SCK
Porosity	n	%	39	SCK
Hydraulic conductivity	k	m/s	1e^{-10}	TNO
Degree of saturation	v	%	100	assumption
Water content	w	%	23,49	calculated
Specific weight water	γ_w	kN/m^3	10	
Bulk modulus water	K_w	MPa	2000	
Gravity constant	g	m/s^2	10	
Pore water overpressure	Δpp	MPa	0	
Coefficient of earth pressure	k_o	-	1	assumption

(*) Effective stress parameters

Table 2.1: Hydromechanical clay parameters and in situ conditions [4, 5, 11,12].

Description	Symbol	Unit	Value
Excavated radius	R	m	2,3
Inner radius	r	m	1,75
Depth centre tunnel	d	m	500
Distance between tunnel centres	L	m	50
Radial stiffness of liming		GPa	5,36

Table 2.2: Geometric parameters

Description	Symbol	Unit	Basic value	Value 2	Value 3
Friction angle	ϕ' (*)	degrees	18	16	23
Cohesion	c' (*)	kPa	300	265	345
Excess pore water pressure	Δpp	MPa	0	5	1
Excavated tunnel diameter	R	m	2,3	1,6	0,6
Depth	d	m	500	225	350
Distance between tunnel centres	L	m	50	40	30

(*) Effective stress parameters

Table 2.3: Parameters used in the sensitivity analyses

In Figure 2.6, the 'convergence-confinement' curves are represented. The loading curve represents a concrete lining with a stiffness of 5,36 GPa. As the support is installed when the initial convergence of 142,7 mm has already occurred, the loading of the support starts at this value. At the sidewall (centre), the equilibrium is reached after an additional convergence of 1,8 mm (total of 144,5 mm), resulting in a support pressure of 4,3 MPa.

In Figure 2.6.c, the two extreme behaviours of the support (null and infinite support stiffness), which are applied for the excavation period and the longterm behaviour (see 2.3.5, 2.3.6 and 2.3.7) are also indicated in dotted lines.

2.3.5 Excavation period (adjacent tunnels)

In comparison to the previous paragraph, an infinite number of parallel tunnels are excavated, mainly to analyse the behaviour of the clay mass between two adjacent tunnels. The infinite number of parallel tunnels is created by introducing symmetrical axes around the vertical boundaries of the model. These boundaries are the vertical lines through the centre of a tunnel and at a distance of 25 m from the centre line. The assumption of an infinite number of tunnels represents well the situation in the middle of the various zones. The load on the two tunnels at the periphery of the zones is probably a little bit smaller. A design for a tunnel in an infinite series of tunnels is therefore a safe approximation.
The support is simulated by a constant radial pressure, applied on the tunnel wall, equal to 4,3 MPA (see equilibrium point on Figure 2.6).

One of the main evaluation criteria is the extent of the plastic zones around the tunnels (see Figure 2.7). The plastic zone is the area surrounding the tunnel, in which the stress state of the clay at equilibrium is situated on or within 0,05 MPa of the yield surface. Even though the plastic behaviour is theoritically an instantaneous behaviour, it is calculated in an iterative way. The plastic zone is more or less elliptic. The plastic zone extends, from the centre of the tunnel about 7 m in the horizontal direction and 6,5 m in the vertical direction. In other words, between two adjacent tunnels

at a centre distance of 50 m, a clay mass of about 36 m remains in the elastic domain. This should be more than enough to create a safe barrier between adjacent storage tunnels and to support the overburden, even if the clay characteristics would even be more disadavantageous (see also 2.3.8).

In comparison to the situation of a single tunnel (see 2.3.4), the application of a constant support pressure of 4,3 MPa to a tunnel surrounded by an infinite number of similar tunnels results in a limited further deformation of the tunnel wall. While for a single tunnel a total convergence after installation of support of 144,5 mm occurs at the sidewall (centre), the value for an infinite number of adjacent tunnels is 146,4 mm.

In Figures 2.8, 2.9 and 2.10, calculated stresses (3 total stress components, pore pressure and 3 effective stress components) and displacements (radial displacement only) along the horizontal and vertical centre lines are presented.

The damaged zone, the peak in the tangential stress and the drop in pore water pressure are clearly illustrated. The peak in effective tangential stress indicates the boundary of the plastic zone. The stresses in the FLAC program are zone-based, which means that they are not calculated in the nodes, but are assumed to be constant over an element. The values at the tunnel wall of the different stresses are obtained by extrapolation of the stresses in the two last elements bordering on the tunnel wall. These extrapolated stresses as well as the displacement of the tunnel wall are summarized in Table 2.4. They show that the influence of the other tunnels situated at 50 m from the tunnel being considered, is as far as the short term response is concerned, limited. Hence, they confirm that in the short term and for the layout considered the stability should be ensured.

2.3.6 Longterm behaviour, impermeable lining, but possibility of flow within clay mass

In this second model, water flow is allowed inside the clay mass, butthe tunnel lining is considered to be impermeable. As in the previous model, no water flows through the boundary defined by the excavation.
In contrast to the elastic/plastic calculations in the foregoing, simulating the water flow has to be conducted in the time domain. The analysis is carried out for a period of 10^9 seconds, corresponding to a period of about 31 years and 8 1/2 months. As for all simulations, the absolute time scale has to be interpreted carefully and some callibration or verification with in situ measurements is necessary.

The graphs depicting the stress distribution in function of the time are given in the figures 2.11 to 2.16. As the stress distribution along the horizontal (Figures 2.11 to 2.13) and along the vertical centre line (Figures 2.14 to 2.16) are similar, only the the stress distribution along the horizontal line is discussed. Comparing the immediate and the 3-year response, a slight decrease of the total tangential stress of 0,05 MPa at the tunnel wall is noted (Figure 2.11.a). At 3,9 m from the tunnel centre this decrease goes with time over in an increase in tangential stress. A maximum difference of 0,3 MPa is reached at 4,7 m from the centre. The difference between the long term tangential stress and the immediate tangential stress becomes negative again at 5,2 m from the centre, from here onwards the long term tangential stress remains smaller than the immediate tangential stress. Note also the kink at 4,7 m.

Description	Symbol	Unit	Excavation period (2.3.5)	Long term, permeable (2.3.7)	Long term, impermeable (2.3.6)
Sidewall (center)					
Plastic zone (Disturbed)	R_{pl} (R_d)	m (m)	6,9 (6,9)	7,6 (7,6)	4,7 (6,9)
Total radial displacement	u_{tot}	mm	146	146 (fixed)	146 (fixed)
Total tangential stress	σ_t	MPa	8,0	7,2	7,9
Total radial stress	σ_r	MPa	4,3 (imposed)	3,7	6,1
Total longitudinal stress	σ_l	MPa	6,3	5,6	7,9
Effective tangential stress	σ'_t	MPa	6,8	7,2	3,0
Effective radial stress	σ'_r	MPa	3,1	3,7	1,1
Effective longitudinal stress	σ'_l	MPa	5,1	5,6	3,0
Pore water pressure	pp	MPa	1,2	0,0 (imposed)	5,0
Roof (crest)					
Plastic zone (Disturbed)	R_{pl} (R_d)	m (m)	6,5 (6,5)	0,0 (6,5)	4,2 (6,5)
Total radial displacement	u_{tot}	mm	138	138 (fixed)	138 (fixed)
Total tangential stress	σ_t	MPa	8,0	8,9	7,7
Total radial stress	σ_r	MPa	4,3 (imposed)	7,0	5,9
Total longitudinal stress	σ_l	MPa	6,4	7,5	7,7
Effective tangential stress	σ'_t	MPa	6,6	8,9	2,7
Effective radial stress	σ'_r	MPa	2,9	7,0	1,0
Effective longitudinal stress	σ'_l	MPa	4,9	7,5	2,7
Pore water pressure	pp	MPa	1,4	0,0 (imposed)	4,9
Floor (bottom)					
Plastic zone (Disturbed)	R_{pl} (R_d)	m (m)	6,5 (6,5)	0,0 (6,5)	4,2 (6,5)
Total radial displacement	u_{tot}	mm	142	142 (fixed)	142 (fixed)
Total tangential stress	σ_t	MPa	8,1	9,0	7,7
Total radial stress	σ_r	MPa	4,3 (imposed)	7,0	6,0
Total longitudinal stress	σ_l	MPa	6,4	7,5	7,7
Effective tangential stress	σ'_t	MPa	6,7	9,0	2,7
Effective radial stress	σ'_r	MPa	2,9	7,0	1,0
Effective longitudinal stress	σ'_l	MPa	5,0	7,5	2,7
Pore water pressure	pp	MPa	1,4	0,0 (imposed)	5,0

Table 2.4: Summary of calculated parameters

The total radial stress increases most markedly at the tunnel wall (Figure 2.12.a): from 4,30 MPa to 6,09 MPa, but the difference between the immediate and the long term response has been reduced to less than 0,08 MPa at 15 m from the tunnel centre. The increased total radial stress has repercussions on the design of the tunnel lining, which has to withstand this increased pressure. This will be discussed further.
The pore water pressure at the tunnel wall rises relatively fast to the hydrostatic pressure (Figure 2.13). Starting from a pore water pressure of 1,18 MPa at the start of the drainage, this pressure would have risen to 1,93 MPa after 1 day, to 3,27 MPa after 10 days, and would after 3 years nearly have reached the hydrostatic pressure. The reason equilibrium is attained relatively quickly, lies partly in the assumption that the clay remains fully saturated at all times, also in the immediate vicinity of the excavation. The considerable and fast increase in pore water pressure has of course its repercussions on the effective stresses.
The effective tangential stress decreases fast and considerably at the tunnel wall: from 6,77 MPa to 3,20 MPa in only 3 months (Figure 2.11.b). The effective tangential stress decrease in the undisturbed zone on the other hand remains limited. The effective radial stress decreases in the vicinity of the tunnel as time elapses, but increases with time beyond approximately 6 m from the tunnel centre (Figure 2.12.b).

The combined effect of the steeply decreasing effective tangential stress, with the less outspoken decrease of the effective radial stress, which is even reverted into a stress increase beyond 6 m, results in a shift of the boundary of the plastic zone. Only the clay within the first 4,7 m from the tunnel centre is being plastically deformed. The clay beyond this limit, has been disturbed in the past, but has returned within the yield envelope.

The results are again summarized in Table 2.4.

In comparison to the simulations without water flow, the extent of the plastic zones have decreased which is positive from a stability and safety point of view. However, these calculations show that if the lining is impermeable precautions could probably have to be taken against the relatively high total radial stress (up to 6 MPa) against the lining. For the case where the impermeable condition is created by the combination lining-saturated backfill, this situation is probably not hazardous, as the backfill counteracts the loading. However, if one would go for an impermeable lining, this finding has to be taken into account during the design.

2.3.7 Longterm behaviour, permeable lining, drained situation

If no special precautions are taken and before the tunnels are backfilled, the tunnel lining has to be considered permeable, and the formation water will drain towards the tunnels. The tunnels are assumed to have an infinite drainage capacity, an assumption which is realistic considering the low hydraulic conductivity of the clay, especially as long as no backfill has been placed.

The stress distribution in between two tunnels is given in the Figures 2.17 to 2.19. The decrease over time in the total stress is outspoken for the radial stress (Figure 2.18.a). Over a three-year period it diminishes from 4,30 MPa to 3,68 MPa at the tunnel wall and even from 10,03 to 7,47 MPa halfway between two adjacent tunnels. The decrease over time in the total tangential stress remains restricted

to the first 13,5 m from the tunnel centre (Figure 2.17.a). From the tunnel to a distance of 6,9 m from the tunnel centre, the decrease in total tangential stress slowly evolves from 0,7 MPa to about 1 MPa, after which the difference in original and long term total tangential stress falls back to 0 MPa over the next 6,5m.
The effective tangential stress however increases markedly over the full zone in between the tunnels as time elapses (Figure 2.17.b). A maximum tangential stress increase of 3,5 MPa is noted at 7,6 m from the tunnel centre. The reason for this sharp increase in effective tangential stress lies in the marked decrease in pore water pressure (Figure 2.19). The terrain surrounding the tunnels is being drained by the tunnels, which have in the model an infinite drainage capacity. The increase in the effective radial stress is most significant in the first 15 m fromthe tunnel centre (Figure 2.18.b), but is with its maximum of 1,5 MPa not as important as the effective tangential stress increase. The change in the effective stresses also results in a lateral increase of the plastic zone (and of the disturbed zone) from 6,9 m to 7,6 m as indicated by the shift in the position of the peak of the effective tangential stress.

The stress distribution above and below a tunnel is given in the Figures 2.20 to 2.22. The stress distribution in the immediate vicinity of the tunnels is very similar above and below the tunnel. The increase over time in the total radial stress (Figure 2.21.a) is limited to the first 12 m measured from the tunnel centre. The largest increase in total radial stress amounts to 2,67 MPa. As this is the radial stress incrase at the tunnel wall, the lining has to be such that it can withstand a stress rise of this magnitude.
The influence of the drainage on the effective radial stress extends to the boundary of the model (Figure 2.21.b) as the drop in pore water pressure Figure 2.22), a consequence of the draining by the tunnels, affects the whole of the clay mass.
The total tangential stress distribution (Figure 2.20.a) and the effective tangential stress distribution (Figure 2.20.b), are also very much determined by the chosen boundary conditions. By applying the lateral symmetry boundary conditions (i.e. fixing the lateral movent of the grid at the right and left-hand sides of the model), the total tangential stress decreases over the full height of the model asa consequence of the consolidation of the clay mass. A refined mesh would be required in the vicinity of the tunnel to comment on the increase in the total tangential stress close to the tunnel wall. The oscillatory nature of both the total and effective tangential stress distribution for the curve depicting the situation after 31 years, as well as the considerable difference near the model boundary between the tangential stresses of the curves describing the situation at the start of the drainage period and after 31 years, point to numerical problems.

The results are again summarized in Table 2.4. The extrapolated stresses at the tunnel wall show that the presence of the other tunnels of the repository have now a marked influence on the response which can be deduced from the different stress values at the sidewall of the tunnels compared to the values at the crest and bottom of the tunnels. In comparison to the two previous cases, the plastic zone has increased to a horizontal distance of 7,6 m from the tunnel center, but the remaining elastic zone is still acceptable (34,6 m) and no hazardous or unstable situation should occur. However, the differential radial loading of the support cannot be omitted during the detailed design of the lining.

2.3.8 Sensitivity analyses (excavation period)

In paragraph 2.3.3, the parameters which are changed in the sensitivity analyses, as well as the alternative values are summed up (see Table 2.3).
The following considerations are taken into account in selecting the parameters for the sensitivity study:

(i) Selected parameters
- To evaluate the sensitivity of the results to a change in mine design, the tunnel diameter and the distance between the tunnels are decreased.
- The experience gained at SCK, Mol, proves that a tunnel can be excavated at a depth of 225 m and that at such a depth a stable configuration can be realized. To get an idea of the influence of the depth, simulations at a depth of 225 m and at 350 m are conducted.
- The extent of the disturbed zone is determined by the yield criterion chosen and the parameters featuring therein. No yield criterion other than the Mohr-Coulomb has been used, but the parameters featuring in this criterion, the cohesion and the friction angle, have both been varied.
  The base value of the friction angle and the cohesion have on the one hand been increased because a larger burying depth could cause these parameters to increase [R.H.B. Rijkers et al., 1998], and they have on the other hand been decreased, because an increase in temperature might cause a change in clay characteristics, with a possible decrease in cohesion and friction angle. The decrease of the values should also give a good indication of the reliability of the conclusions derived in the previous three paragraphs.
- The pore water pressure was in first instance assumed to be equal to the hydrostatic pressure. An increase in temperature might result in a (temporary) increase in pore water pressure in the vicinity of the tunnel. Two simulations have therefore been carried out with an excess pore water pressure.

(ii) Non-selected parameters
- The elastic modili (Young's modulus E' and Poisson's ratio v') have not been changed, as the extent of the plastic zone, and the stress levels are mainly determined by the plastic behaviour of the clay.
- The bulk modulus of the water K_w, has not been varied either. A decrease in K_w due to gases being dissolved in the water could decrease the value of K_w considerably, which in turn would lead to an increase in the extent of the plastic zone [C. Grégoire, 1996; V. Labiouse et al., 1997].
- The specific weight of the clay and its porosity have not been altered. A decrease in porosity might cause a decrease in permeability.
- Instead of varying the dilatation angle, other models describing the clay behaviour should be utilized that take account of the overconsolidation ratio, and that relate the specific volume to the stress state. This would however require the determination of the relevant parameters.

For each of the 13 alternative cases, first the corresponding 'convergence-confinement' curve is calculated, followed by the short term simulation, as decribed above. The results of the parameter study are summarized in Tables 2.5 and 2.6. The total convergence, radius of the plastic zone (from the tunnel axis), as well as the stresses (total stress components, pore pressure and effective stress

components) at the tunnel side wall are brought together in Table 2.5. All the values listed are taken in the centre of the tunnel side wall. The relative variances are given in Table 2.6, and were calculated as follows:

$$\frac{\left(\begin{array}{l}\text{Resulting value associated with highest value of parameter -}\\ \text{Resulting value associated with lowest value of parameter}\end{array}\right)}{\text{(Resulting value associated with highest value of parameter)}} \times \frac{\text{(Highest value parameter)}}{\text{(Highest value parameter - lowest value parameter)}}$$

The graphs depicting the trend for varying the input parameters are given in appendix B.

In evaluating the influence of a parameter on the results, one has to take the following in consideration:

- the sensitivity in the real sense, i.e. the relative changes of the results in relation to a change in the input parameters,
- the trend in the results; the change of an input parameter can, up to a certain level be negligible, after which it becomes significant,
- the possible fluctuations the input parameter can be subject to,
- the absolute changes of the results, which reflects the coupling of the fluctuations in input parameters to the relative changes.

From Table 2.5, it becomes clear that the results, and especially the convergence and the extent of the plastic zone are very sensitive to a change in friction angle. The trend of the extent of the plastic zone and of the convergence in function of the friction angle indicate moreover that the influence of a change in friction angle becomes more important as the friction angle decreases. At room temperature, the friction angle is assumed to increase marginally as the depth increases. The variation in friction angle due to a substantial temperature increase (to e.g. 80°C in the vicinity of the heat generating waste) requires however more research, as this could lead to a decrease in the friction angle. A further decrease of the friction angle with a few degrees would increase the extent of the plastic zone with a few metres, and the convergence of the tunnel wall with a number of centimetres. For a friction angle of 16° the remaining elastic zone is however still more than 30 m. Only a moderate influence of the friction angle on the radial stress is noted. The radial stress increase associated with an increase in friction angle is not expected to pose problems for the support.

The influence of the cohesion on the stresses seems to be rather small. For the range of the values chosen for the sensitivity study (+ and - 15% of the basic value), the trend for the results in function of the cohesion seems to be linear. The relative increase in the extent of the plastic zone, as well as the convergence are, although not negligible, not as important for a change in cohesion as what they are for a change in friction angle or in depth (see further).

Parameter		conv. mm	R_{pl} m	σ_t MPa	σ_r MPa	σ_l MPa	pp MPa	σ_t' MPa	σ_r' MPa	σ_l' MPa
ϕ	16°	193	8,4	7,56	4,23	6,03	0,95	6,61	3,29	5,08
	18°	146	6,9	7,95	4,30	6,25	1,18	6,77	3,12	5,07
	23°	91	4,7	8,91	4,47	6,80	1,76	7,15	2,71	5,04
c	265kPa	154	6,9	7,88	4,29	6,21	1,14	6,75	3,15	5,08
	300kPa	146	6,9	7,95	4,30	6,25	1,18	6,77	3,12	5,07
	345kPa	136	6,3	8,08	4,34	6,33	1,26	6,82	3,08	5,07
d	225m	41	4,7	4,03	2,07	3,09	0,82	3,21	1,24	2,27
	350m	86	6,3	5,81	3,07	4,52	0,98	4,83	2,10	3,54
	500m	146	6,9	7,95	4,30	6,25	1,18	6,77	3,12	5,07
Δpp	0MPa	146	6,9	7,95	4,30	6,25	1,18	6,77	3,12	5,07
	5MPa	192	8,4	7,55	4,20	6,00	1,43	6,12	2,77	4,57
	1MPa	282	11,1	7,08	4,10	5,71	1,62	5,46	2,43	4,09
L	50m	146	6,9	7,95	4,30	6,25	1,18	6,77	3,12	5,07
	40m	150	7,0	8,00	4,30	6,24	1,14	6,83	3,16	5,10
	30m	160	7,9	8,00	4,30	6,24	1,10	6,88	3,20	5,14
	25m	175	8,6	8,00	4,30	6,24	1,10	6,89	3,20	5,15
R	23m	146	6,9	7,95	4,30	6,25	1,18	6,77	3,12	5,07
	16m	97	4,6	8,00	4,35	6,30	1,29	6,71	3,06	5,01
	0,6m	56	1,9	7,13	3,53	5,56	0,88	6,25	2,65	4,68

Table 2.5: Results of the parameter study at tunnel side wall (centre)

	conv.	R_{pl}	σ_t	σ_r	σ_l	pp	σ_t'	σ_r'	σ_l'
tanΦ	-3,45	-2,38	0,47	0,16	0,35	1,42	0,23	-0,66	-0,03
c	-0,56	-0,43	0,11	0,05	0,08	0,43	0,05	-0,10	0,00
Δpp	0,48	0,38	-0,12	-0,06	-0,10	0,27	-0,24	-0,28	-0,24
d	1,31	0,58	0,90	0,94	0,92	0,55	0,96	1,09	1,01
L	-0,40	-0,49	-0,01	0,00	0,00	0,14	-0,04	-0,06	-0,03
R	0,84	0,98	0,14	0,24	0,15	0,34	0,11	0,21	0,11

Table 2.6: Relative change in the results

The reason for including the excess pore water pressures in the parameter study is the observation that the strength of an undrained clay sample decreases with up to 28% as the temperature is increased from 20°C to 80°C [D. De Bruyn et al., 1996]. An increase in pore water pressure can be used to model such a behaviour, but it could be the actual cause of the behaviour as well. It should be noted that, if a temperature increase causes an excess pore water pressure, this effect is tempory, and the pore water pressure returns to an equilibrium as the clay mass drains. The relative decrease in effective stress is more or less uniform for the different stress components. Although the relative influence of the increase in excess pore water pressure is not as important as for most of the other parameters, the excess pore water pressure may vary quite considerably, such that this parameter becomes one of the more important characteristics.

The main difference between the geometric factors and the hydromechanical parameters is the control one has over the former. The input range is indeed well defined, and a study of these parameters serves to optimize the design rather than to establish the sensitivity of the design to the parameter in question.

The repository to be designed has to be situated at a minimum depth of 500 m. To enable a comparison with the work carried out at SCK, Mol, and to illustrate the influence of increasing the depth, a set of calculations is carried out at a depth of 225 m and 350 m. The influence of a variation in depth is nearly directly related to a variation in both total and effective stress levels. The depth is therefore the single most important factor in determining the loads the support is subjected to (about double when comparing the depths of 225 m and 500 m). The important radial support required at greater depth, has a possitive effect on the extent of the plastic zone. Although the relative increase of the disturbed zone remains important, this increase remains smaller than the increase of most of the other resulting values appertaining to the depth increase. The trend of the curve indicates moreover that the beneficial effect of the radial stress on the disturbed zone mounts with the depth. The depth proves to be an important factor governing the convergence as well, which has a direct effect on the overexcavation gap.

The influence of the centre distance between the tunnels on the results being discussed in this paragraph is negligible for distances up to 40 m. The behaviour of the clay mass is very similar to the behaviour of a clay mass surrounding an isolated tunnel (for the immediate response). The result most significantly affected by the distance between the tunnels, is the extent of the plastic zone, which enlarges considerably as the tunnel centres approach each other. The extent of the plastic zone becomes larger than the zone reacting linearly when the tunnels centres are less than 30 m apart. Hence the remaining elastic zone decreases even stronger.

The extent of the plastic zone is proportional to the tunnel diameter, provided the boundary conditions, such as the radial support pressure, do not change. The required radial support pressure itself does however depend on the tunnel diameter, on the distance between the face and the last support panel and on the lining itself. It is assumed, that the minimum distance from the face to the last support element as well as the excavation-support sequence are independant of the tunnel diameter. This means that different radial support pressures are mobilised for each of the tunnel diameters. The extent of the plastic zone therefore decreases in absolute size as the tunnel diameter decreases, but the extent of the plastic zone relative to the tunnel diameter increases with decreasing tunnel diameter.

2.3.9 Discussion of results, hydromechanical response

In the underground laboratory at SCK, Mol, one has shown that excavating circular tunnels at a depth of 225 m is feasible. Based on the various numerical simulations discussed in the previous paragraphs, one can conclude that this should also be feasible at a depth of 500 m, at least if the clay characteristics do not deteriorate with depth. The current knowledge indicates that the clay should rather improve from a geotechnical point of view. The most critical parameter found so far is the friction angle. A value of 18° is used as basic value for the friction angle (effective stresses). A decrease of 2° only (about 10%) has already a significant effect on the total plastic zone.

In the above simulations the short and longterm behaviour is considered and a hydromechanical coupling is applied. Based on these simulations, a centre distance of 40 m to 50 m between adjacent galleries seems to be safe. If one would decrease the centre distance to 30 m or less, the remaining elastic zone in the clay mass between galleries becomes small.
When the clay mass around the tunnels is drained, specific attention should be given to the differential radial loading of the support, in addition to the high total radial stress (up to 7 MPa), when designing the lining. A situation in which the clay mass is drained could for example be encountered when the lining is permeable. When the lining would on the other hand be impermeable, precautions should also have to be taken against the relatively high total radial stress (up to 6 MPa) against the lining. A combination of a permeable lining and a saturated backfill leads to conditions around the shroud comparable to the situation in which the lining is impermeable. This situation is probably not hazardous, as the backfill counteracts the loading and as long as the shroud withstands the stresses.

All simulations consider a perfect elasto-plastic behaviour and a Mohr-Coulomb failure criteria. Other more complex failure criteria can also be applied and more complex stress-strain relations could be used too. In these simulations the stress-strain response is always considered to be immediate. A visco-plastic approach would introduce a time dependent reaction of the mass due to loading. These more complex constitutive laws and failure-flow criteria will add additional insight in the behaviour of the clay mass around the excavations. However, the accurate determination of all additional input parameters may not be underestimated. The much longer calculation time is another restriction to their use.

In conclusion, a rectangular grid of 40 m x 50 m or a square grid of 50 m x 50 m seems to be a good choice for further studies.

2.4 Spatial distribution of the heat generating waste

2.4.1 Design approach

So far, the effect of placing heat generating waste in the galleries on the temperature distribution in the surrounding rock mass and on the stability of the galleries has not been considered. The zones in which the high radioactive waste that does not generate heat and in which the middle and low radioactive waste are stored, do not undergo any additional temperature effect. The findings of this paragraph do not have to be applied to these zones.

To quantify the influence of the heat generating waste on the temperature distribution in the clay, use is made of a number of analytical formulas and of the three dimensional boundary element code MAP3D [Mine Modelling Ltd, 1997]. The analytical formulas are used to obtain an idea of the evolution of the temperature front in function of the time. The MAP3D simulations are used to calculate the steady state temperature distribution in the clay mass for a given temperature of the storage galleries. The calculations give, besides the temperature distribution, also an indication of the stress increase one may expect as a consequence of a rise in temperature. Coupled thermomechanical-groundwater simulations with a time dependant heat source arenot conducted; this would form a research project on its own.

The initial boundary element model considers one heat generating canister only. In successive models the number of heat sources is increased (1, 2 and 24) till a total number of 320 canisters is reached. By increasing in successive steps the amount of heat sources, one gets a good idea of the three dimensional effect. In first instance the canisters are placed at centre distances of 50 m in the one direction and at a distance of alternatively 26 m and 24 m in the other direction (see Figure 2.23.a). This configuration corresponds to a square pattern of galleries (centre distances at 50 m x 50 m). Afterwards, an additional simulation is carried out for the situation that the centre distances between galleries is increased to 100 m. For this geometry, the canisters are at 100 m in the one direction and at 26 m and 74 m in the other direction (see Figure 2.23.b).
For all boundary element models, the stationary situation is determined at various distances above the repository and for different temperatures of the storage sites.

To obtain an idea of the time required to reach the steady state situation, use is made of analytical formulas. This time scale is then compared to the evolution of the heat generating power of the waste in function of the time.

2.4.2 Input parameters for simulations

The additional soil parameters, and the subsurface temperature data required for the thermal calculations are summarized in Table 2.7. The soil parameters are obtained from SCK, Mol, while the information relating to the subsurface temperatures stems from research conducted by K.U.Leuven [N. Vandenberghe et al., 1988; N. Vandenberghe et al., 1989].

As the location of the repository is not known, the ambient temperature and the temperature featuring in the calculations are also estimates. It should be noted that the ambient temperature at a depth of 500 m can vary considerable from site to site; temperatures ranging from 15°C to 30°C have been recorded at a depth of 500 m in the Belgian underground [N. Vandenberghe et al., 1989]. For the purpose of the calculations, the temperature distribution and the temperature gradient of northern Belgium are utilized. This seems to be justified considering that:

- No special temperature anomalies are encountered in the North of Belgium at a depth of 500 m. (i.e. there is no evidence of either hot spots or cold spots.).
- The formations encountered in the North of Belgium are likely to be similar to the formations encountered in the area to be used for the disposal of radioactive waste in the Netherlands. The temperature maps for the Dutch underground, included in the Car II report confirm this assumption [R.H.B. Rijkers et al, 1998].

Description	Symbol	Unit	Value	Source
In situ temperature at 500 m	T_0	°C	25	KULeuven
Temperature gradient	ΔT	°C/100 m	3	KULeuven
Specific heat	c_p	J/(kg °C)	1400	SCK
Thermal conductivity	λ	W/(m °C)	1,69	SCK
Thermal diffusivity	a	m^2/y	18,6	Calculated
Drained linear dilatation coefficient	α'	/°C	$0,8e^{-5}$	SCK
Undrained linear dilatation coefficient	α	/°C	$4,19e^{-5}$	SCK

Table 2.7: Thermal parameters [N. Vandenberghe et al., 1988; N. Vandenberghe et al., 1989; R.H.B. Rijkers et al., 1998; SCK, 1994].

Based on the temperature distribution maps of Vandenberghe and Fock [N. Vandenberghe et al., 1989], and on the data recorded in the Meer well [N. Vandenberghe et al., 1988], an ambient temperature of 25°C is considered a fair estimate of the prevailing temperature at a depth of 500 m. The temperature gradient is taken to be 3°C/100 m. Although it may be argued that this is an overestimate in the tertiary clay, it approaches very well the average of 2,9°C/100 m, measured in the Tertiary of the Meer well in between 100 and 834 m [[N. Vandenberghe et al., 1988].

It is further assumed that the temperature at the boundary clay-lining never exceeds 80°C. This assumption is independent of the radius of the tunnel in which the waste is to be stored. This implies that if the waste is stored in small diameter tunnels it has to remain on surface for a longer period than when it is stored in larger diameter tunnels.

2.4.3 Temperature distribution in rock mass

Firstly, the influence of the number of heat sources (1, 2, 24, 320) being modelled is investigated. The temperature profile above a canister in the centre of the repository is used as a measure (Figure 2.24). The details of the model and the boundary conditions applied are discussed in Appendix C, the graphs presented in this section are the results of calculations carried out for 1,2 m diameter tunnels.

The markedly different curves in Figure 2.24.a obtained from the calculations on the 24-source model and on the model containing all the heat sources proves that a full three-dimensional analysis, including all the heat sources is required to obtain accurate results. It can further be pointed out that the temperature falls with more than 18°C over the first 5 m, while it decreases with only 9°C over the next 45 m when the heat sources are spaced 50 m apart. For the 100 m x 100 m pattern (Figure 2.24.b) the temperature decrease over the first 5 m amounts to 26°C and it decreases a further 10°C over the next 45 m.

If one would use the temperature increase at the top of the clay layer, situated in the models 50 m above the storage, as a design criteria, one has to conclude that too large a temperature increase

occurs. In the case of the basic grid (50 m x 50 m), the increase is about 30°C relative to the virgin temperature; in the case of the enlarged grid (100 m x 100 m) it remains high (about 20°C). In Belgium, one hopes to limit the temperature increase at the top of the clay layer to 4°C. However, it has to be pointed out that the time dependancy has been omitted so far and therefore the above negative conclusion is premature. On the one hand, the rock mass needs time to heat up, but at the same time the temperature of the source is decreasing. This is discussed and analysed in more detail in the next paragraph (2.4.4).

The influence of the size of the storage galleries is illustrated in Figure 2.25. A decrease in the diameter of the storage gallery from 3,2 m to 1,2 m corresponds with a decrease of the temperature of the modelled heat source (i.e. with the temperature of the tunnel wall) from 80°C to 67,5°C for a 3,2 m tunnel.

Even for a constant heat source, a full scale analysis of the influence of a temperature increase on the stresses would require a simulation whereby the influence of a time dependent temperature increase on both the behaviour of the pore water pressure and on the clay skeleton is evaluated, taking the hydraulic conductivity of the clay in consideration, and whereby the effective stresses are used to determine the elasto-plastic response of the clay. Such a fully coupled analysis lies beyond the scope of this study. The analysis was limited to an evaluation of the total stress increase one would obtain if the clay mass was to react elastically. The following considerations should be made in interpreting the results.

- By the time the HLW canisters are brought into place, the clay mass is partially consolidated. The temperature increase leads to a stress increase as further convergence is limited by the stiff lining.
- The cubic dilatation coefficient of water ($\gamma = 2{,}1e^{-4}$/°C) is considerably higher than the cubic dilatation coefficient of the drained clay ($\gamma = 2{,}4e^{-5}$/°C). A fast temperature increase in the poorly permeable clay therefore gives rise to an increase in pore water pressure. A slow temperature increase would lead to a much smaller stress increase, as the water would drain as it dilates. The total stress increase would in such a case be equivalent to the effective stress increase, and the drained clay characteristics should be used.
  The increase in total stress, calculated with the undrained dilatation coefficient is here considered as a pore water pressure increase. This assumption overestimates the actual pore water pressure increase, but it allows to calculate an upper limit to the extent of the plastic zone.

The maximum stress increase obtained by increasing the temperature of the tunnel wall from 25°C to 80°C for a 3,2 m tunnel amounts to 1,45 MPa. The extent of the plastic zone for an increase in pore water pressure of 1,45 MPa increases from approximately 4,6 m to 7,5 m (from centre of tunnel).

2.4.4 Thermal analysis, time related aspects

The generated power decreases exponentially. The generated heat per canister is given in Figure 2.26. The contribution of both the fission products and the actinides [R.J. Heijboer et al., 1988; J.J. Heijdra et al., 1995] is taken into account. The graph has been derived for a burn-up of 33 Gwd/Tonne U; a three year cooling period before chemical reprocessing and a 30 year cooling period after reprocessing have been allowed for. At the end of this 30 year cooling period, the waste is stored

underground. All time indications are in what follows referred to the end of the cooling period, when the waste is stored underground. The HLW canisters are assumed to be of the Cogema type, filled with 150 l of vitrified waste, which contains the waste generated by 1,33 tonnes U.

Figure 2.27 gives the evolution of the temperature in function of the time at various heights above the repository (for a tunnel diameter of 3,2 m), assuming that the tunnel wall remains at a constant temperature of 80°C [H. Hens, 1992; A. Whillier, 1982] (see appendix C for details of the calculations). The temperature in the vicinity of the tunnels increases relatively fast. Ten meters above the repository, the temperature 10 years after the storage is already more then 50°C. Twenty five meters above the repository, 50°C is only reached after about 65 years. The absolute temperatures reached after 30, 100 and 300 years is given in Table 2.8. The temperature increase (relative to virgin temperature), expressed as a percentage of the asymptotic temperature increase (also relative to virgin temperature) is indicated between brackets.

An alternative way of presenting the advance of the temperature front is given in Figure 2.28, where the temperature distribution in function of the distance is depicted for different points in time, while the tunnel wall is kept at a constant temperature of 80 °C.

Height above repository	**Virgin Temperature °C**	**30 years °C**	**100 years °C**	**300 years °C**	**Asymptotic Temperature °C**
10 m	24,70	34,0 (76 %)	38,7 (87%)	41,1 (92%)	69,2
25 m	24,25	18,8 (45%)	28,2 (68%)	33,7 (81%)	65,6
50 m	23,50	5,1 (14%)	15,6 (41%)	24,1 (64%)	61,4

Table 2.8: Temperature evolution at various heights above the repository for a tunnel at 80°C. [Percentages refer to the increase, relative to virgin temperature]

In the Belgian context, the maximum temperature increase at the top of the clay layer, about 50 m above a possible repository, should not be more than 4°C [F. Bernier, 1998]. Such a rise in temperature would be attained after a period of 25 years for tunnels kept at a constant temperature of 80°C, after 35 years for tunnels kept at a constant temperature of 60°C, and after 90 years for tunnels at a temperature of 40°C.
If the distance in between the secondary galleries and in between the tertiary galleries in which the HLW is stored would be increased from 50 m to 100 m, and if the tunnel diameter would at the same time be decreased from 3,2 to 1,2 m, the period required to obtain a temperature rise of 4°C would increase to 40 years (instead of 25 years) for tunnels at a temperature of 80°C, to 65 years (instead of 35 years) for tunnels at a temperature of 60°C and to 550 years (instead of 90 years) for tunnels at a temperature of 40 °C.

The heat generation decreases with about 50% over a period of 30 years. Ninety years after being stored underground it has fallen back to about 25% of the power that was being generated at the time of storage. The relation between the heat generation and the temperature of the tunnel wall has not

been calculated, but the temperature distribution 50 m above the repository in function of the time for tunnels being kept at a constant temperature is given in Figure 2.29. To calculate the temperature of the tunnel wall in function of the time, taking account of the heat being generated in the canisters. This would also require a detailed knowledge of the backfill and lining material.

2.4.5 Discussion of results, temperature effect

Although the exact temperature variation in function of the time of the combination heat generating waste, canister, backfill material and lining is not known, some usefull conclusions can be derived.

First of all, a three dimensional approach is essential to study this problem. It has been shown that the number of heat sources stored influences the temperature distribution significantly. Even with a regular grid, the geometry is too complex to solve the problem analytically. The boundary element method provides however a useful tool for the analyses.

In the vicinity of the tunnel, the temperature increases fast. For example 10 m above the repository the temperature increases by about 30° during the first 10 years. This temperature increase has an effect on the behaviour of the clay: on the one hand, the material characteristics change, and on the other hand, the pore water pressure and the effective stresses change. For both aspects, detailed further research is required to gain a better understanding of the phenomena involved and to quantify more accurately the effect of the temperature increase.

If one would use as prerequisite a maximum increase of 4° at the top of the clay layer (50 m above the storage level), all simulations indicate that it is unlikely to satisfy this condition with a 50 m x 50 m pattern. A larger spatial distribution of the heat generating canisters could be a solution. Further study is required to determine whether a doubling of the distance between galleries (area multiplied by a factor 4) would result in a temperature distribution, conform with the plus 4° prerequisite. Making the centre distance between galleries larger has not only a direct effect on the economics, but also on the mining and storing operations. These operations become less efficient, as for example the total tunnel length to be ventilated and the transport distances would increase.
Another solution would be combining both types of high level radioactive waste (heat generating and not heat generating waste) in the same mining zone (e.g. alternatively, placing a warm and cold canister). The mining operation would remain similar, but the number of heat sources per area decreases. An important disadvantage, however, is that both zones are not segregrated anymore. This is one of the conditions suggested to make the waste more easily retrievable. Therefore, combining both zones is not further considered.
A solution to the problem of high temperature in the rock mass, would be the storage of the heat generating waste for a longer time period on the surface. This solution could fit in the global strategy of retrievable waste without too many consequences.

As the choice of the ideal centre distance for the zone containing the heat generating high level waste requires further research and more detailed calculations, it is suggested to consider centredistances of 50 m between adjacent galleries as acceptable. This scheme is then also used for further planning and calculations of the mining operations. At least, with a grid of 50 m x 50 m, two prerequisites linked to the requirement of retrievability are fulfilled, namely that each canister can be accessed

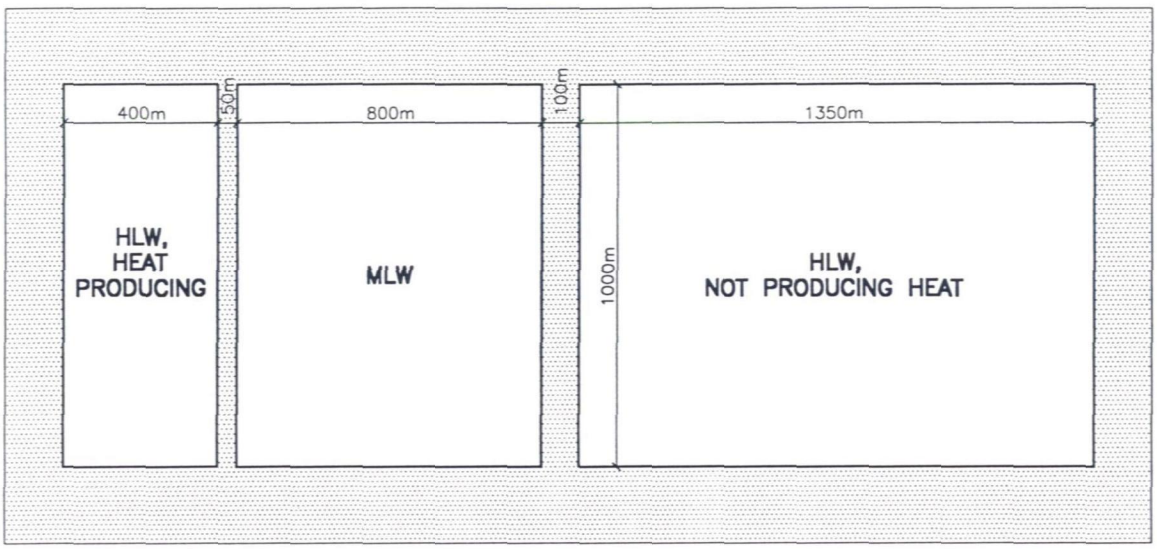

Figure 2.1.a: View of three separated zones (horizontal plane)

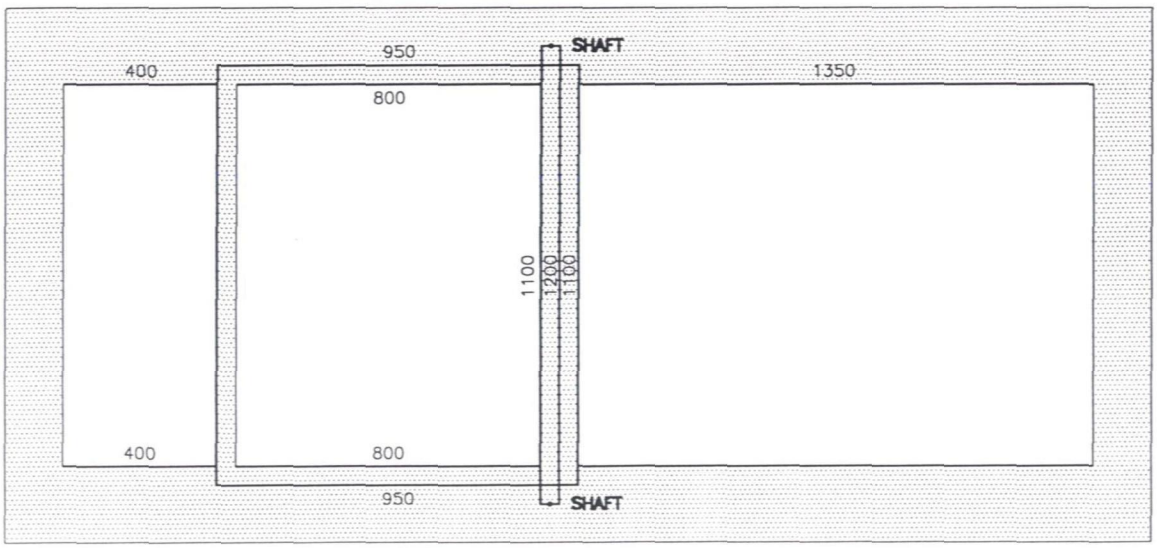

Figure 2.1.b: Primary galleries (horizontal plane)

individually and that the three types of waste (heat generating high level, not heat generating high level and low/middel level) are stored in three different mining zones. However, it is advised to consider a long cooling period of the waste in surface facilities. Only more complex calculations and a better knowledge of the temperature variation of a canister surrounded by backfill and a clay mass can assist in an accurate estimate of the required cooling period in a surface storage facility.

2.5 Layout, discussion

Based on the general layout principles (paragraph 2.1), on the results of the hydromechanical simulations (paragraph 2.3) and partly on the considerations formulated following the temperature calculations (paragraph 2.4), two basic grid sizes are suggested for further planning operations. For the waste that does not generate heat (high and low/middle radioactive waste), a rectangular pattern is applied with centre distances of 50 m for the secondary galleries and of 40 m for the tertiary galleries. For the heat generating high radioactive waste a square pattern is applied with centre distances of 50 m for the secondary and tertiary galleries.

For the high level waste (both types), each canister is individually accessible via the secondary galleries. For the heat generating high level waste, 300 canisters have to be stored. This could be realised by a grid of 16 x 19 = 304 storage points (see Figure 2.1.d). For the high level waste not generating heat, 1260 drums have to stored. A grid of 54 x 24 = 1296 fullfills this requirement.
The middle and low radioactive waste is stored in a different way. As explained above, for this type of waste the constraint of retrievability is not imposed and, hence, the drums may be stacked on top of each other. In total 52508 drums of 200 l and 3780 drums bigger than 1 m^3 have to be stored. It has been calculated that 16 secondary galleries and 24 tertiary galleries would suffice for that purpose (see Figure 2.1.d).

A mine plan at a scale of 1/2500 representing this layout is added to this report. The further mine planning, presented in chapter 3, is based on this plan.

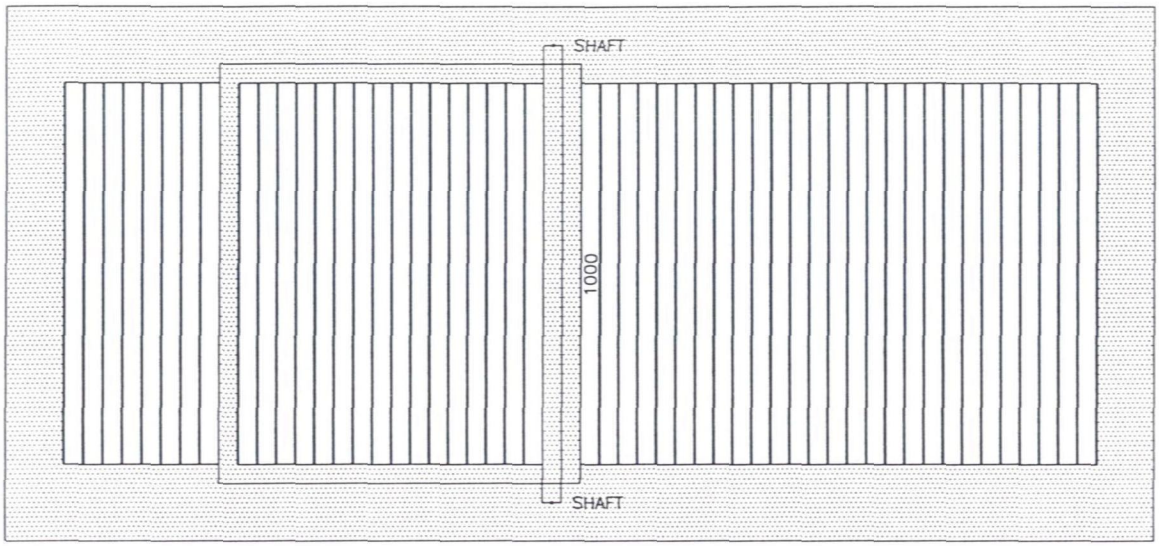

2.1.c: Secondary galleries (horizontal plane)

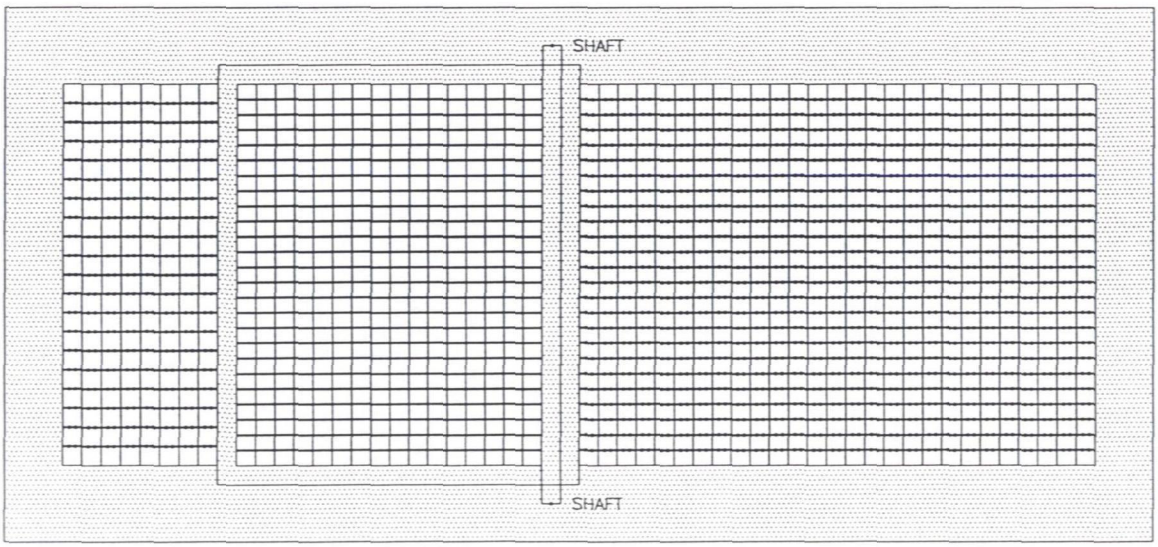

Figure 2.1.d: Tertiary or waste storage galleries (horizontal plane)

Figure 2.1: Mine layout of waste disposal

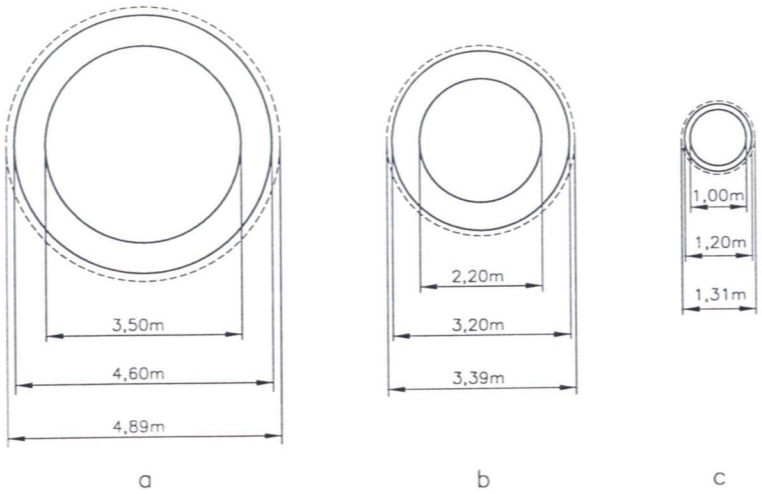

Figure 2.2: Cross-section and dimensions of a) primary and secondary gallery, b) tertiary gallery and c) alternative for tertiary gallery

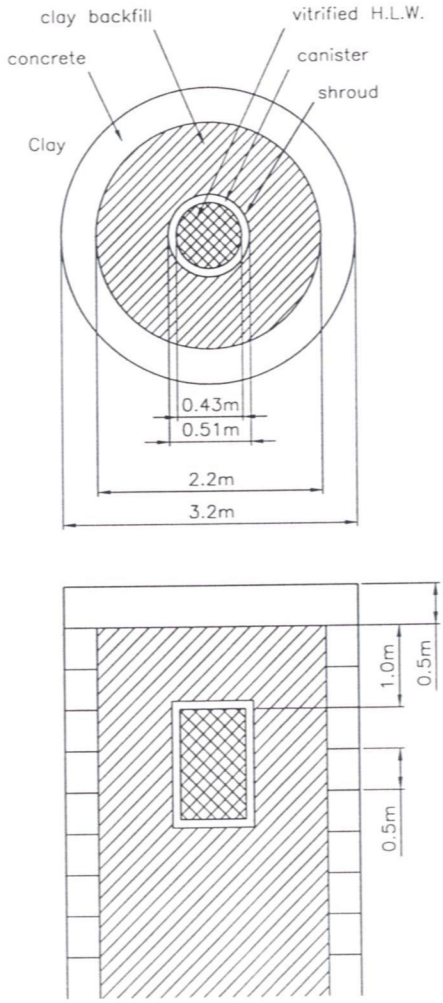

Figure 2.3: Position of the high level waste canister in the tertiary gallery

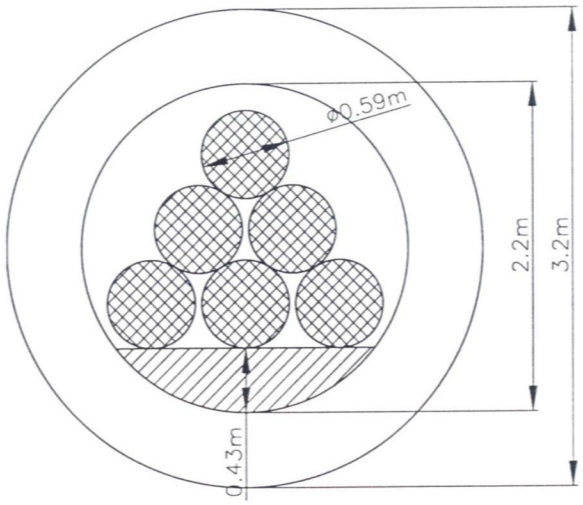

Figure 2.4: Storage drums containing middle and low level waste

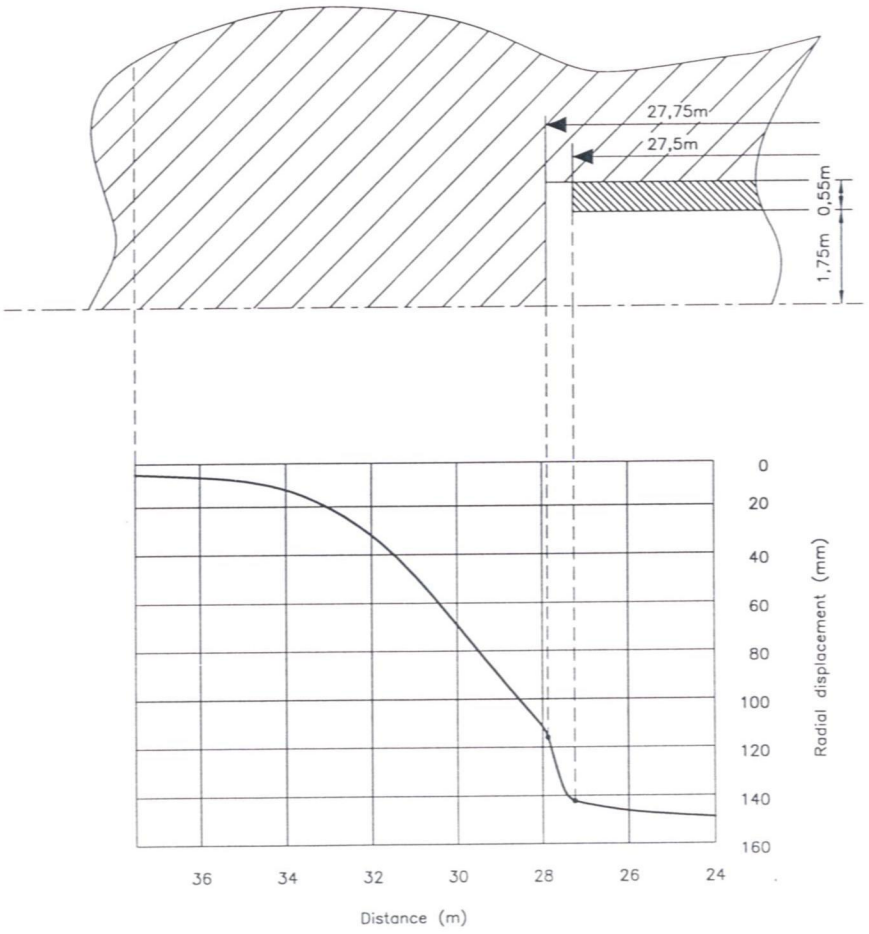

Figure 2.5: Convergence of the tunnel. Based on an axisymmetric model

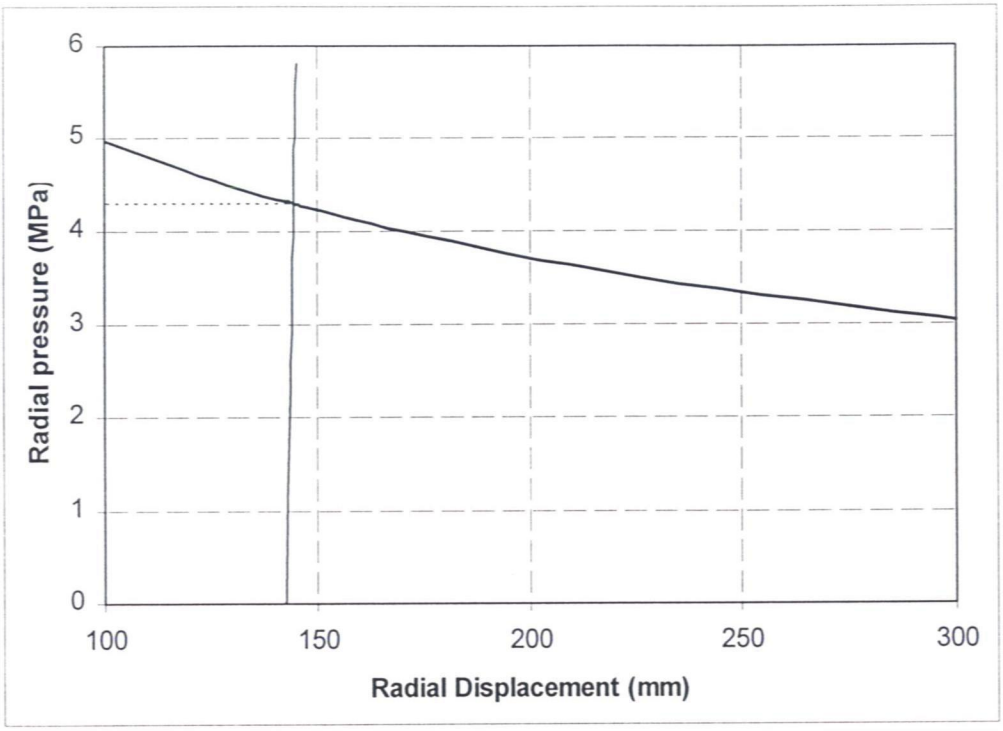

Figure 2.6.a: Convergence-confinement curve: convergence curve for single tunnel; confinement curve for concrete support

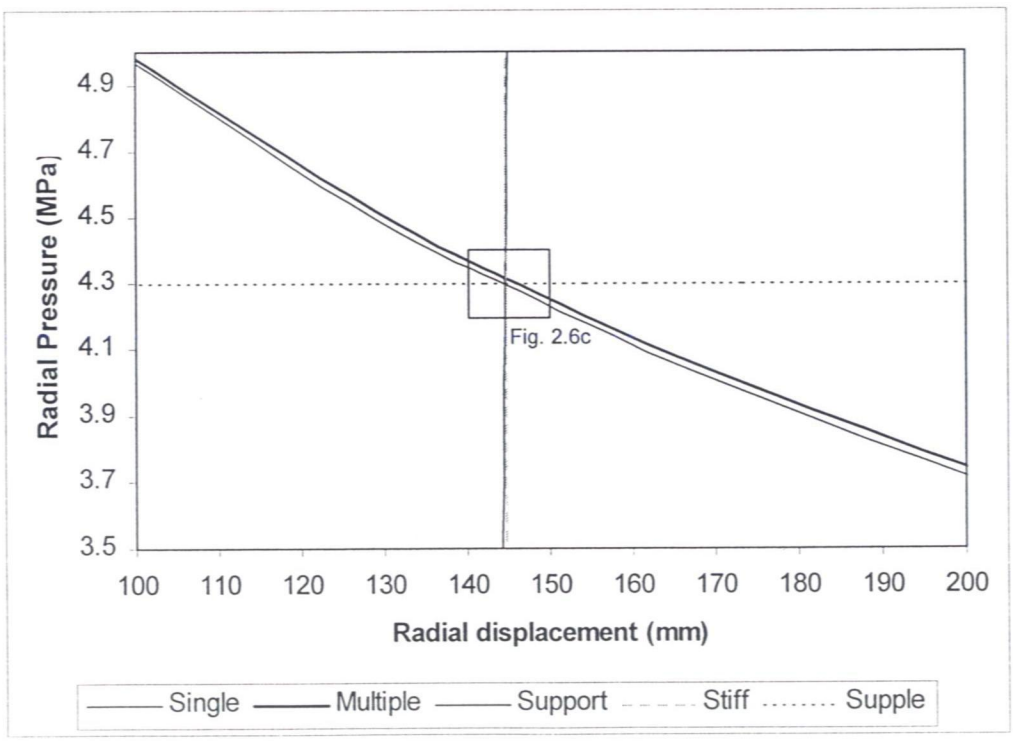

Figure 2.6.b: Convergence curve for single tunnel and for a tunnel surrounded by other tunnels with the support characteristic if the concrete support, an infinitely still support and a support with zero stiffness

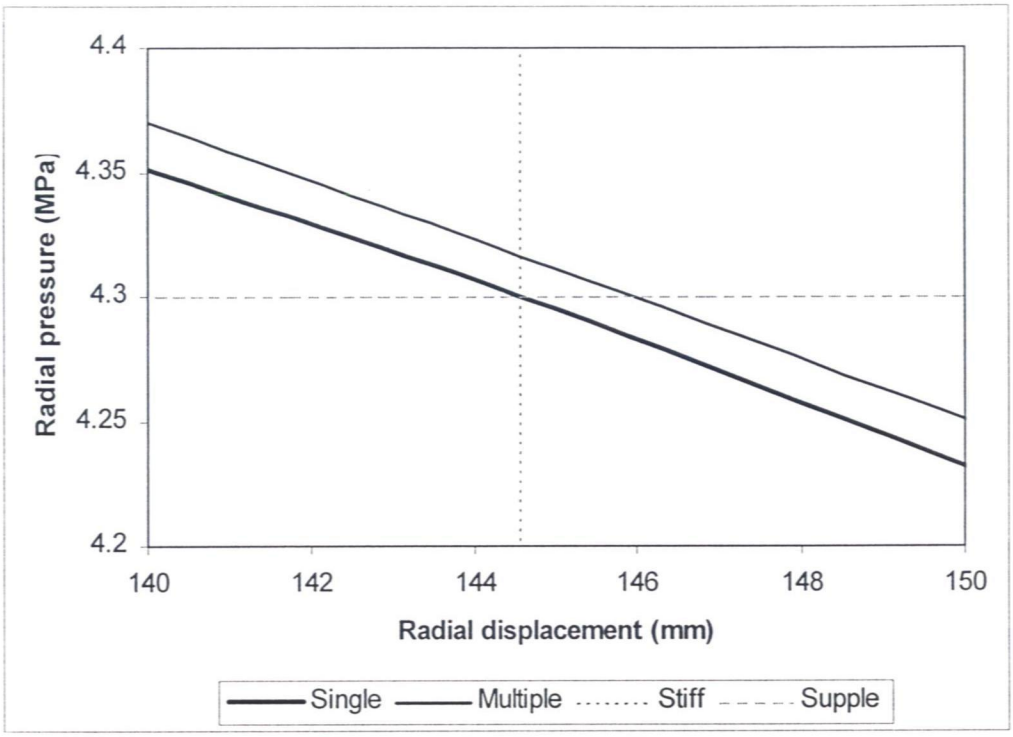

Figure 2.6.c: Detail of Figure 2.6.b [The concrete support characteristic is omitted]

Figure 2.6: Convergence-confinement curves

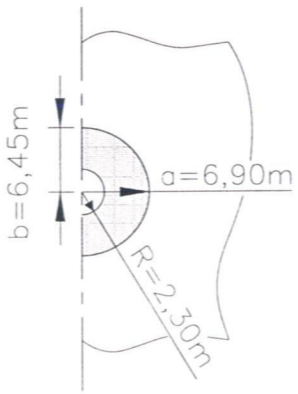

Figure 2.7: Extent of the plastic zone around one tunnel surrounded by an infinite number of parallel tunnels

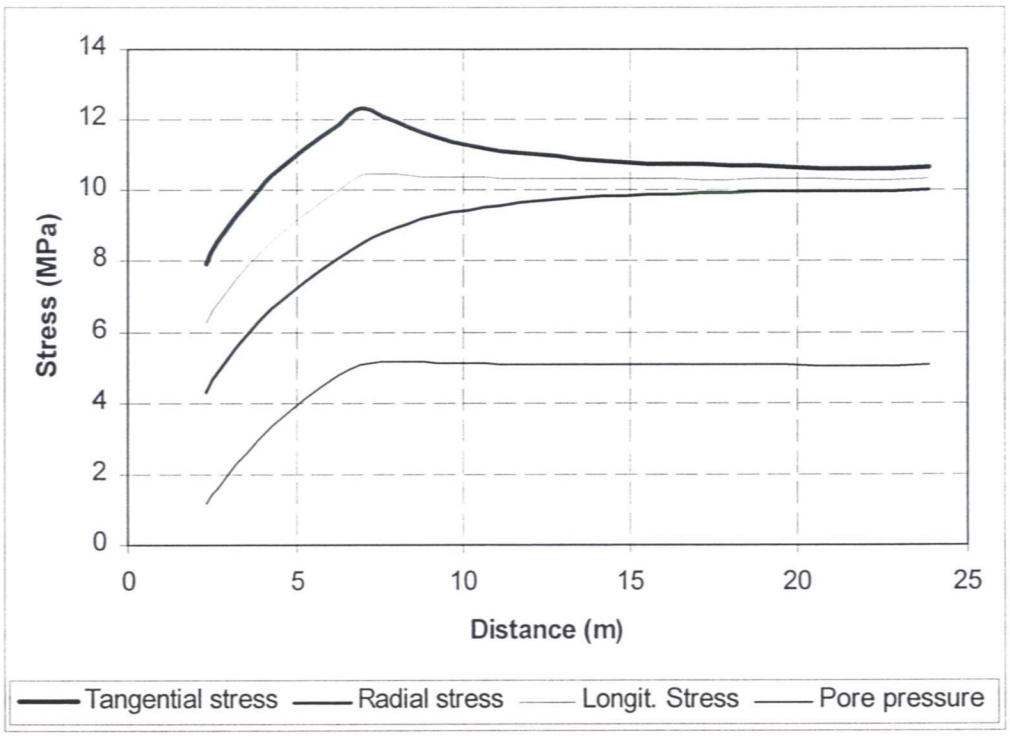

Figure 2.8.a: Along horizontal centre line

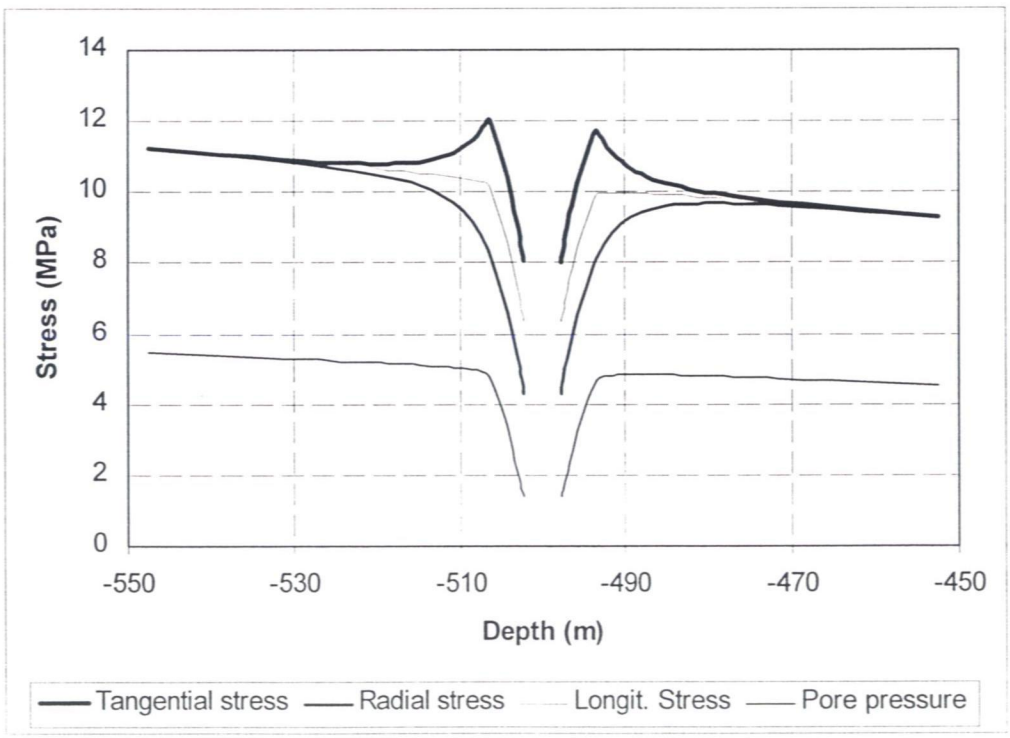

Figure 2.8.b: Along vertical centre line

Figure 2.8: Total stress components and pore pressure (excavation period)

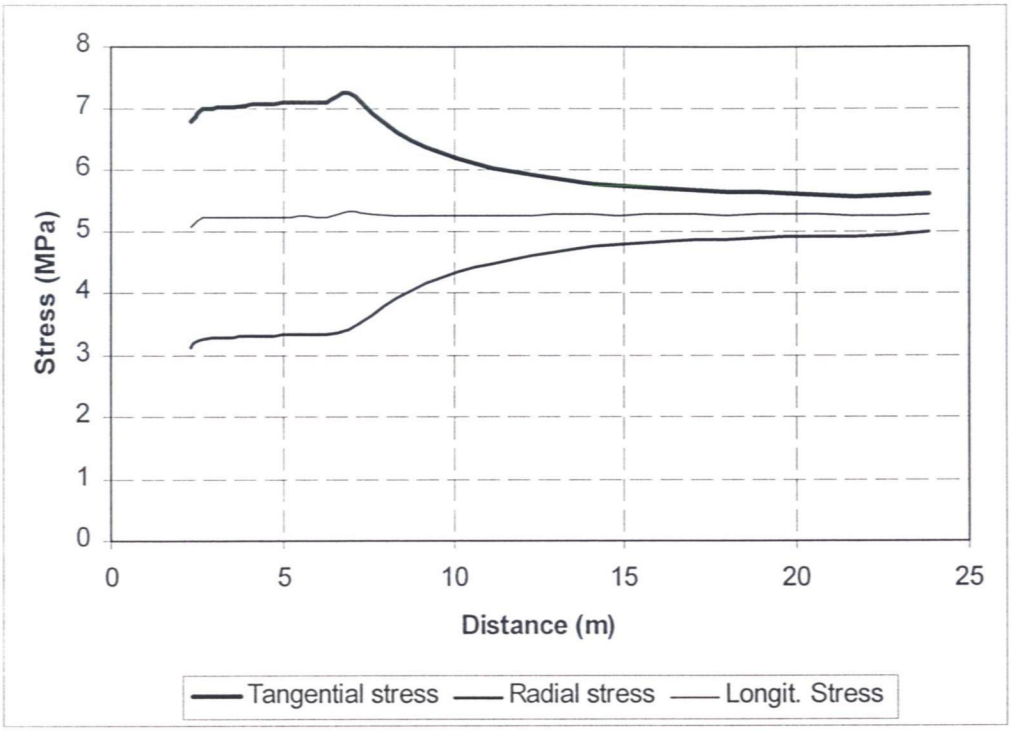

Figure 2.9.a: Along horizontal centre line

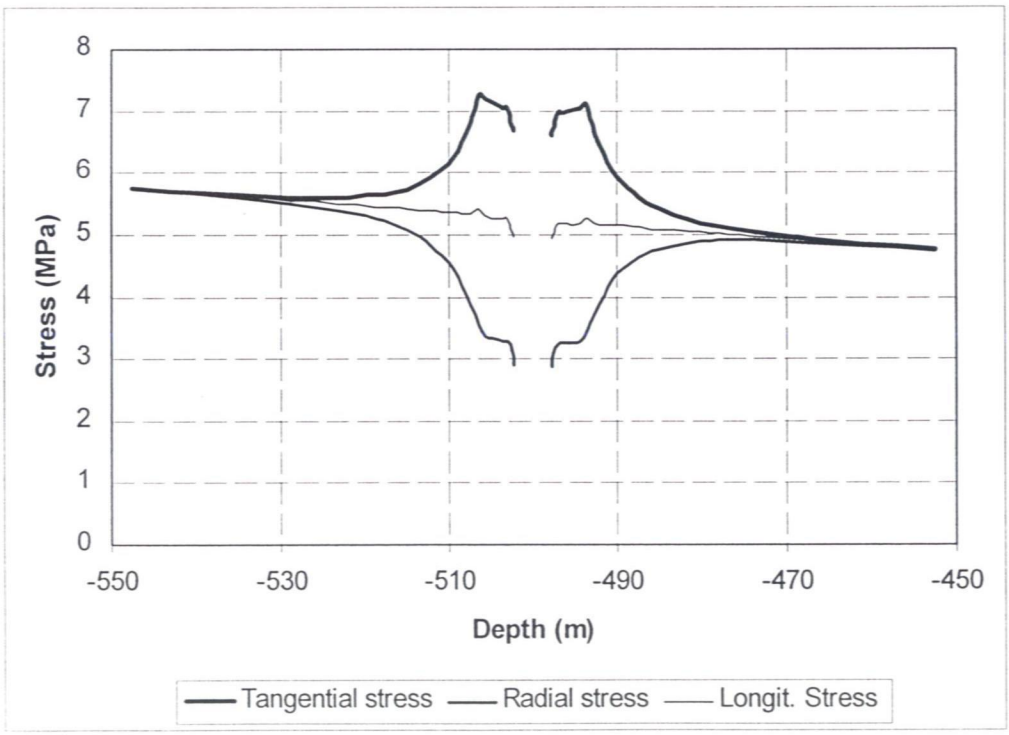

Figure 2.9.b: Along vertical centre line

Figure 2.9: Effective stress components and pore pressure (excavation period)

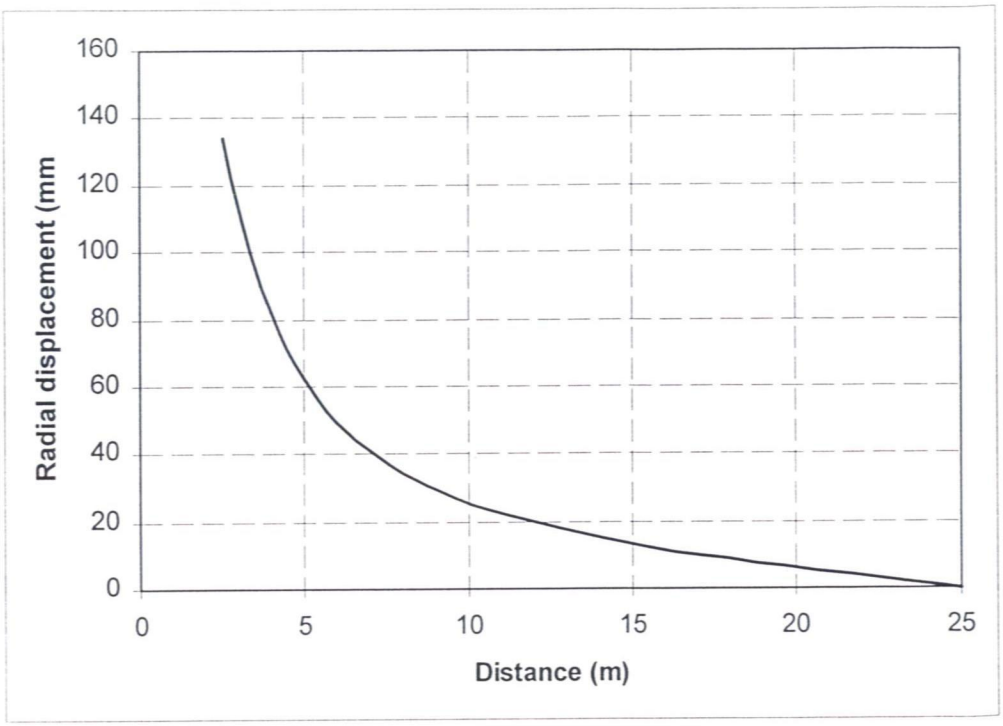

Figure 2.10.a: Along horizontal centre line

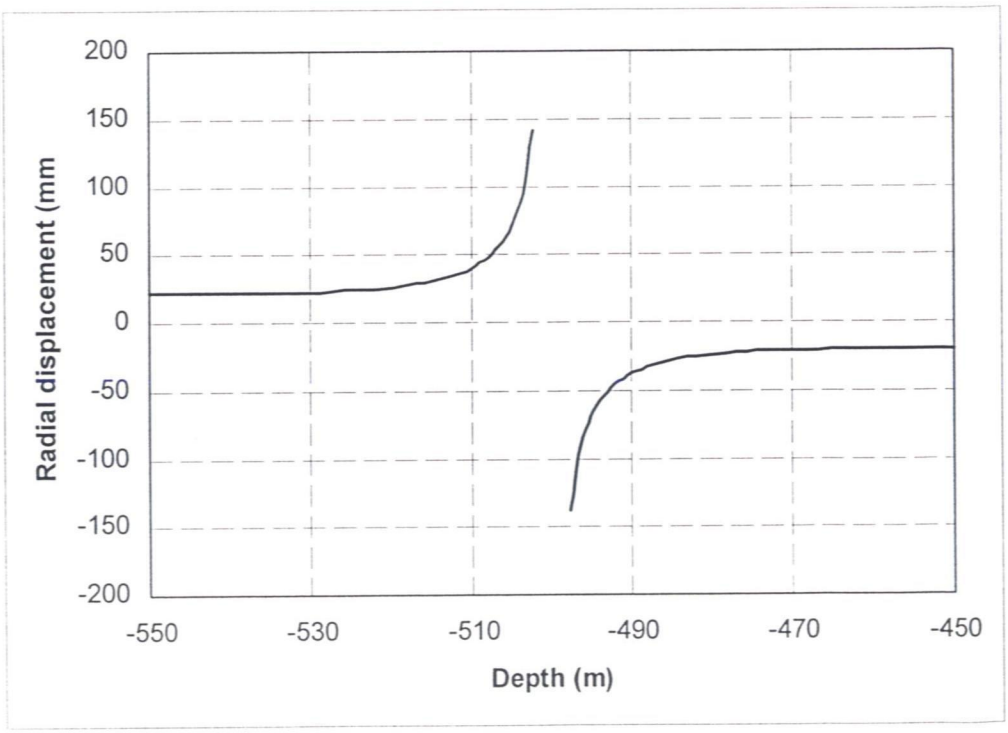

Figure 2.10.b: Along vertical centre line

Figure 2.10: Radial displacement (excavation period)

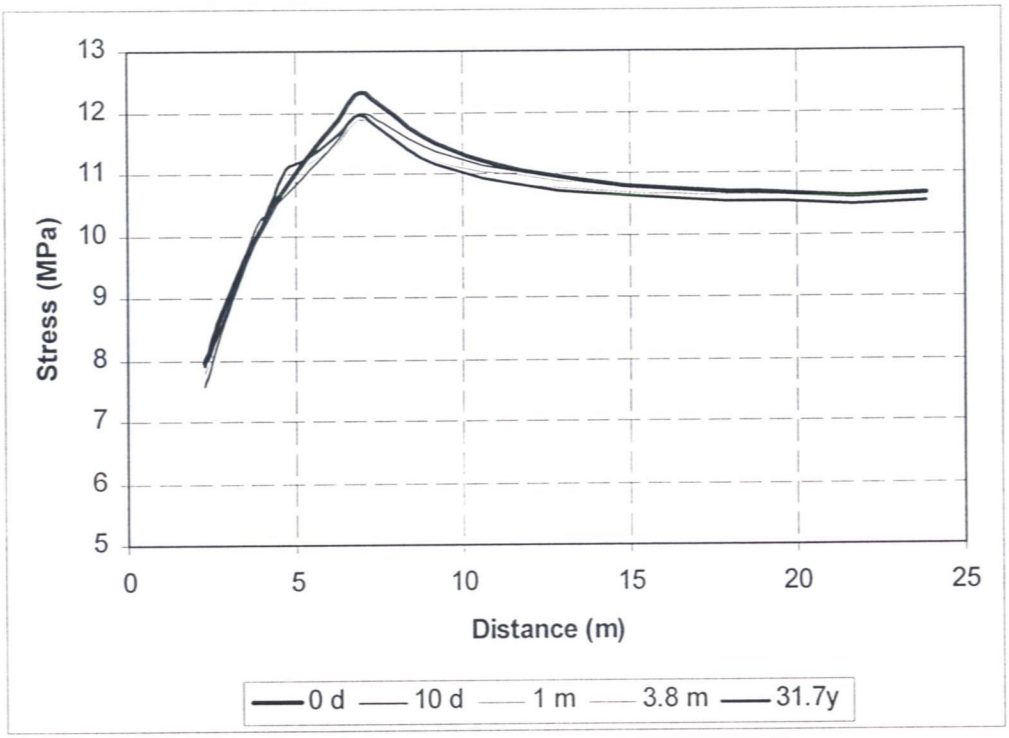

Figure 2.11.a: Total tangential stress

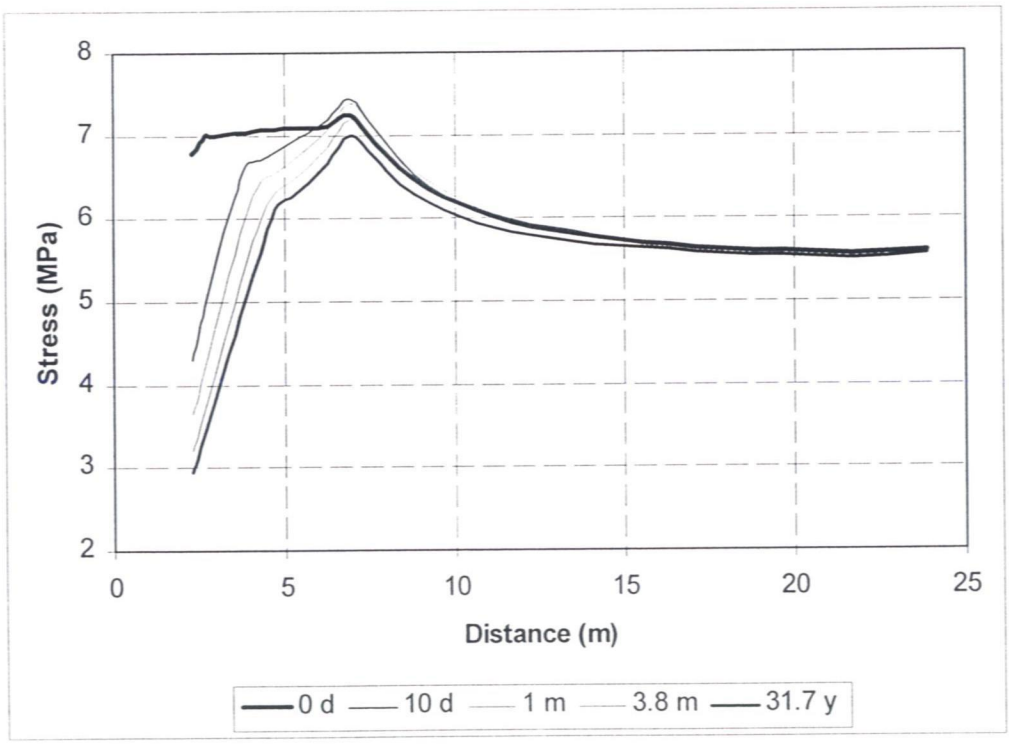

Figure 2.11.b: Effective tangential stress

Figure 2.11: Tangential stress component along horizontal centre line (evolution over time with an impermeable lining)

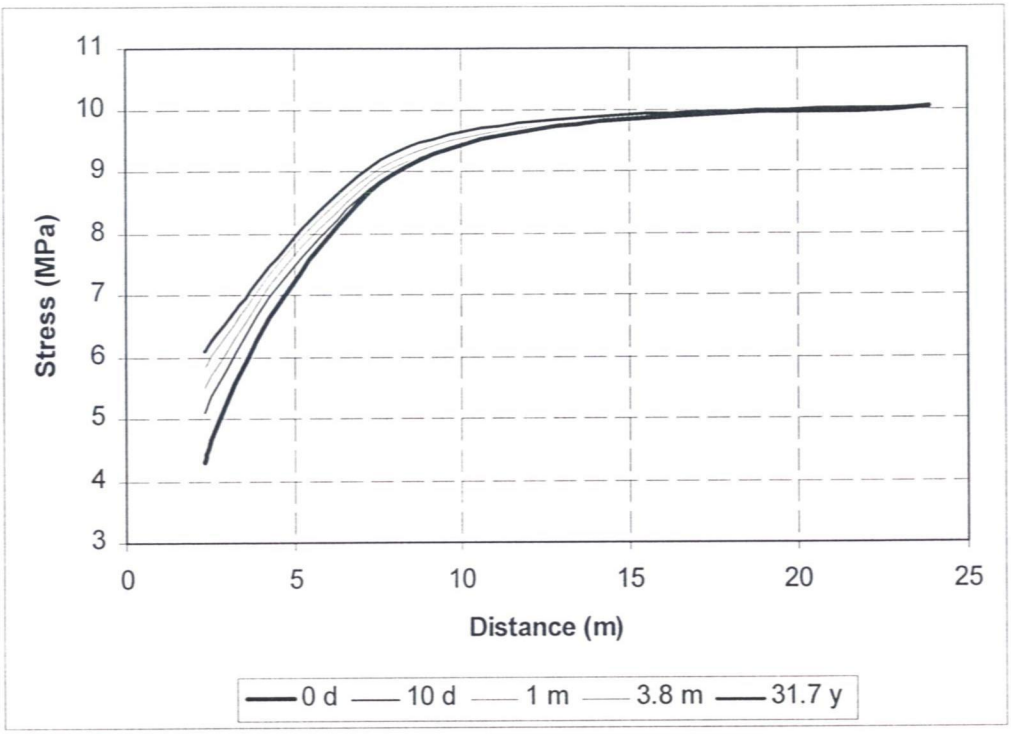

Figure 2.12.a: Total radial stress

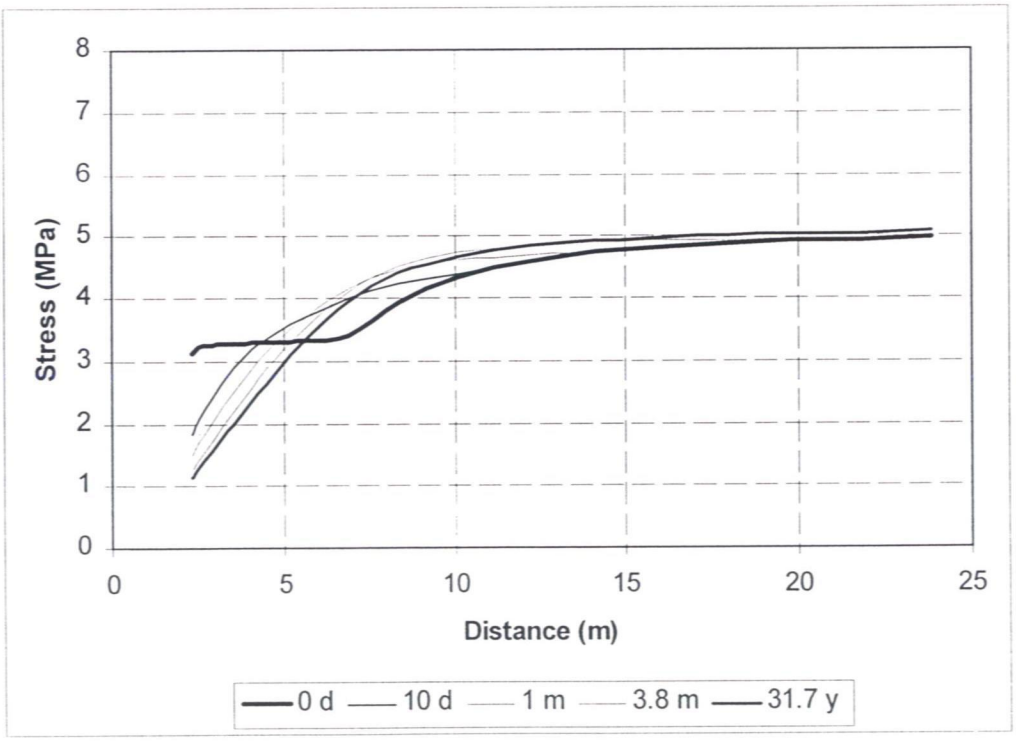

Figure 2.12.b: Effective radial stress

Figure 2.12: Radial stress component along horizontal centre line (evolution over time with an impermeable lining)

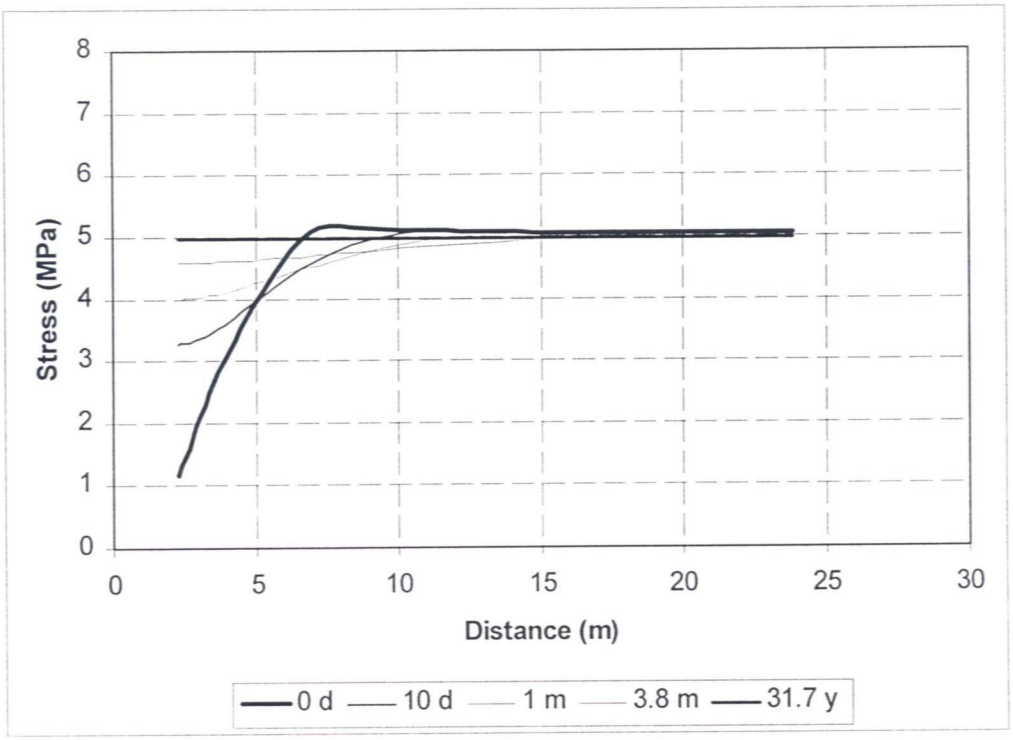

Figure 2.13: Pore water pressure along horizontal centre line (evolution over time with an impermeable lining)

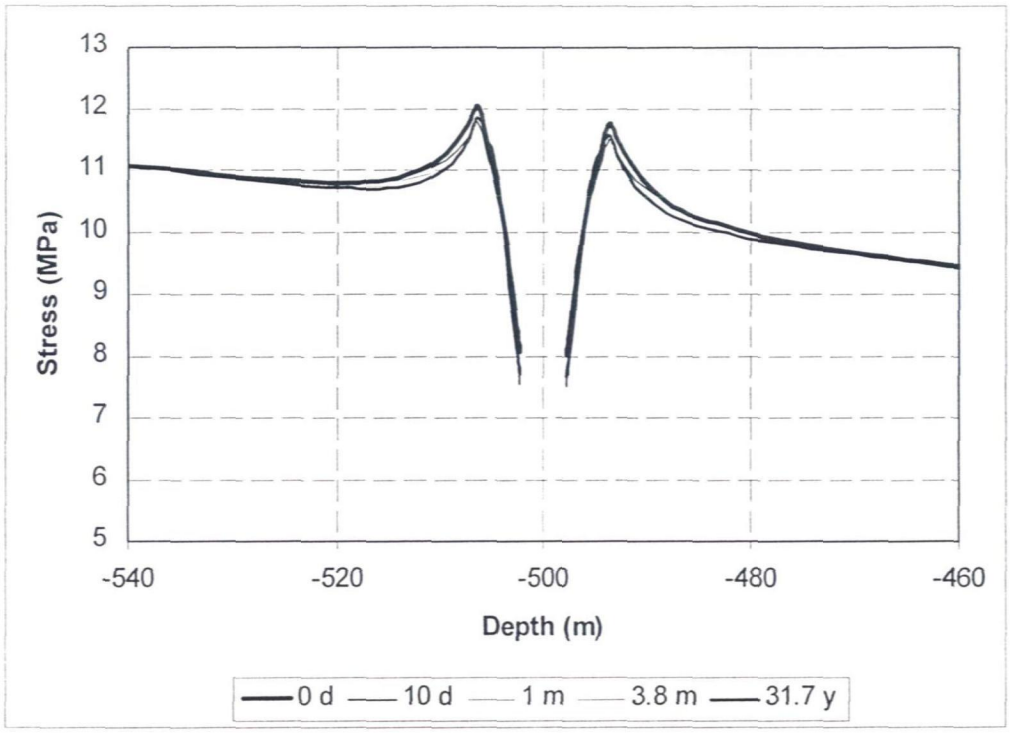

Figure 2.14.a: Total tangential stress

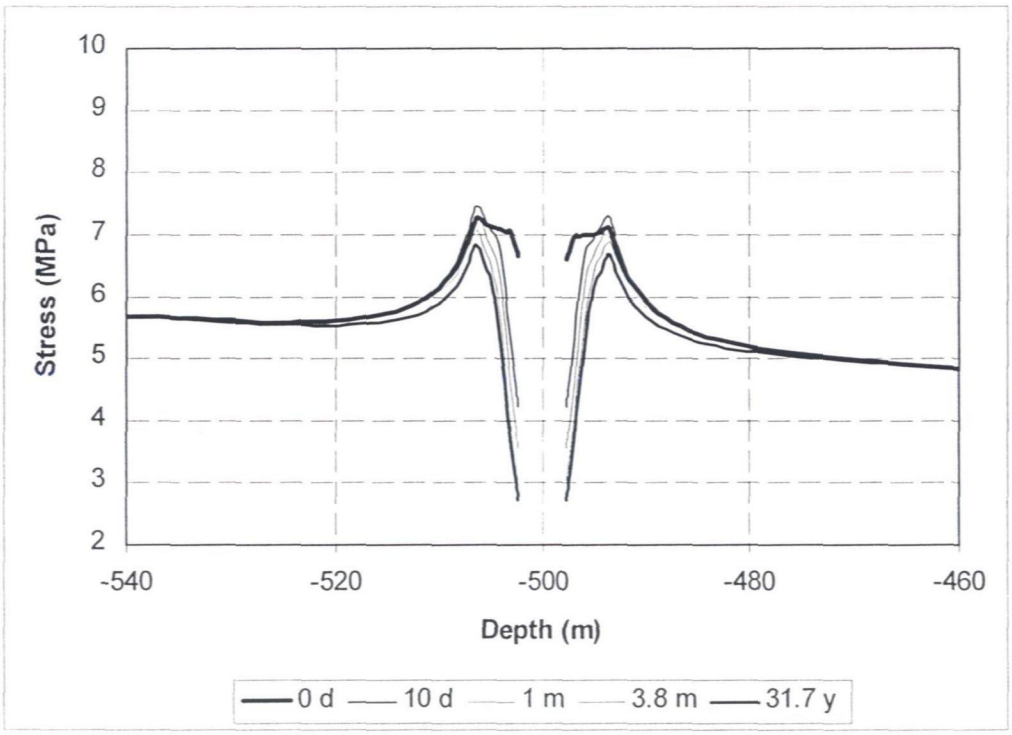

Figure 2.14.b: Effective tangential stress

Figure 2.14: Tangential stress component along vertical centre line (evolution over time with an impermeable lining)

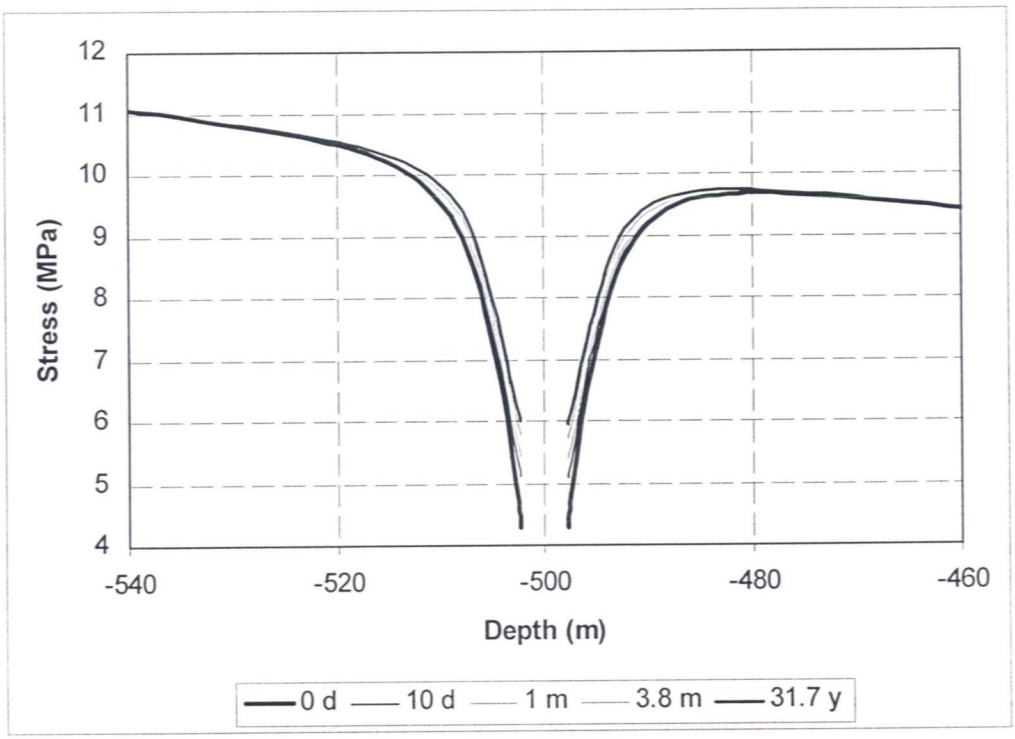

Figure 2.15.a: Total radial stress

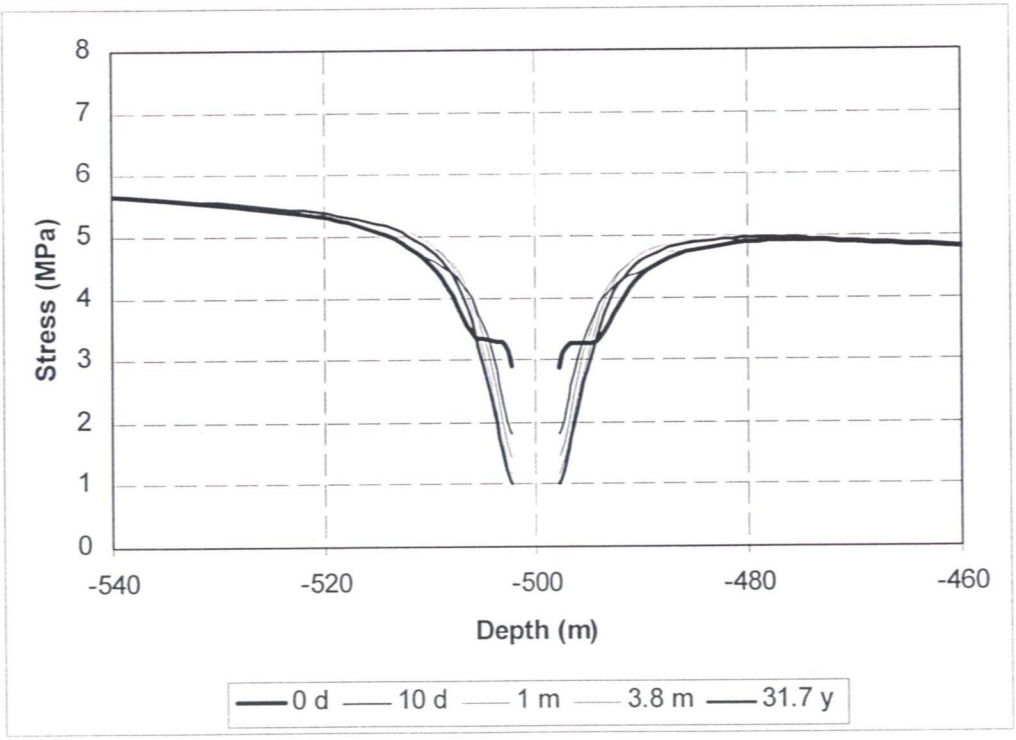

Figure 2.15.b: Effective radial stress

Figure 2.15: Radial stress component along vertical centre line (evolution over time with an impermeable lining)

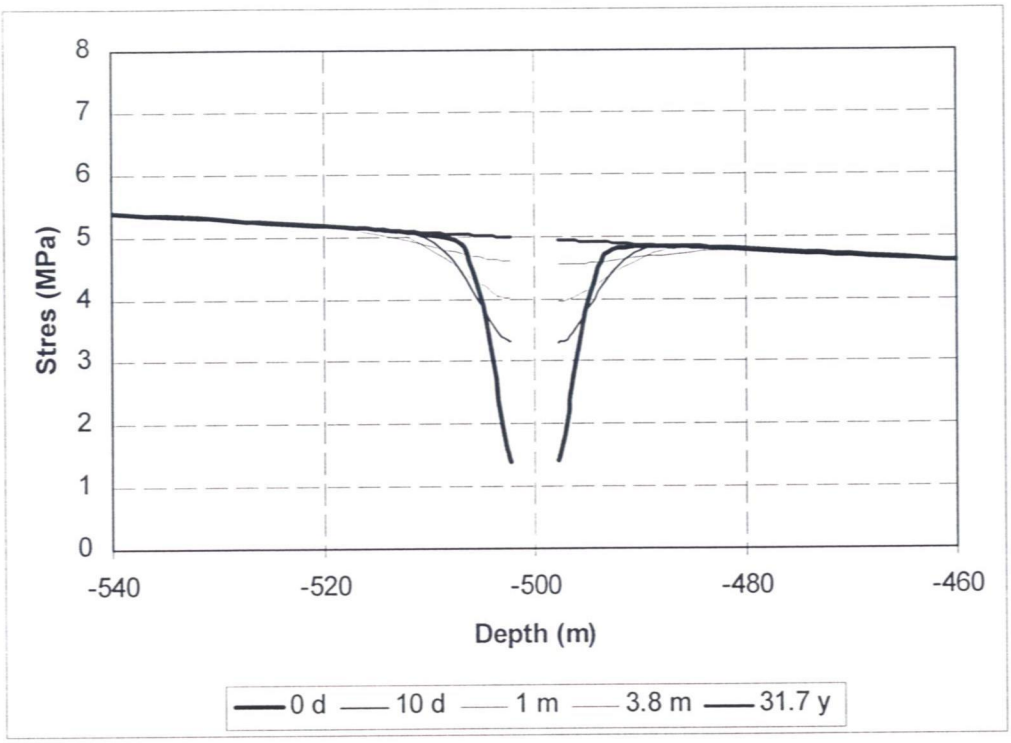

Figure 2.16: Pore water pressure along vertical centre line (evolution over time with an impermeable lining)

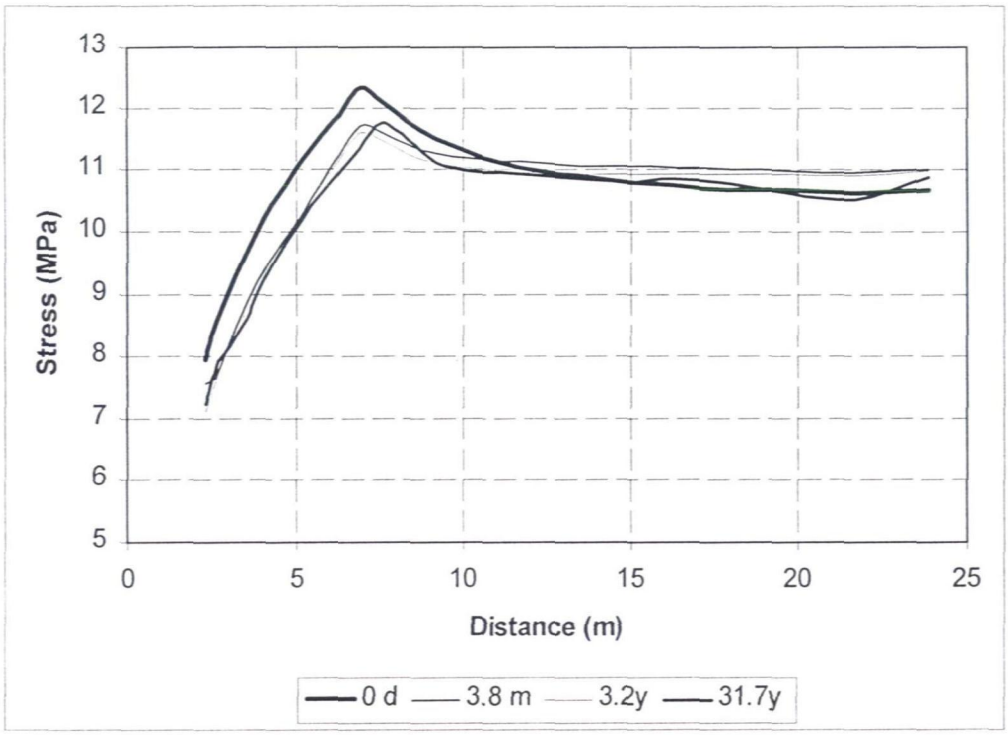

Figure 2.17.a: Total tangential stress

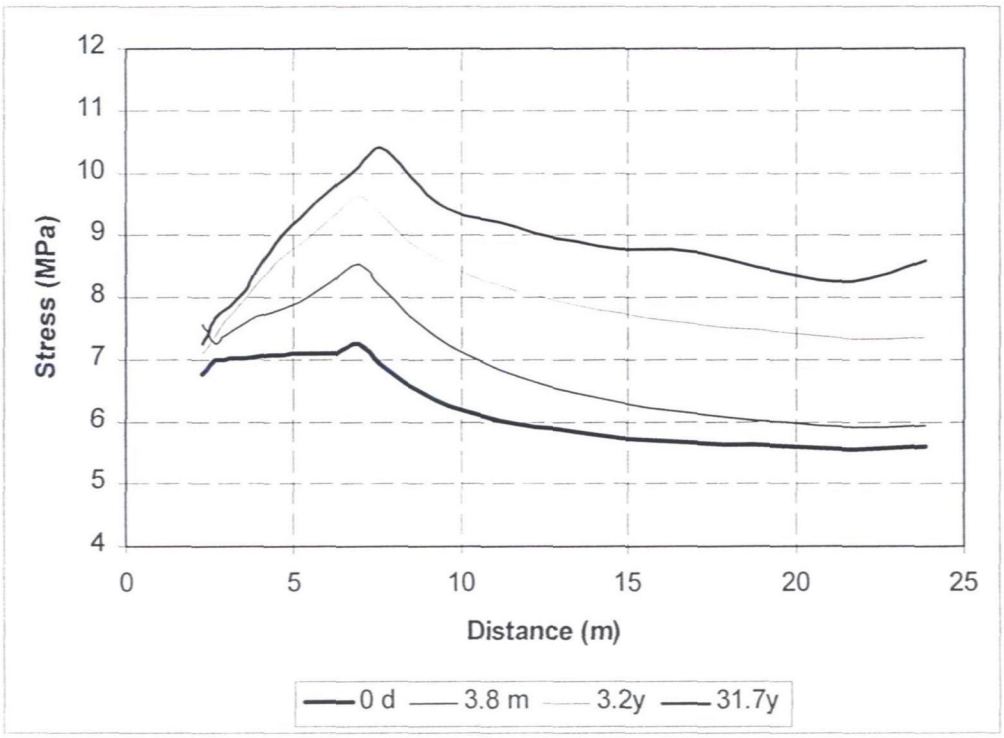

Figure 2.17.b: Effective tangential stress

Figure 2.17: Tangential stress component along horizontal centre line (evolution over time with a permeable lining)

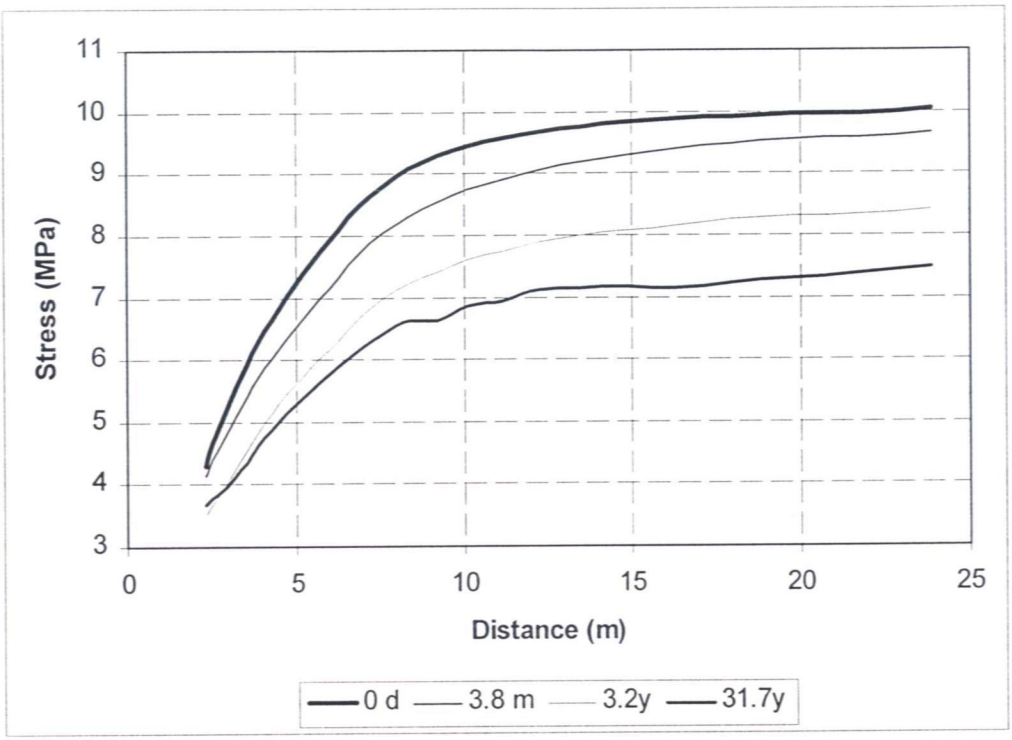

Figure 2.18.a: Total radial stress

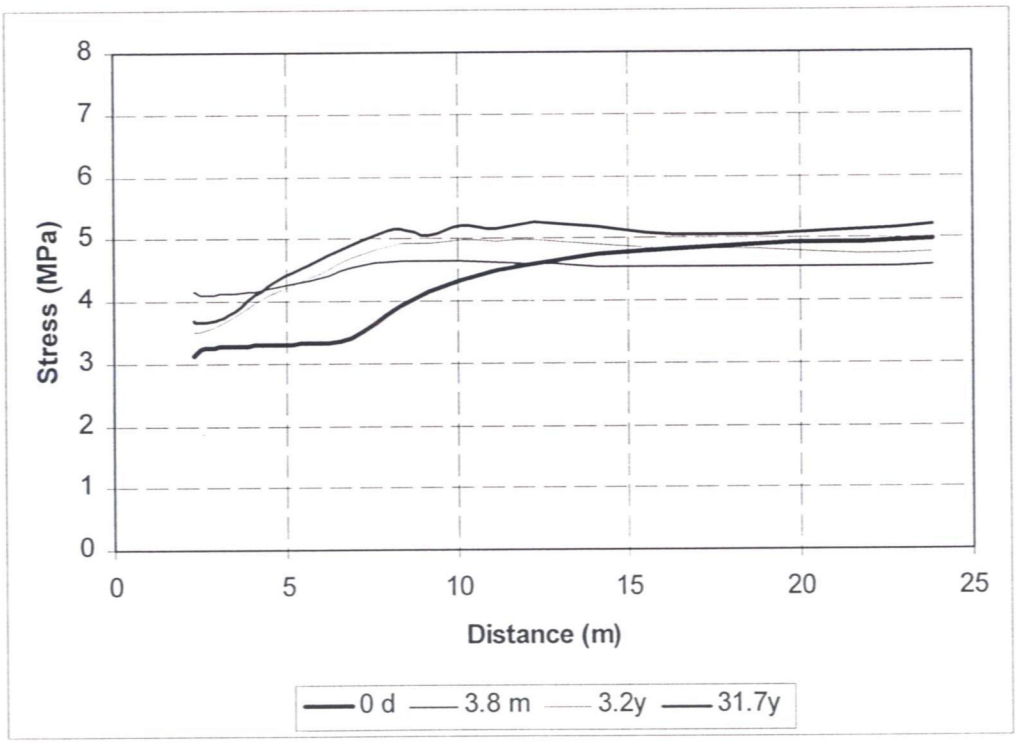

Figure 2.18.b: Effective radial stress

Figure 2.18: Radial stress component along horizontal centre line (evolution over time with a permeable lining)

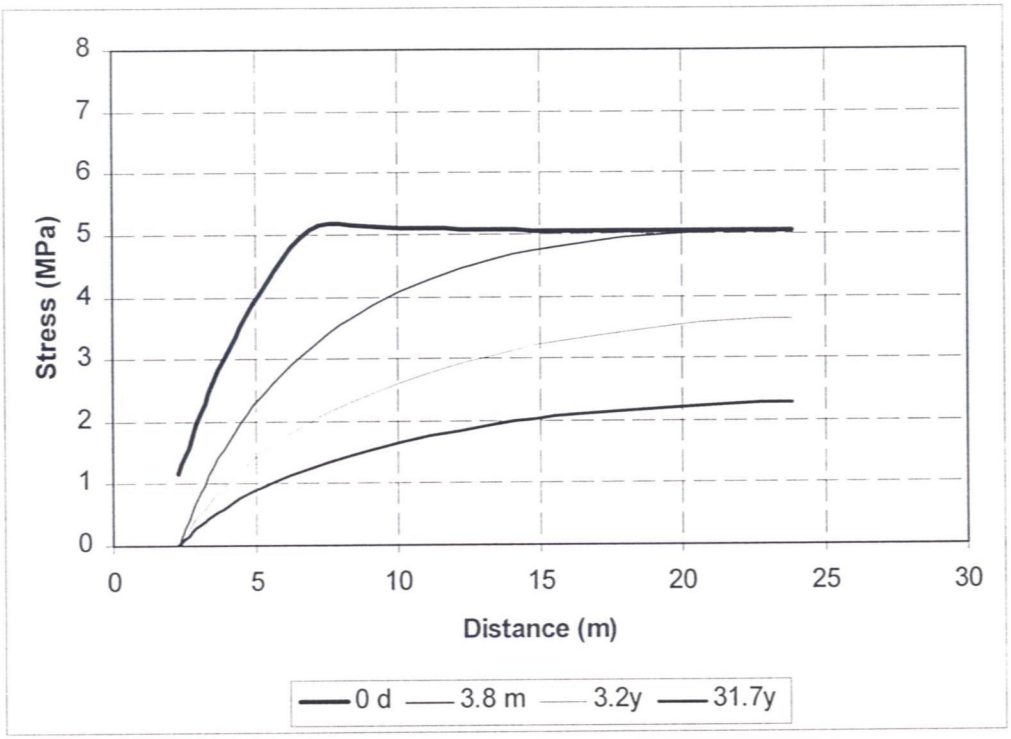

Figure 2.19: Pore water pressure along horizontal centre line (evolution over time with a permeable lining)

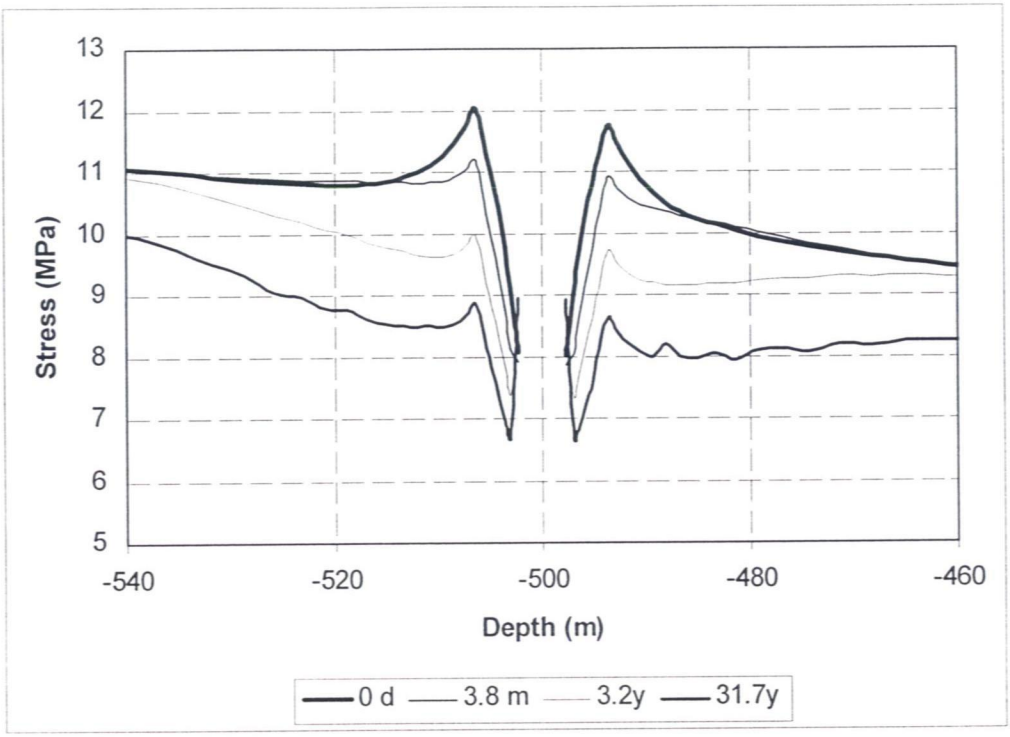

Figure 2.20.a: Total tangential stress

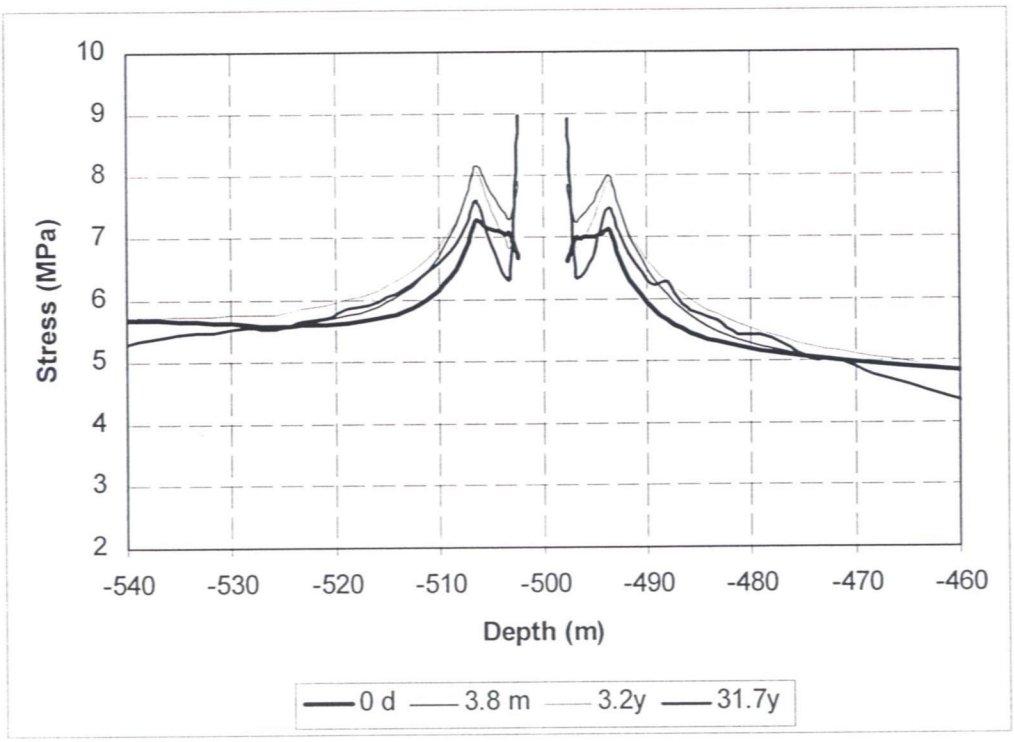

Figure 2.20.b: Effective tangential stress

Figure 2.20: Tangential stress component along vertical centre line (evolution over time with a permeable lining)

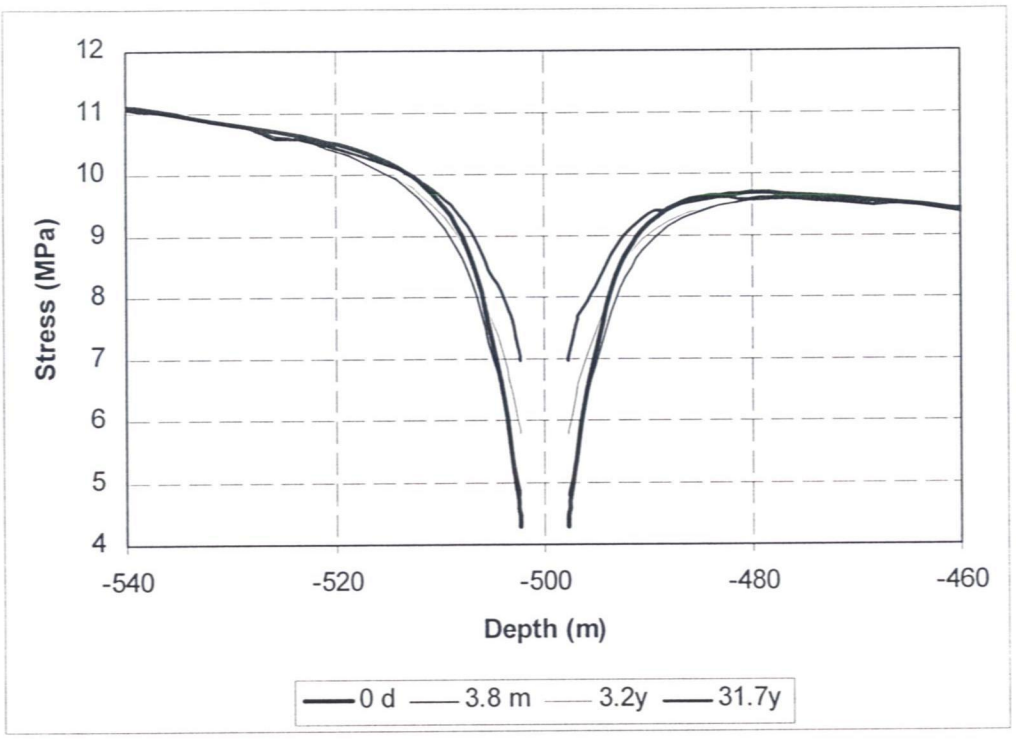

Figure 2.21.a: Total radial stress

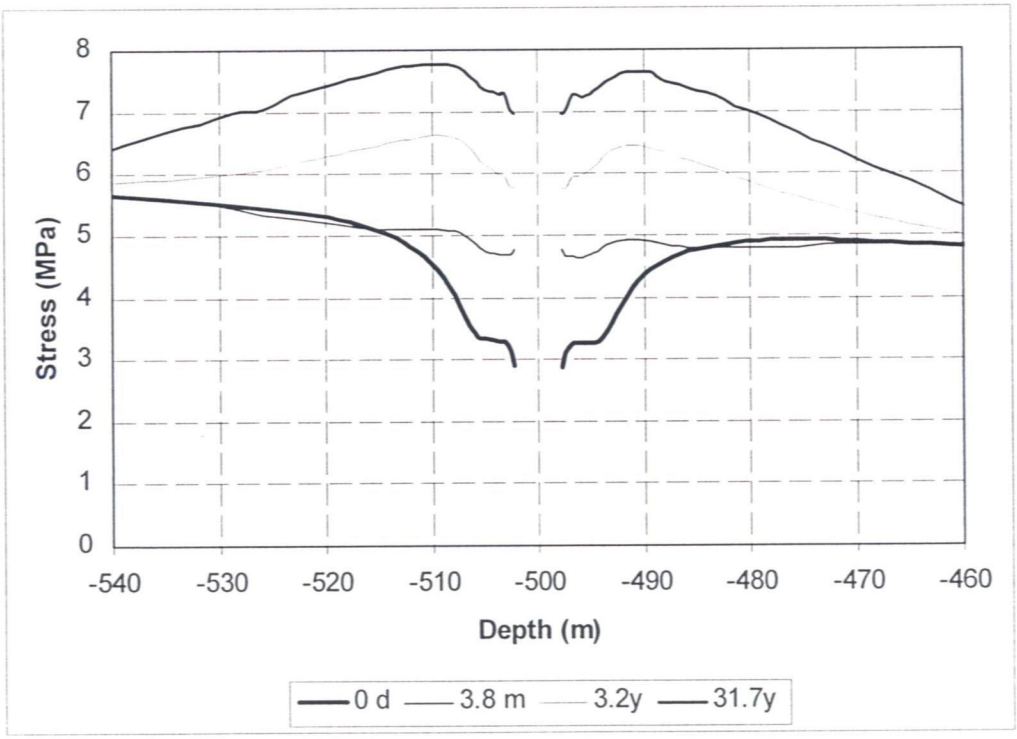

Figure 2.21.b: Effective radial stress

Figure 2.21: Radial stress component along vertical centre line (evolution over time with a permeable lining)

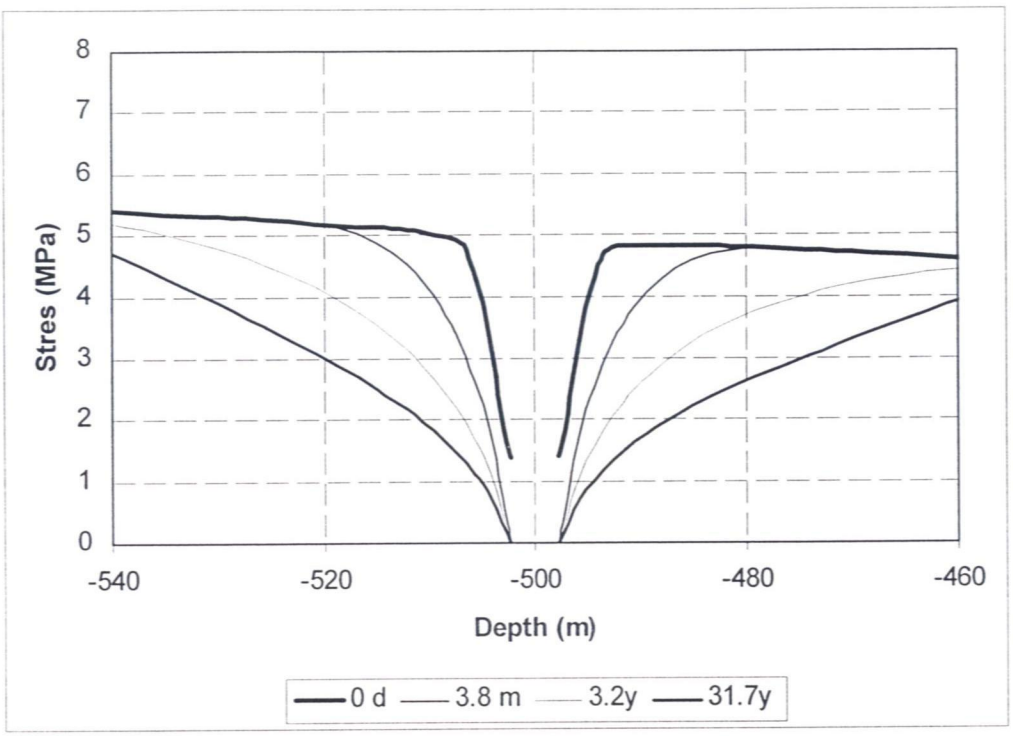

Figure 2.22: Pore water pressure along vertical centre line (evolution over time with a permeable lining)

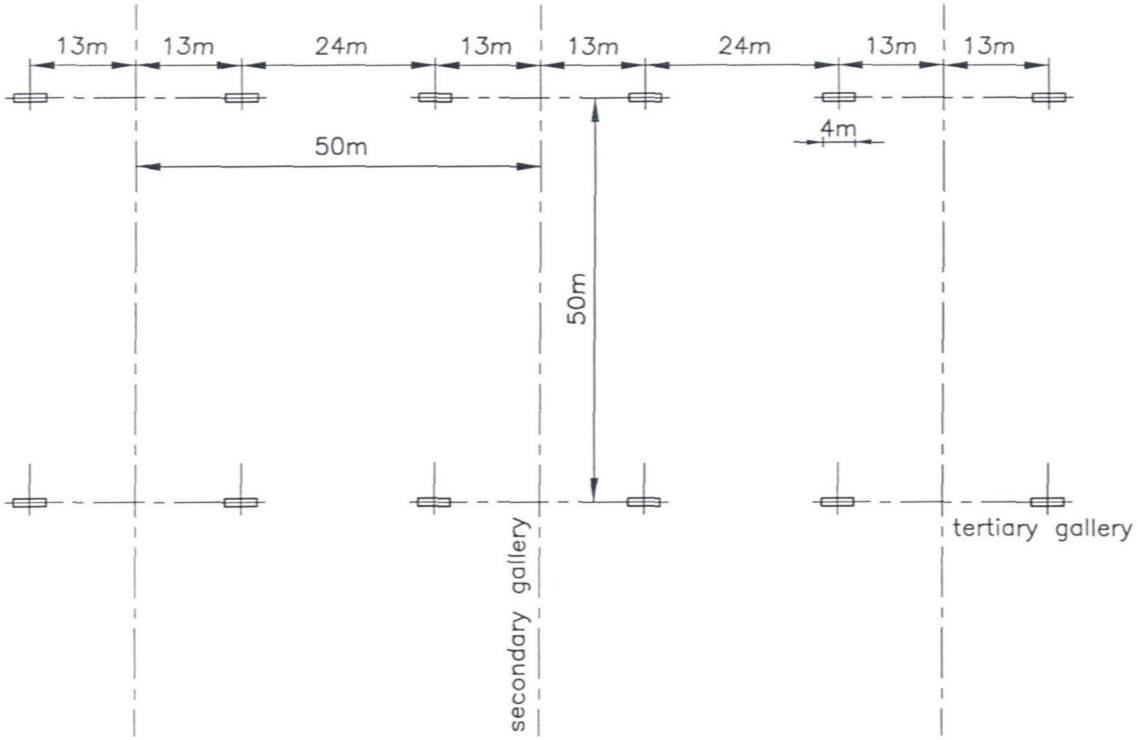

Figure 2.23.a: Basic grid pattern of 50 m x 50 m

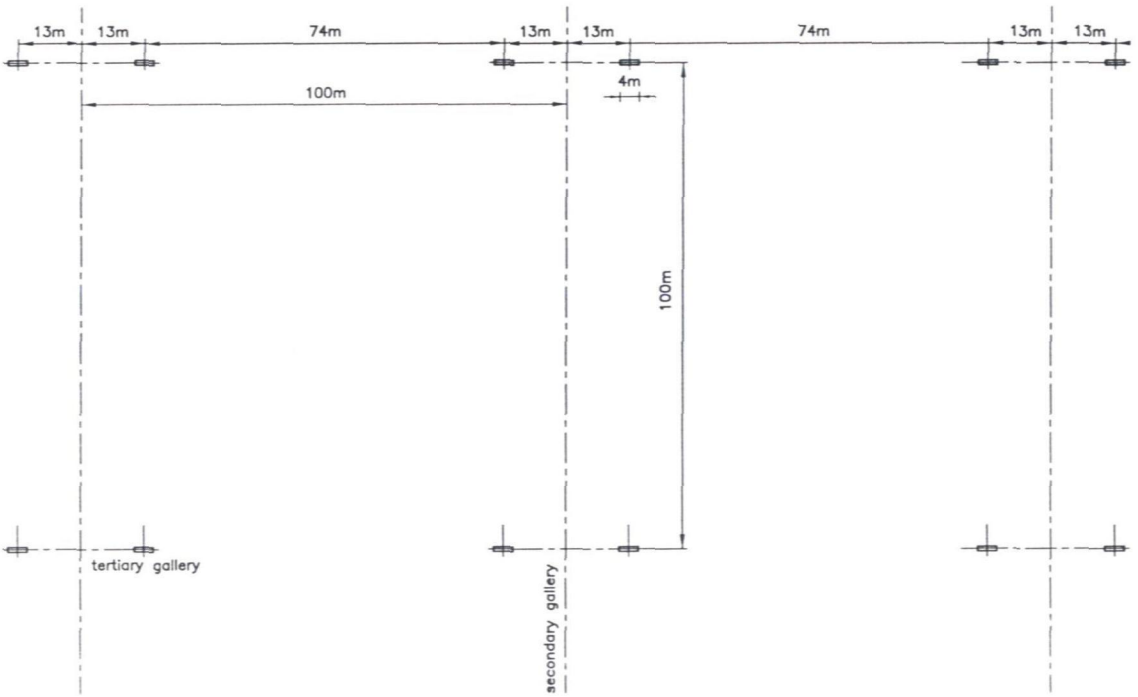

Figure 2.23.b: Basic grid pattern of 100 m x 100 m

Figure 2.23: Positions and dimensions of high temperature zones in the boundary element model (horizontal plane)

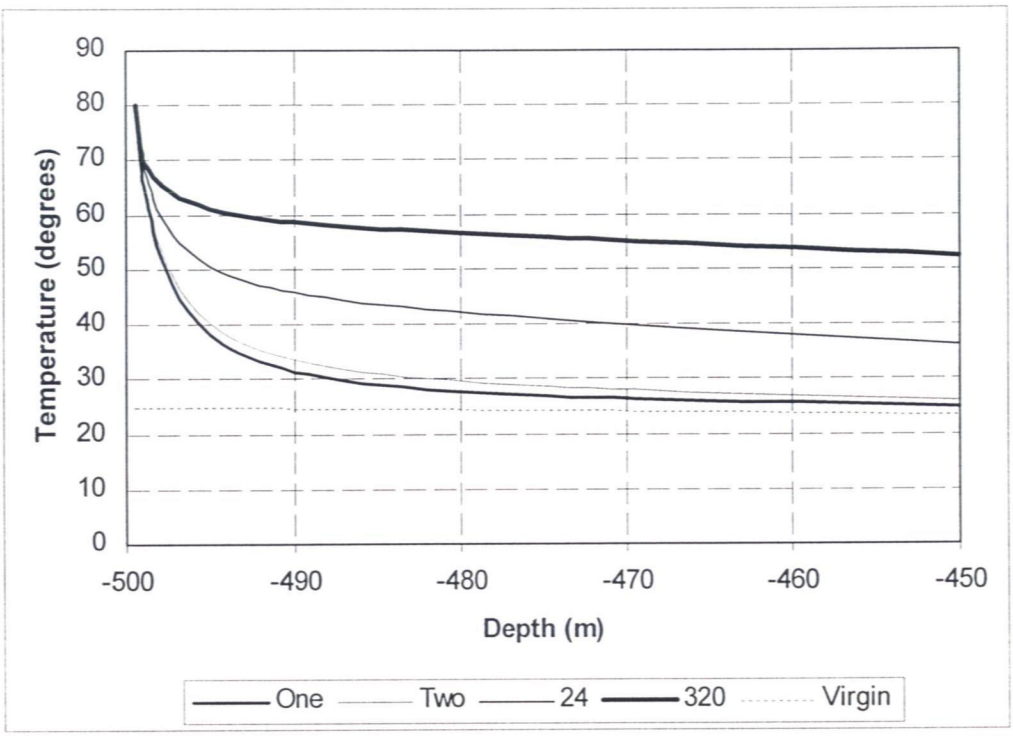

Figure 2.24.a: Basic grid of 50 m x 50 m

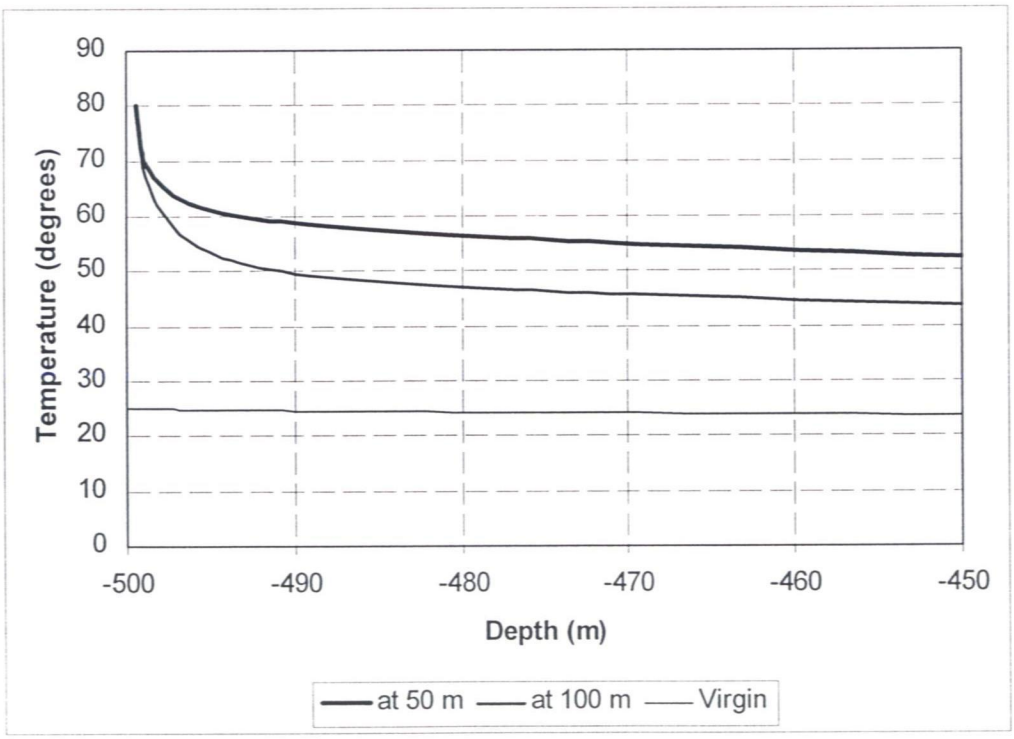

Fig.2.24b: Comparison of grid sizes (50 m x 50 m vs 100 m x 100 m), 304 canisters

Figure 2.24: Temperature distribution above the central canister

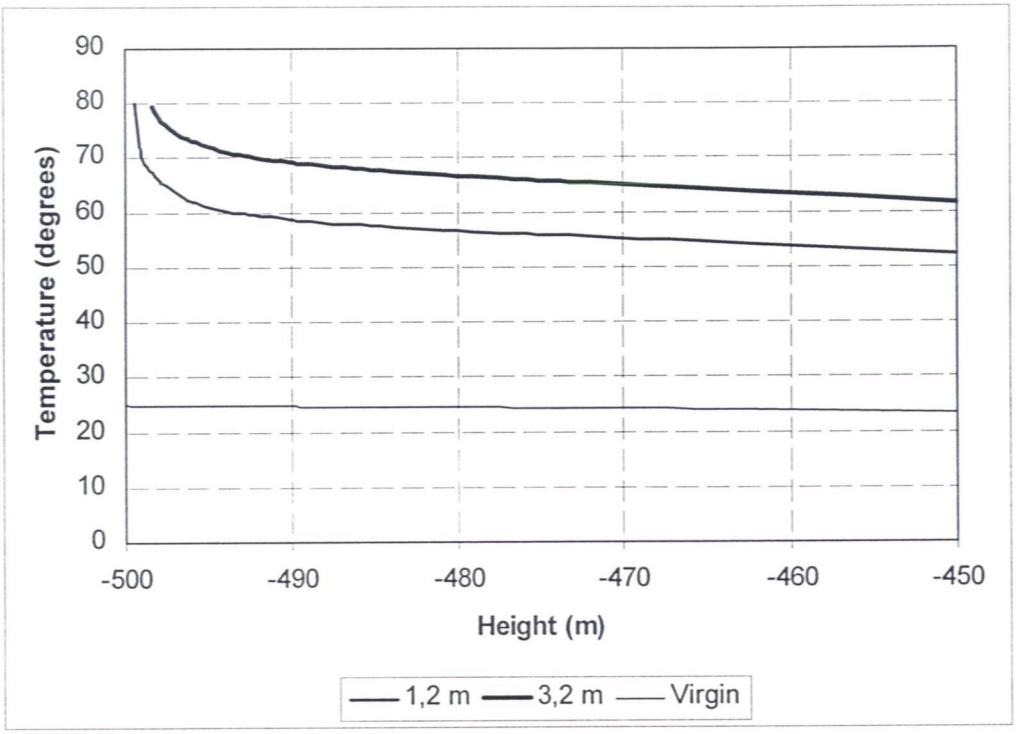

Figure 2.25: Influence of tunnel diameter on the temperature distribution above the repository. The tunnel wall is kept at a constant temperature of 80°C

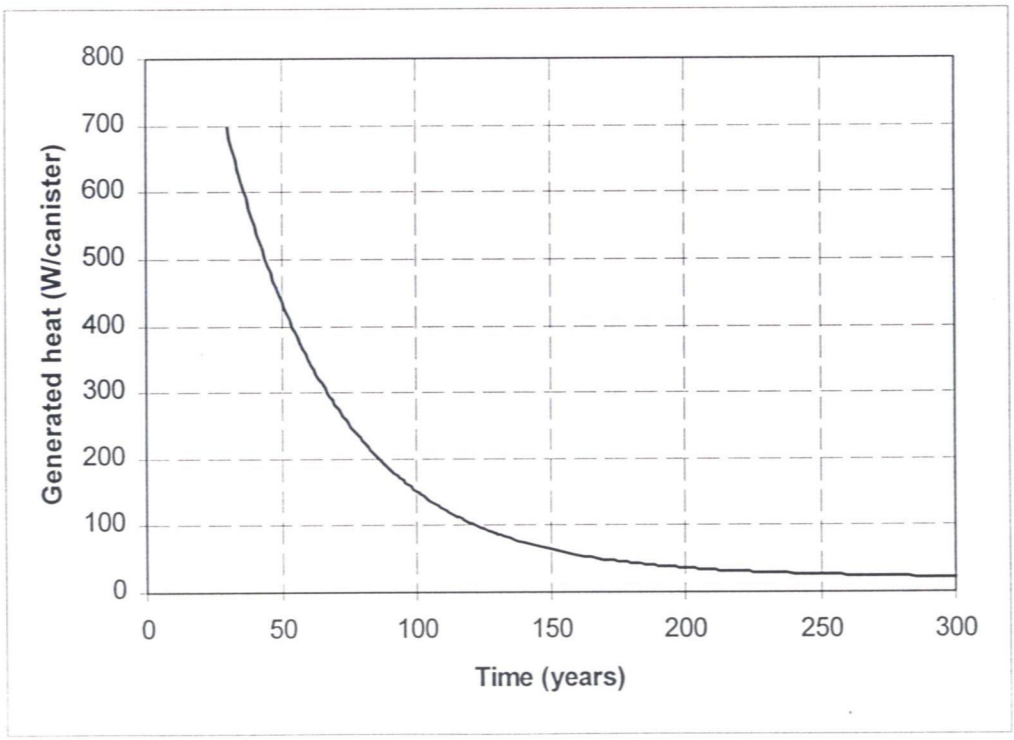

Figure 2.26: Generated heat per canister [R.J. Heijboer et al., 1988; J.J. Heijdra et al., 1995]

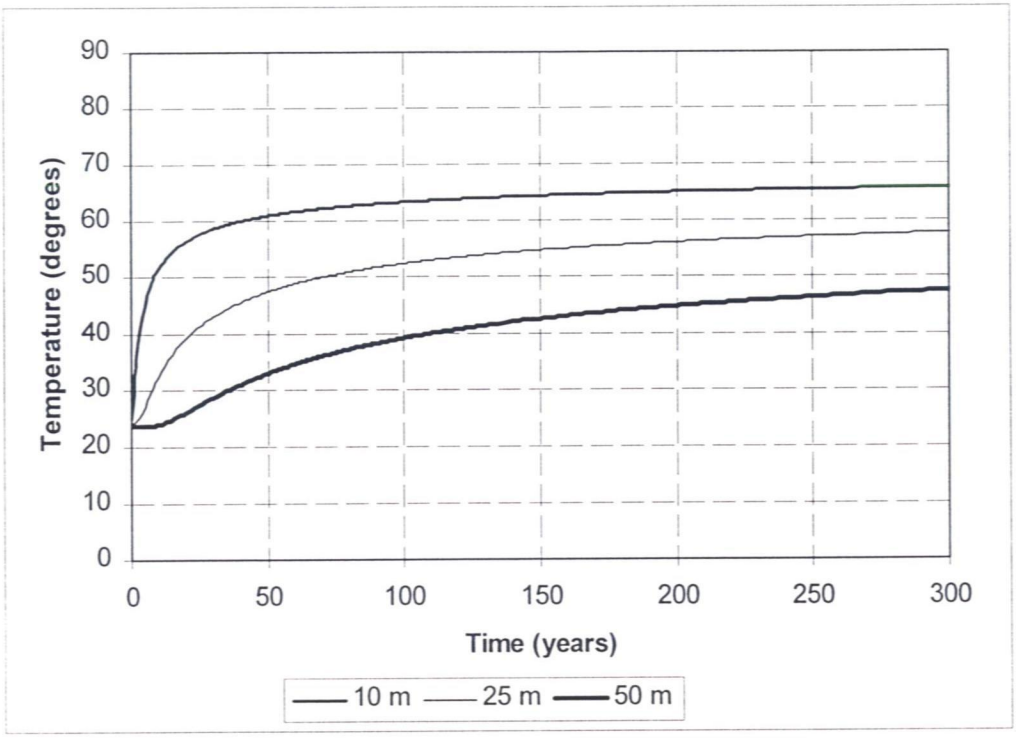

Figure 2.27: Temperature distribution at various heights above the repository in function of the time

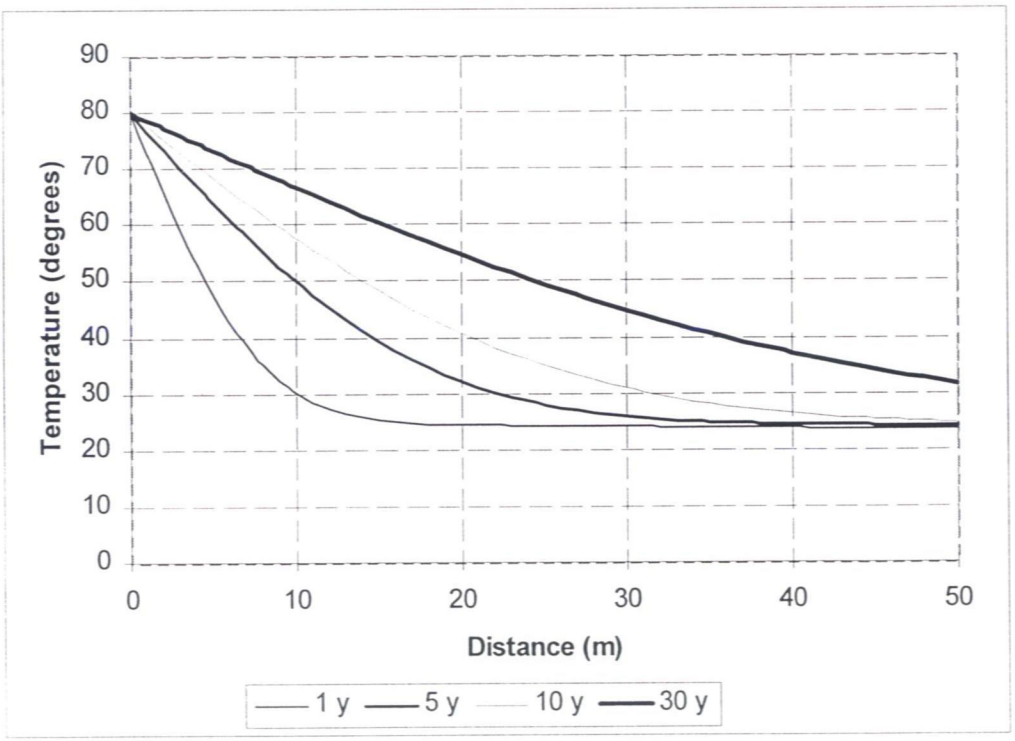

Figure 2.28: Temperature distribution in function of the height above the repository at various points in time

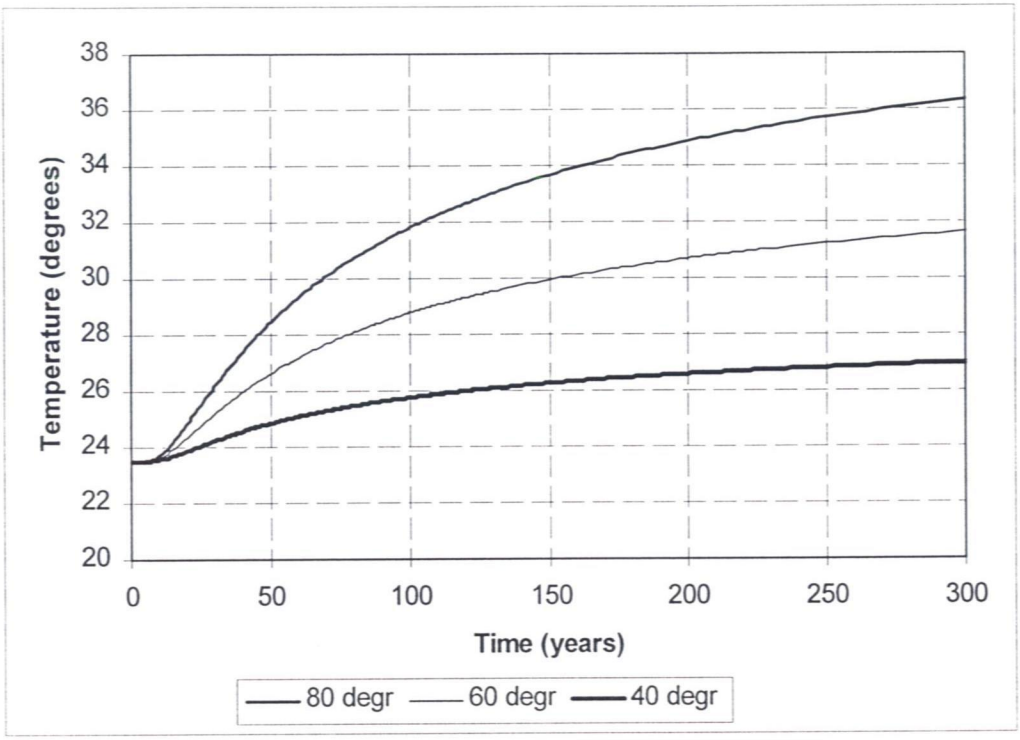

Figure 2.29: Temperature distribution in function of the time for different tunnel wall temperatures (50 m above depository)

3 Planning and time schedule

3.1 Aim of planning and time scheduling exercise

The aim of this planning and time scheduling exercise is twofold. One wishes in the first place to obtain an idea of the time required to establish the repository, to store the waste and to carry out the work necessary for closing the facility permanently. The scheduling provides in the second place an estimate of the number of working faces. This allows to decide on the number of machines required for the excavation of the clay and for the transport of the excavated material, the support material and the backfill material. The number of working faces also determines the required ventilation volumes.

3.2 Description of successive phases

In total, eight different phases are considered. The first five cover the excavation period. The sixth is the actual storage of the waste and the backfilling of the voids surrounding the canisters. The filling of the primary and secondary tunnels are considered in the last two phases. Reference is made to the mine plan attached at the end of the previous chapter.

3.2.1 Excavation

Phase 1, Shafts and shaft areas

Phase 1 concerns the shaft sinking (phase 1a) and the development in the vicinity of the shaft (phase1b). The shaft sinking operations include the site establishment, the freezing operations and the equipping of the shaft. The advance attained in the shaft sinking is specified at 2 m/day. The site preparation is assumed to require three months. The equipping of the shaft and the installation of the hauling machinery is assumed to take 3 months as well. These figures are considered to be realistic estimates; they are partly based on the current experience with shaft sinking at SCK, Mol. In the vicinity of the shaft, the tunnels are excavated manually (phase 1b, see Figure D.1). The excavated diameter of these tunnels is assumed to be 5,4 m instead of 4,6 m. The larger diameter in the vicinity of the shaft provides additional height for equipment used in loading and unloading material from the cage, and an additional cross-section for ventilation purposes. The scheduled advance for the manual digging is 2,5 m/day. The preparation work preceding the actual excavation is fixed at 1 week (= 5 working days)

Phase 2, basic primary layout

Phase 2 involves the digging of the connection between both shafts (phase 2a) (Figure D.2) and the construction of the loops giving access to the separate sections (phase 2b) (Figure D.3). The connection between the shafts has to be realized as soon as possible, not only to provide a second escape route, but also for ventilation purposes. The excavated diameter of these galleries amounts to 4,6 m. From phase 2 onwards, all excavation operations are fully mechanized. Special tunnel excavation machines to be designed for the purpose are required. Some possible designs by the contracting companies Fairclough, Smet-Boring and Howden, are presented in [Van Cotthem et al., 1997]. The daily advance these machines can attain is for the purpose of the schedule fixed at

10 m. The dismantling, repositioning and re-assembly of these machines is assumed to require 5 working days.

Phase 3, primary galleries and part of secondary galleries

Phase 3 pertains to the digging of the remaining primary galleries (Figure D.4), and the secondary galleries at the boundaries of the concession, connecting them. At the end of phase 3, all galleries along the boundary of the excavation are developed. The ventilation is now available at the outermost parts of the repository, thereby minimizing the distances that have to be ventilated by secondary ventilation in the following phases. The advance rate and the time required for repositioning remain unchanged from phase 2 at 10 m/day and 1 week respectively since the same machines are used as in phase 2.

Phase 4, secondary galleries

Phase 4 is, of the different excavation stages, the stage that takes most time. In this phase, the remaining secondary galleries are excavated (Figure D.5). At the end of this phase, all 4,6 m diameter tunnels are completed. The same advances and repositioning times as in phase 2 and 3 are used. It can be noted that the scheduling is carried out as if the secondary galleries are 1000 m long. While the distance between the centre lines of the primary galleries is indeed 1000 m, the distance to be excavated is actually decreased by about two times 2,3 m which is considered to be negligible in the planning. The lining of the primary gallery has to be holed through, both upon starting and upon finishing a secondary gallery. No additional time has been allowed for realizing these holings. The same argument applies to phase 5 for the tertiary galleries, and is also applicable for some of the galleries in phase 2 and 3.

Phase 5, tertiary galleries

Phase 5 is the last excavation phase. The tertiary galleries are being developed. This phase is however quite distinct from the phases 2, 3 and 4, in that other tunnel excavation machines have to be used because the excavated tunnel diameter of the tertiary gallery is 3,2 m instead of 4,6 m. In phase 5a, the digging of the tertiary galleries in the MLW zone is scheduled, while in phase 5b, the digging of the tertiary galleries in the HLW zones is scheduled. The reason for splitting the excavation of the tertiary tunnels in two separate sub-phases, lies in the different nature of the tunnels in the MLW zone and the HLW zones. A tertiary tunnel in the MLW zone interconnects two secondary galleries, while a tertiary tunnel in the HLW zones extends 15 m from the secondary tunnel centre only. The design of the machines used in phase 5a will probably be very similar to the design of the machines for the excavation of the 4,6 m diameter tunnels. The advance rate and the repositioning time are therefore also equal for both machines: 10 m/day advance rate and a 1 week repositioning time have been maintained. The tunnelling machine is also assumed to cross the secondary galleries. In other words, the excavation machine is not dismantled each time it holes into a secondary gallery, but it carries on over the full width of the MLW zone.

The machines used in the HLW zones (phase 5.b) will be of a different design, as they have only to advance 12,7 m into the clay. A pipe jacking technique might be envisaged. The different nature of these excavations also warrants a different approach to the advance rates and repositioning times. Three different types of repositioning have to be considered:

- The repositioning of the machine from one side of a secondary gallery to the other side. This movement consists only of retracting the machine and redirectioning it by turning it around.
- The second type of repositioning, is the lateral movement over a distance of 50 m or 40 m (depending if it concerns the HLW heat generating zone or the HLW zone where no heat is generated). This lateral movement has to be made each time one moves to another, parallel tertiary gallery in the same secondary gallery.
- A third type of repositioning involves the dismantling and re-assembly of the machine, and has to be planned for each time the machine has to be moved to another secondary gallery.

The third type of repositioning is scheduled explicitly, and is fixed at 1 week, similar to phases 2 to 4. The first and the second type of repositioning are scheduled implicitly though, by providing 5 working days for the excavation of two 12,7 m tunnels situated opposite each other. These 5 days include one movement of the first type to the opposite side and one lateral movement (second type). For the excavation of one tertiary gallery without having to excavate one on the opposite side, 3 working days are provided (i.e. for all tertiary galleries ending on secondary galleries at the boundary of the zones). These 3 days include the excavation of 12,7 m of gallery and the lateral movement over a distance of 40 m or 50 m.

3.2.2 Storage of waste

Phase 6, storage of waste

Phase 6 encompasses the waste storage period. It has to be clearly differentiated from the previous stages, as it concerns a total different activity. Phase 6 should not necessarily follow phase 5 immediately, several years may elapse between the completion of the repository, and the start of the waste storage. The three different types of waste can be stored simultaneously or in entirely separated time periods. For example, it should be feasible to store the waste not generating heat (high and middle/low level) relatively fast after the excavation period, but to wait with the storage of the heat generating high level waste till it has cooled down sufficiently.

The storage of the heat generating high level waste is described in phase 6a; the storage of the high level waste that does not generate heat is treated in phase 6b. The storage of both types of waste includes the backfilling of the tertiary galleries as well. The emplacement of a canister, the backfilling of the tertiary tunnel and the sealing of this gallery form all integral part of the waste storage process. The schedule is based on the assumption that the whole storage process of one canister in one tertiary gallery, including preparation of the storage site and backfilling, requires three days. One day is allowed for the preparation of the storage site, one day for the transportation and the emplacement of the canister, and one day for the backfilling. It is further assumed that maximum one heat generating canister and two HLW drums that do not produce any heat can be transported per day. The preparation, emplacement and backfilling operations for respectively three sites can take place simultaneously, which means that the heat generating waste can be stored at the rate of one per day, and the other HLW can be stored at a rate of two per day.

The storage of the low and medium level radioactive waste is described in phase 6c. No back-filling of the spaces in between the drums is envisaged. It is assumed that fifty containers of low and medium level radioactive waste can be brought in place per day.

3.2.3 Filling of access galleries

After all the radioactive waste has been disposed of, the workings are monitored and are kept accessible such that the HLW waste may be retrieved at any desired moment.

Phase 7, Filling of secondary galleries

Before closing the repository, the secondary galleries in the HLW zone is backfilled to ensure a good sealing of the potentially hazardous waste. The filling of the secondary galleries in the HLW zone where the heat generating waste is stored is the subject of phase 7a, while the filling of the HLW zone where the waste that does not generates heat is the subject of phase 7b. The galleries are filled at a rate of 500 m^3/day.

Phase 8, Filling of primary galleries

Phase 8 is the last step preceding total closure: the primary galleries connecting the HLW zones to the shaft area are being filled. After this phase the underground facility can remain open, or it can be decided to proceed to a complete closure of the repository as well. A filling rate of 500 m^3/day is envisaged for this phase as well.

It can be noted that phase 7 and phase 8 could either immediately follow the storage of the waste, or it could be decided to monitor the behaviour of the canisters for a certain time before one goes over to the phases 7 and 8, or it could be decided to make phases 7 and 8 part of the total closure activities. The ease of access to the waste canisters themselves decreases once phase 7 and 8 have been carried out, the barriers to be broken through by any possible contamination on the other hand are enlarged.

3.3 Discussion of results

The actual schedule and the detailed figures are given in appendix D. The schedule in appendix D specifies the following:

- the number of working places,
- the zones in which each machine is deployed during each phase,
- the number of working days each machine spends in the zones in which it is deployed,
- the day a machine starts and the day a machine finishes work per phase (expressed in working days),
- the approximate volume of clay excavated, expressed in cubic metres of in situ material,
- the total gallery length excavated per phase.

The data of the time scheduling is summarized in Table 3.1. For the assumptions specified above, the total time required to excavate the entire mining complex is estimated to be 2950 working days. This would correspond to about 13 years (46 workings weeks of 5 days considered in one year). If one would be able to increase the speed of excavating by 50 %, but keeping the same time for e.g. repositioning, the total time period is only reduced by about 600 working days. Under these conditions the mine could be finished in about 10 years.
If the three types of waste are stored in successive phases, it would require 2060 working days or about 9 years. To store the middle and low level radioactive waste requires 1126 working days or just

below 5 years. The storage time for the two types of high level radioactive waste is less: 302 working days for the heat generating waste and 632 working days for the waste not generating heat.
The final filling of the secondary and primary galleries would require maximum 815 working days or 3,5 years. This could be reduced if one works at the same time in the various zones.
In conclusion, a minimum period of about 20 years should be provided for, between starting the shaft excavation and sealing off the repository. This if no mayors delays are experienced between the consecutive phases.

Phase	**Activity**	**Time required (# working days)**	**Total time period since start**
Excavation			
1a	Shaft	380	
1b	Shaft area	85	465
2	Basic primary layout	320	785
3	Primary galleries	290	1075
4	Secondary galleries	1000	2075
5	Tertiary galleries	875	2950
Storage			
6a	HLW (Heat)	302	-
6b	HLW (Cold)	632	-
6c	MLW	1126	-
Filling			
7	Secondary galleries		
7a	HLW (Heat)	172	-
7b	HLW (Cold)	537	-
8	Primary galleries		
8a	HLW (Heat)	50	-
8b	HLW (Cold)	56	-

Table 3.1: Overview of time schedule for the excavation of the mine, the storage of the waste and possible successive closure

Another finding of this planning exercise is the total volume of rock that has to be excavated, and that consequently has to be dumped somewhere. In Table 3.2, the total volume of rock is summarized. For all excavations it amount to 1358400 m^3. This would require an area of about 13,6 ha if the clay is to be stacked 10 m high and if no swell is taken into consideration. Part of it can probably be used in the process of filling. In the phases 6, 7 and 8, filling material with a volume of respectively 71700, 354700 and 52900 m^3 is required. The total volume amounts to 479300 m^3.

Phase	Activity	Volume (1000 m^3)
1a	Shaft	31,4
1b	Shaft area	8,9
2	Basic primary layout	102,7
3	Primary galleries	117,8
4	Secondary galleries	794,0
5	Tertiary galleries	303,6
	Total	1358,4

Table 3.2: Total volume of rock excavated

4 Ventilation

4.1 Introduction

The workings have not only to be ventilated during the period people are employed underground, but at least the possibility has to be maintained to ventilate the repository after the waste has been stored, and this until total closure of the underground facilities. In the light of the required retrievability, the zone in which the high level radioactive waste is stored has either to be ventilated permanently after the canisters have been brought in place, or the possibility to ventilate this zone with sufficient air to enable re-entry has to be provided for. Such a re-entry should be possible at short notice.

The reasons why, in general, high standards of ventilation are required in an underground environment are manifold. The people working underground have of course to be provided with sufficient fresh air. Adequate air quantities are required to dilute and evacuate the exhaust gases of diesel equipment as well as to render harmless any accumulation of any other noxious fumes that may be produced either during mining activities or in the course of repair work being carried out. The allowable limits of the most harmful substances found in the underground mine atmosphere are generally laid down in government regulations. The air velocities should be sufficiently high to evacuate air borne dust that may be generated as a consequence of the breaking of rock or as a consequence of the mining activities in general. These velocities should at the same time remain low enough as not to be a hindrance to people working or travelling underground. A velocity of 4 to 5 m/s is generally considered a maximum. The quantities and the temperature of the ventilation air have to be such that any excess heat can be evacuated. The wet bulb temperature of the ambient air in the workings should not exceed 27,5°C since productivity decreases dramatically above this temperature [R.G. Gürtunca, 1998].

It is envisaged that most of the machinery employed in the excavation of the clay and in the transport is powered electrically. The absence of diesel equipment implies that the calculations of the ventilation requirements should not be based on the amount of diesel consumed or on the installed diesel power, but can be derived from the other factors governing the ventilation requirements. An excavation process in wet clay does not resort in the category of dust creating operations. Therefore, one can disregard this aspect as well in the ventilation calculations.

In summary, the ventilation of the mining operation considered in this project should be such that it is ensured that:

- The people employed underground are provided with sufficient oxygen and fresh air.
- Any harmful gases or vapours that may be generated are diluted and evacuated. Such gases and vapours may be generated by normal industrial activities such as welding, flame-cutting and the like or they may escape from machinery installed underground (air loaded with oil particles, hydrogen set free during battery charging operations, etc.).

The required flow rates are determined for the different excavation phases. An estimate is also provided of the air quantities required to keep the temperature rise of the ambient air below 2,5 °C once the heat generating sources have been brought in place.

4.2. Required flow rates

Quite some standards exist determining the minimum ventilation requirements. Several of these standards specify the minimum required flow rates to be maintained to satisfy the health and safety norms. If specific or exceptional sources of air pollution are present under any form, the required air volumes have to be increased. Other standards are more oriented to workings where the main sources of pollution are the exhaust fumes of diesel equipment. If the virgin rock temperature is such that a problem could arise with the atmosphere underground or where special sources of heat are present in the workings, as with the heat generating zone in the repository under consideration, the air quantities and the allowable temperature of the inlet air have to be determined. The heat exchange between the ventilation air and the rock mass have thereby to be taken into consideration.

An overview of some of the standards and recommendations found in the literature to calculate the normal air requirements, reflects the different functions of the ventilation air:

- An air quantity of 0,1 m^3/s to 0,5 m^3/s per person underground [F.C. Bossard et al., 1983].
- A minimum of 0,25 m^3/s per square metre of cross zone in shafts being sunk [N. Thorp, 1982].
- A minimum of 0,15 m^3/s per square metre of cross sectional area for any heading which is advanced [Reg.10.7.2, 1991].
- An air velocity of 0,15 m/s to 0,25 m/s depending on the circumstances in all headings [W.A. Bardswick, 1973].
- A minimum of 0,025 m^3/s for each tonne mined per shift [J. Burrows et al. 1982].
- An air quantity of 0,025 m^3/s to 0,1 m^3/s per tonne of ore and waste mined [F.C. Bossard et al., 1983]
- An air quantity of 60 to 65 m^3/s per MW rated diesel capacity at the point of operation [J. Burrows et al. 1982]
- A total amount of air of 2400 m^3 per kilogram of diesel consumed [J. Patigny, 1982].

The standard selected for the ventilation calculations in this study has been borrowed from N. Thorp for the shaft sinking (0,25 m^3/s per square metre of cross zone in shafts being sunk), and from Bardswick for the headings being advanced (an air velocity of 0,25 m/s, which corresponds to a quantity of 0,25 m^3/s per square metre of cross sectional area).

In the excavation and storage schedule, schematized in appendix D, the required total downcast flow rates are given for each phase. The following aspects were taken into account in determining the downcast volumes:

- the actual flow rates required at the working face, determined in accordance with the chosen standards (see above),
- the leakage and the fresh air commitments,
- the autocompression.

The leakage is the difference between air send to a working place and the actual volume reaching this working place. The leakage is dependent on the extent of the underground workings, on the type of mining, and on the materials used for regulating the air reticulation. The simple, regular layout of the repository and the methods and materials that are used for ventilating the working places enable an efficient use of the air. Leakages ranging from 0% to 20% of the total downcast air quantity, are taken into account. The percentage of leakage increases as the extent of the mine increases and is

indicated for each phase in appendix D. The fresh air commitments are the volumes of air that are not intended for the working places but that are allowed for the ventilating of e.g. the underground electrical substations, pump stations, compressor houses etc.

The volumes of air sent down the shaft, the volumes at the bottom of the downcast shaft, the volumes at the bottom of the upcast shaft and the volumes to be handled by the fans at the top of the upcast shaft are different.
The air going down the shaft will undergo a compression, and associated therewith a temperature and density increase. This process, known as autocompression is discussed in more detail in appendix E. The opposite process of decompression arises in the upcast shaft. For a repository at a depth of 500 m, the volume decrease due to autocompression amounts to 5%. (see appendix E). The decompression in the upcast shaft offsets the autocompression in the downcast shaft. The volumes to be handled by the fans, are however 5% higher than the volumes required underground.

Besides the change in volume and temperature due to autocompression, the volume of the ventilation air is also influenced by the changing air temperature due to heat exchange between the clay mass and the air. The temperature of the air leaving the mine is assumed to remain fairly constant at ± 20 °C throughout the year. The temperature of the air entering the downcast shaft varies considerably though between winter and summer. The increase in volume at the top of the downcast shaft comes to 0,33% to 0,38% per degree the temperature rises, depending on the initial temperature. An increase in temperature of e.g. 20° (inlet air temperature of 0°C) results in a volume increase of 7,35%. Because the downcast air temperatures are calculated, this phenomenon does not influence the calculated volumes. The volume increase due to the pressure drop realized by the fans is also not taken into account. This volume change is again largest just in front of the main fans. These factors have to be taken into account in designing the fan capacities.

Besides the change in volume of the ventilation air, the mass of the air leaving the repository may also exceed the mass of the air entering the workings by about 1% (figure obtained from Barenbrug's psychrometric chart [R. Hemp, 1982]). The reason for this, is that its moisture content may increase as it moves through the workings because of the evaporation of water present underground. As the ventilation calculations are based on the volumes, this does not have a bearing on the figures in appendix D.

4.3 Ventilation practice

The main fan is to be installed on surface at the top of the upcast shaft, and it extracts air from the workings. The main advantage of this configuration relates to transport and leakage. Using the downcast shaft as main shaft for the transport of men and material, one avoids interference with the ventilation system. Travelling in the shaft in which the main fan is installed is a major cause of air leaks.

The ventilation of the headings themselves has to be ensured by the auxiliary ventilation. This signifies that a fan forces the air into the heading being developed (force fan), or extracts the air from the face (exhaust fan). The use of force fans is recommended as it ensures that good quality air can be delivered at high velocities, and as leakage is always from the ducting column and hence easily

detected. To avoid recirculation (i.e.: that air leaving a heading re-enters the same heading), the fans are placed 15 m upstream from the entry to the heading (see Figures D3 to D5 in Appendix D). The volume of air running over the fans has to exceed the volumes of air forced to the face. The volume of air in the through ventilation roads is therefore the double of the volumes of air required at the headings being ventilated from that specific through ventilation road. As no blasting operations are envisaged, and as hardly any diesel equipment is used, few noxious fumes are produced during normal operations. Serial ventilation is therefore acceptable.

The ducts used in auxiliary ventilation can consist of galvanized iron piping, fibre glass piping, rigid plastic piping, or flexible plastic ducting. The common ducting size of 760 mm diameter has been selected for the ventilation of the shafts, the primary and the secondary galleries. The tertiary galleries are ventilated with 570 mm ducting. The pressure drop in the ducts, has to be delivered by the auxiliary fans. This pressure drop is determined by the length of the ducting, the friction factor and the air velocity. The pressure drops tabled in the scheduling summary of Appendix D, are calculated as follows:

$$\Delta p = K\frac{L C v^2}{A}$$

where Δp : pressure drop (MPa),
K : Atkinson's friction factor (kg/m^3), it takes account of the shape of the ducts and the surface roughness, and is only valid for air,
L : length of the duct (m),
C: circumference of the inside of the duct (m),
v : velocity of the air (m/s),
A: cross sectional area of the duct (m^2).

4.4 Removal of heat

One of the functions of the ventilation is the removal of heat. In the zones where the heat generating waste is stored, the capacity of the air to remove heat becomes an important factor. The air, required to maintain the temperature of the environment at an acceptable level is calculated in appendixE. The calculations are based on a very modest temperature increase of 2,5°C as an example. The temperature of the air at the entrance to the section is hereby in equilibrium with the temperature of the virgin clay (i.e. 25°C), and it is fully saturated with water vapour. The calculation is carried out for the heat generated at the moment the drums are stored (i.e. when the generated power is maximal). The maximum allowable temperature is fixed at 27,5°C. The moisture content of the air is assumed to remain constant. It is further assumed (see appendix E) that 13,5% of the heat generated in the canisters has to be removed by the ventilation.
Under these conditions, 1,2 m^3/s of air would suffice per secondary gallery to remove the excess heat, resulting in 9,6 m^3/s for the entire heat generating section. This should be compared with the 2,40 m^3/s required in each secondary gallery where people are travelling or working.

4.5 Discussion of results

To provide a healthy working environment and to evacuate excess heat generated by the heat generating canisters, sufficient ventilation has to be provided. Attention is paid to both the main and the auxiliary ventilation during the excavation period. The flow rate required to keep the temperature at acceptable levels once all the heat generating canisters have been brought in place is determined as well.

During the development of the secondary galleries, the ventilation requirements are maximal. The required flow rate of the downcast air attains at this stage 50,7 m^3/s. The maximum air velocities associated with this flow are encountered close to the shaft, and amount to 3,2 m/s, an acceptable velocity in the intake airways. In conventional mining operations, one singular fan has a capacity between 25 to 350 m^3/s and often several fans are combined to support the air flow in one shaft. Hence, the selection of the main fan(s) should not pose any problem.
Once all the heat sources have been placed, a flow rate of 9,6 m^3/s is needed in the zone where the heat generating waste is stored to keep the temperature at acceptable levels. The demands placed on the main ventilation are not exceptional, and no technical difficulties are envisaged for the main ventilation.

As the length of the blind headings is quite considerable, good auxiliary ventilation is of the utmost importance. It is proposed to use force fans for this purpose. The substantial length of the ducts requires fans that are able of handling 4,15 m^3/s at up to 10,4 kPa. During the shaft sinking stage and the initial underground development, the auxiliary fans have to provide 7,5 m^3/s at pressures up to 8,6 kPa. The application discussed here cannot be considered standard, and although the material and the fans to meet these demands are available on the market, the selection of suitable fans, preferably axial flow fans, should not be underestimated.

5. References

W.A. Bardswick; Ventilation for environmental control - metal mines. In *SME Mining Engineering Handbook*, Volume 1, 1973, p 16.56 - 16.67.

F. Bernier; Pers. Comm., 1998.

F.C. Bossard, J.J. LeFever, J.B. LeFever and K.S. Stout; A manual of mine ventilation design practices, 1983.

J. Burrows, R. Hemp, W. Holding and R.M. Stroh; Planning ventilation and refrigeration requirements. In *Environmental Engineering in South African Mines*, 1982, p 953-974.

S.L. Crouch, A.M. Starfield; Boundary element methods in solid mechanics, 1983.

D. De Bruyn and J.-F. Thimus; The influence of temperature on mechanical characteristics of Boom clay: The results of an initial laboratory programme. *Engineering Geology* 41, 1996, p117-126.

D. De Bruyn and J. Verstricht; The design of the PRACLAY experiment and the behaviour of Boom Clay at elevated temperature. In *Feasibility and Acceptability of Nuclear Waste Disposal in the Boom Clay Formation*, 1997, p 27-33.

C. Grégoire; Comportement hydro-mécanique de l'argile de Boom autour d'un forage piezométrique. MSc thesis FPMS, 1996.

J. Grupa; Overzichtslijst OPLA strategie A, Pers. Com., 1998.

R.G. Gürtunca; Mining below 3000 m and challenges for the South African gold mining industry. In *Mechanics of Jointed and Faulted Rock*, 1998, p 3-10.

R.J. Heijboer et al.; Nuclide-inventaris, warmteproduktie en gammastraling van kernsplijtings-afval. Eindrapportage deelrapport 11, 1988.

J.J. Heijdra et al.; Retrievability of radioactive waste from a deep underground disposal facility, 1995.

R. Hemp; Psychrometry. In *Environmental Engineering in South African Mines*, 1982, p 435-463.

H. Hens; Bouwfysica 1: Warmte- en massatransport, 1992.

Itasca Consulting Group Inc.; FLAC user's manual, 1995.

V. Labiouse and F. Bernier; Hydro-mechanical disturbances around excavations. In *Feasibility and Acceptability of Nuclear Waste Disposal in the Boom Clay Formation*, 1997, p 15-26.

Mine Modelling ltd; MAP3D user's manual, 1997.

G.N. Pande, G. Beer and J.R. Williams; Numerical methods in Rock Mechanics, 1990.

M. Panet; Le calcul des tunnels par la méthode convergence-confinement, 1995.

J. Patigny; Nota's bij de cursus mijnventilatie, 1982.

Reg. 10.7.2.; Minerals Act and Regulations (Republic of South Africa), 1991.

R.H.B. Rijkers et al.; Inventarisatie geomechanische, geochemische en geohydrologische eigenschappen van Tertiare kleipakketten - CAR Fase II. Conceptrapportage, 1998.

Rijksgeologische dienst; Kartering slecht doorlatende laagpakketten van Tertiare Formaties, Project CAR - Fase I, 1996.

SCK-CEN; Hades Tour guide, 1994.

N. Thorp; Auxiliary ventilation Practice. In *Environmental Engineering in South African Mines*, 1982, p 277-311.

A. Van Cotthem, J.P. Minon and B. Neerdael; Construction of geological repositories for radioactive waste. *Fourth European Conference on Management and Disposal of Radioactive Waste*, 1997, p 299-310.

N. Vandenberghe, M. Dusar, P. Laga and J. Bouckaert; The Meer well in North Belgium. *Toelichtende verhandelingen voor de Geologische en Mijnkaarten van België*, verhandeling 25, 1988.

N. Vandenberghe and W. Fock; Temperature data in the subsurface of Belgium. *Tectonophysics*, 164, 1989, p 237-250.

A. Whillier; Elementary Thermodynamics. In *Environmental Engineering in South African Mines*, 1982, p 395-411.

A. Whillier; Heat transfer. In *Environmental Engineering in South African Mines*, 1982, p 465-494.

Appendix A: Hydromechanical modelling

The different models used in paragraph 2.3 are discussed in this appendix. The appendix is subdivided in different parts, each treating a different aspect of the hydromechanical modelling. In a first paragraph, the model used to determine the initial convergence u_{ini} is discussed. In a second paragraph the convergence-confinement method is reviewed; attention is paid to the line characterizing the support reaction, to the method and to the model utilized to determine the convergence curve. In a third paragraph the model is discussed that is used to calculate the response of a tunnel forming part of a repository. In a fourth and last paragraph the models appertaining to the long term response are considered.

A1 Determination of u_{ini}

An axisymmetric model is used to determine the initial convergence (Figure A1) before the support is installed.

As both geometric factors and clay characteristics determine the initial convergence, a different model has to be run each time a parameter is changed. Using an axisymmetric model places a number of constraints on the model; the gravity cannot be taken into account, and only a single isolated tunnel can be modelled. The advantage is of course that a three-dimensional situation can be simulated in an otherwise two-dimensional code.

The method being employed to determine the initial configuration, relies on a simulation of the excavation-support process. It is hereby assumed, that if this process is simulated a number of times, the calculated convergence close to the face tends towards the unknown initial convergence. The simulation consists in other words of a number of models (106 in this case), calculated the one after the other, in which the excavation and the support process gradually advance.

The initial configuration consists of a tunnel with a length of 10,25 m of which 10,0 m is supported, and 0,25 m is unsupported. The support consists of concrete panels, assumed to react linearly elastically. Their characteristics are summarized in Table A1. The model itself is 12,5 m wide and 37,5 m long, which corresponds to a cylinder with a diameter of 25 m and a height of 37,5 m.

	Symbol	**Unit**	**Value**
Specific weight concrete	γ_b	kN/m^3	25
Coefficient of Poisson	ν	-	0,33
Young's modulus	E	MPa	20000
Length panels	w	m	0,5

Table A1: Characteristics of the concrete panels.

The following boundary conditions are applied:

- The radial movement of the gridpoints on the axis of the model is prevented (necessary boundary condition for an axisymmetric problem).

- No axial movement is allowed of the gridpoint at the right (= the beginning of the tunnel) and left side of the model. This corresponds to the assumption that at some distance ahead of the tunnel the ground movement is not influenced by the approaching tunnel, and that as the face has advanced some distance each plane perpendicular to the tunnel axis can be considered as a plane of symmetry.
- A constant radial pressure equal to the (isotropic) in situ ground pressure of 10,25 MPa is applied at the boundary parallel to the axis. A pore pressure equal to the hydrostatic pressure of 5 MPa is applied to this boundary as well.
- The movement of the outer boundary in the radial direction is unrestricted.

The following initial conditions are imposed:

- An in situ total stress of 10,25 MPa, and a pore water pressure of 5 MPa are applied to the part of the model consisting of clay. The radial, tangential and axial stresses are all initiated at this value, corresponding to the assumption that the stress distribution is isotropic.
- The saturation in the whole model is fixed at 1 (= fully saturated).
- The lining already in place is not prestressed.
- As the hydraulic conductivity is very low (10^{-10} m/s), the excavation-support process may be considered fast, and an undrained analysis is warranted. No water flow is therefore allowed.

After bringing the initial configuration to equilibrium, 35 consecutive excavation-support phases are simulated. Each excavation-support cycle consists of:

- A first excavation step advancing 0,25 m.
- Convergence to equilibrium.
- A second excavation step advancing 0,25 m.
- Convergence to equilibrium.
- Installation of support (0,5 m long).
- Convergence to equilibrium.

At the end of this 35 cycle excavation-support cycle, the maximum radial displacement is assumed to be the initial convergence u_{ini}. At this stage, the tunnel has a total length of 27,75 m of which 27,5 m is supported. Note that the unsupported span varies between 0,25 m and 0,75 m.
To appraise the sensitivity of the model to the size of the excavation step, two similar models with different excavation steps are carried out: a first one with two excavation steps of 0,25 m each and a support step of 0,5 m and a second one with two excavation steps of 0,167 m each and with a support step of 0,33 m. The difference in u_{ini} amounts to 6,5 mm for the base configuration (about 4,5% of u_{ini}), resulting in a radial stress difference of 0,084 MPa, which is less than 2% of the required 4,295 MPa. All further axisymmetric simulations are carried out with the second configuration.

A2 Convergence-confinement curve

A2.1 Introduction

The convergence-confinement curve is illustrated in Figure 2.6 (2.3.4). The convergence curve represents the response of the ground, while the confinement curve characterizes the support. The soil-support equilibrium is reached at the intersection point of the two curves. The initial convergence u_{ini} (see A1) as well as the slope of the support characteristic have an influence on the equilibrium.

A2.2 Confinement or support loading curve

To determine the slope of the support characteristic, the response of a model consisting of a ring subjected to a uniform isotropic pressure is determined. It should be noted that the purpose of this simulation is to obtain an idea of the stiffness of this type of support. The detailed design of a suitable lining, taking the anisotropic stress distribution caused by the gravity and by the presence of the other tunnels into consideration falls outside the scope of this research project. The material characteristics used previously (see Table A1) were utilized here as well. The calculations yield a radial stiffness of 5,36 GPa, whereby the radial stiffness is defined as:

$$E_{rad} = \frac{R_{out} P_{rad}}{u_{out}}$$

where: E_{rad} : Radial stiffness
R_{out} : Outer tunnel radius
P_{rad} : Applied radial pressure
u_{out} : Radial displacement of the outer radius of lining

The confinement curve is the line with slope 2,33 GPa/mm (= E_{rad} /R_{out}).

A2.3 Convergence curve

To determine the convergence curve, a number of simulations have to be performed whereby a uniform, constant pressure is applied to the tunnel wall. The convergence curve is firstly established for a single tunnel. The gravity is taken into account, leaving only the vertical through the tunnel centre as an axis of symmetry. Using this symmetry, only half the tunnel is modelled. The area modelled is 100 m high and 50 m wide. The purpose of each simulation is to determine the convergence corresponding with a certain support pressure. A number of support pressure - convergence pairs, allows to trace the convergence curve.

The following boundary conditions are applied (see also Figure A2):

- The horizontal movement of the gridpoints situated on the vertical through the tunnel centre is prevented, representing the symmetry that exists with respect to this line.
- The vertical movement of only one gridpoint is restricted: the gridpoint on the right-hand boundary situated at the same depth as the tunnel centre. The restriction of the vertical movement of at least one gridpoint is necessary to prevent the vertical movement of the model as a whole due to a possible small imbalance in the vertical forces.
- A constant vertical total pressure is applied to the top and the bottom of the model; the pressure being equal to the ground pressure applicable to the depth in question. The vertical movement of these boundaries is unrestricted as well as the horizontal movement (except for the gridpoint on the vertical through the centre).
- A horizontal total pressure, varying with depth, is applied to the right-hand boundary. Both the vertical and the horizontal movement of this boundary are free, except for the vertical movement of the one gridpoint mentioned earlier.
- A pore water pressure, equal to the hydrostatic pressure at the applicable depth is imposed along the

top, the bottom and the right-hand boundary of the model.
- A uniform radial support pressure is applied to the tunnel wall. This radial support pressure is decreased in 2500 steps from the in situ ground pressure reigning at the tunnel centre, to the desired support pressure. Once the desired support pressure has been reached, it is held constant and the model is brought to equilibrium. The radial movement of the tunnel wall is totally unrestricted.
- The pore pressure at the tunnel wall remains free.

The following initial conditions are imposed:

- The initial stresses are function of the depth, and are equal to the virgin in situ stresses.
- The saturation in the whole model is fixed at 1 (= fully saturated).
- No lining is modelled.
- As the hydraulic conductivity is very low (10^{-10} m/s), the excavation process may be considered fast, and an undrained analysis is warranted. No water flow is therefore allowed.

It should be noted that the boundary conditions for the top, the bottom, and the right-hand boundary of the model are nearly identical. They only differ due to the influence of the gravity, and because of the one gridpoint that has to be fixed in the vertical direction. From the symmetry of the excavation, it can therefore be expected that the response, such as the stress distribution and the displacement are similar as well.

A3. Response around a tunnel being part of a repository

In the calculations carried out so far, only one tunnel is modelled. To evaluate the influence other tunnels may have on the stress distribution and on the extent of the plastic zone, the model has to be extended to take account of the other tunnels. An infinite series of tunnels can be simulated by a suitable choice of the boundary conditions. It is further assumed that the radial pressure exerted on the lining remains constant. This last assumption seems justified considering the convergence curve for a single tunnel and for a tunnel surrounded by other tunnels (Figure 2.6). For the same support pressure, the radial convergence of the side wall of the tunnel increases with less than 2 mm when additional tunnels are modelled (basic configuration). As an increase in convergence is noted when a support pressure is applied, it can be expected that the initial convergence increases as well when multiple tunnels are considered instead of a single tunnel. This would mean that the intersection point of the confinement curve with the x-axis also would shift slightly to the right. Maintaining the support pressure at the value obtained from the convergence-confinement equilibrium for a single tunnel, would, therefore lead to a slightly higher convergence, as would be obtained by shifting the confinement curve to a higher convergence.

The following boundary conditions are applied (see also Figure A3):

- The horizontal movement of the gridpoints situated on the vertical through the tunnel centre is prevented, representing the symmetry that exists with respect to this line (same boundary condition as for the single tunnel).
- The horizontal movement of the gridpoints situated on the right-hand boundary is prevented. The right-hand boundary is situated halfway between two tunnels. Fixing the horizontal movement of the gridpoints on a vertical, implies that this line is an axis of symmetry. The presence of two parallel axes of symmetry signifies that the feature modelled in between these two lines is mirrored

an infinite number of times.

- The vertical movement of only one gridpoint is restricted: the gridpoint on the right-hand boundary situated at the same depth as the tunnel centre. The restriction of the vertical movement of at least one gridpoint is necessary to prevent the vertical movement of the model as a whole. This could happen due to a possible small imbalance in the vertical forces (same boundary condition as for the single tunnel).
- A constant vertical total pressure is applied to the top and the bottom of the model; the pressure being equal to the ground pressure applicable to the depth in question. The vertical movement of these boundaries is unrestricted as well as the horizontal movement (with the exception of the gridpoint on the vertical through the centre, same boundary condition as for the single tunnel).
- A pore water pressure, equal to the hydrostatic pressure at the applicable depth is imposed along the top and the bottom of the model (same boundary condition as for the single tunnel).
- A uniform radial support pressure is applied to the tunnel wall. This radial support pressure is decreased in 2500 steps from the in situ ground pressure reigning at the tunnel centre, to the support pressure obtained from the equilibrium point in the convergence-confinement curve. Once the desired support pressure is reached, it is held constant and the model is brought to equilibrium. The radial movement of the tunnel wall is totally unrestricted (same boundary condition as for the single tunnel).
- The pore pressure at the tunnel wall remains free (same boundary condition as for the single tunnel).

The following initial conditions are imposed:

- The initial stresses are function of the depth, and are equal to the virgin in situ stresses (same initial condition as for the single tunnel).
- The saturation in the whole model is fixed at 1 (= fully saturated) (same initial condition as for the single tunnel).
- No lining is modelled (same initial condition as for the single tunnel).
- As the hydraulic conductivity is very low (10^{-10} m/s), the excavation process may be considered fast, and an undrained analysis is warranted. No water flow is therefore allowed (same initial condition as for the single tunnel).

A4. Long term response

Two models simulating the long term response have been considered in 2.3.6 and 2.3.7: one in which the lining is assumed to be permeable and one in which the lining is deemed impervious. The physical interpretation, and the circumstances in which the one or the other could be encountered are already discussed in 2.3.2. Only the boundary conditions applicable to the tunnel itself differ from the boundary conditions applied to the models described in A3:

- The position of the gridpoints on the tunnel wall is fixed in the position they have attained at the end of the short term response. This boundary condition implies that the lining is infinitely stiff, a simplification that could be accepted considering the radial stiffness of the lining (Figure 2.6b). An additional radial pressure of 2,33 MPa, would cause an additional radial displacement of 1 mm. This should be compared with a radial displacement of e.g. 146 mm at the beginning of the long term period.
- The pore water pressure at the tunnel wall remains free if an impervious lining is simulated. If a permeable tunnel lining is simulated, the pore water pressure at the tunnel wall is however fixed at 0 MPa.

The stresses resulting from bringing the model described in A3 to equilibrium are used as input for both types of long term simulations. Because the time scale being considered becomes important, a drained analysis is carried out, and water flow is therefore allowed. Water can enter or leave the model at the boundaries on which the pore pressure has been fixed. Water can in other words enter the model at the top and at the bottom of the model (pore water pressure fixed at the hydrostatic pressure), and can leave the model at the tunnel wall in the model with the permeable lining (pore water pressure fixed at 0 MPa). No water is allowed to enter or to leave along the boundaries where the pore water pressure remains free to change: no water can leave the model at the tunnel wall in the model with the impermeable lining and no water can enter or leave the model along the right hand or left-hand boundaries for both the long term models, as in each of these cases the pore water pressure is free to increase or decrease. The consequence of leaving the pore water pressure free at the right and left-hand boundary (i.e. that no water can flow through these boundaries), is also in agreement with the applicable symmetry conditions.

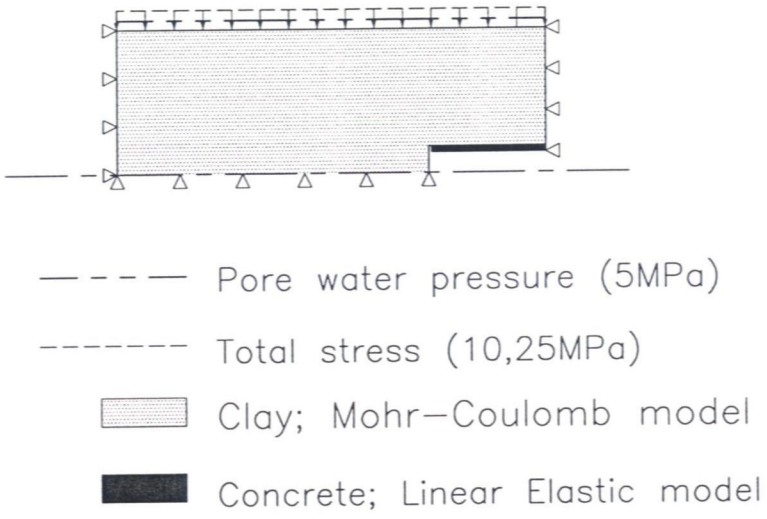

Figure A1: Axisymmetric model used to determine the initial convergence

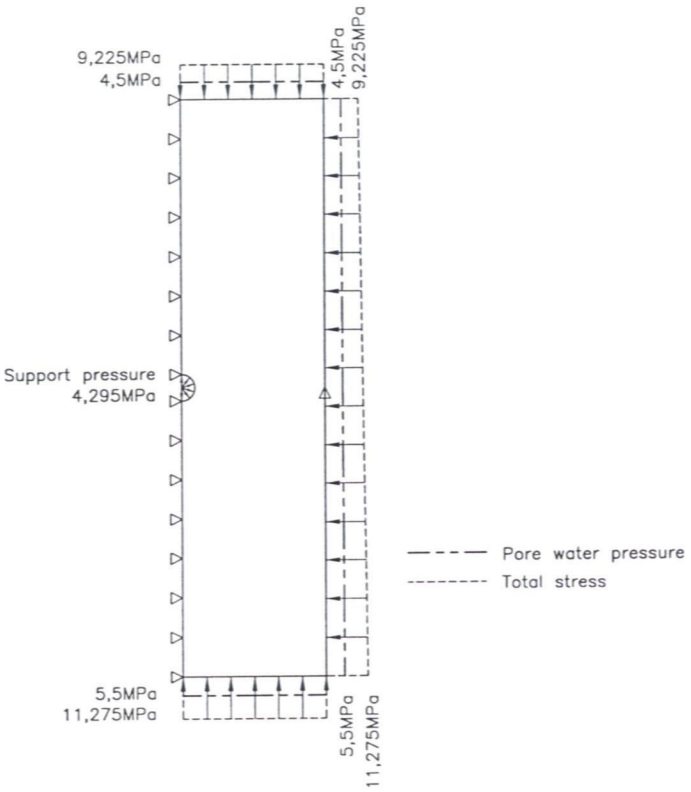

Figure A2: Single tunnel model used to determine the convergence

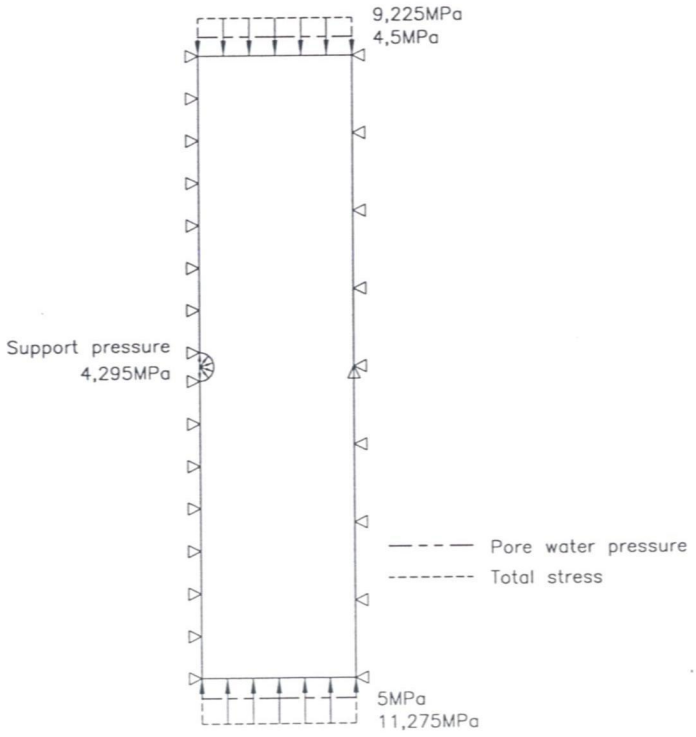

Figure A3: Model used for the short term response, simulating an infinite number of tunnels

Appendix B: Parameter study, clay characteristics

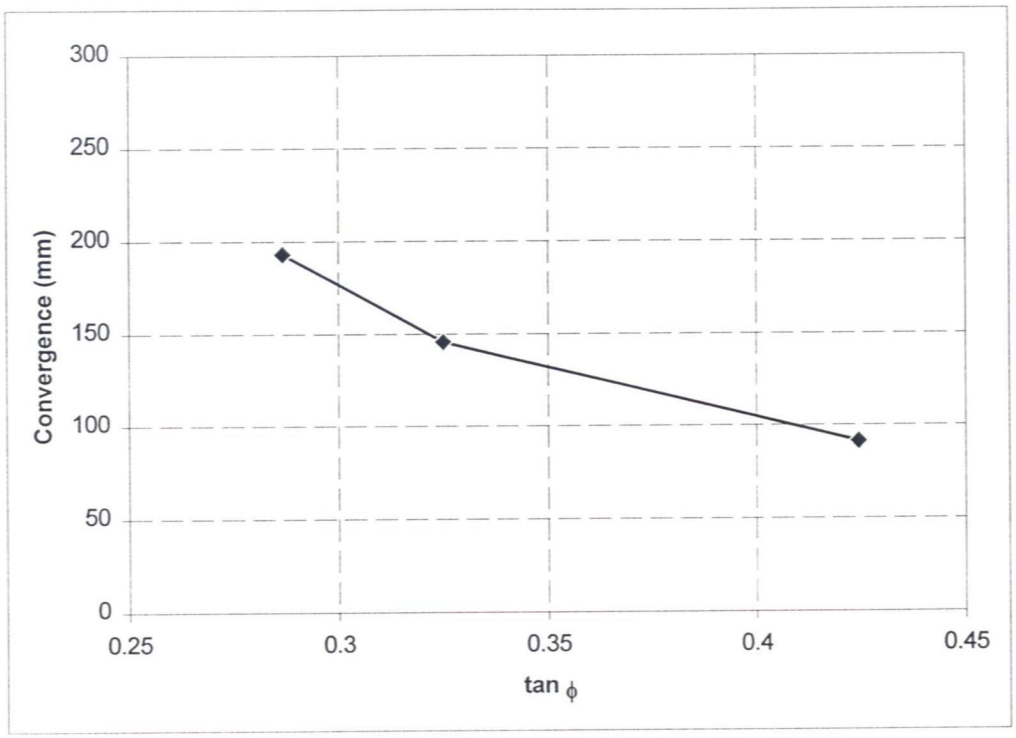

Figure B1: Influence of the friction angle on the convergence

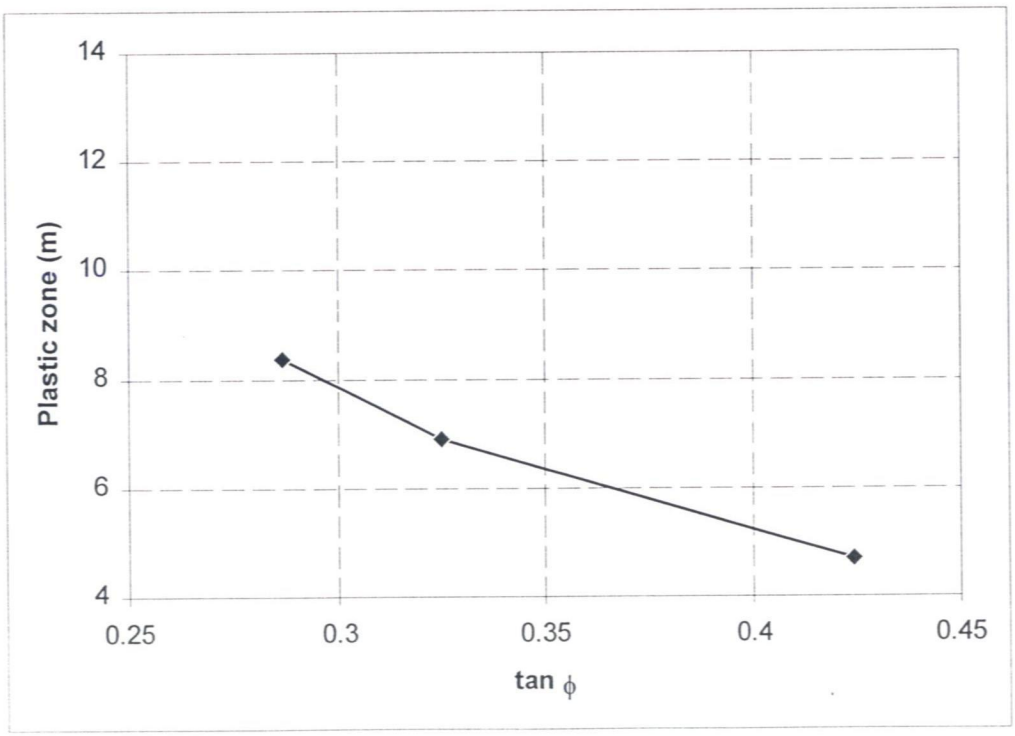

Figure B2: Influence of the friction angle on the extent of the plastic zone

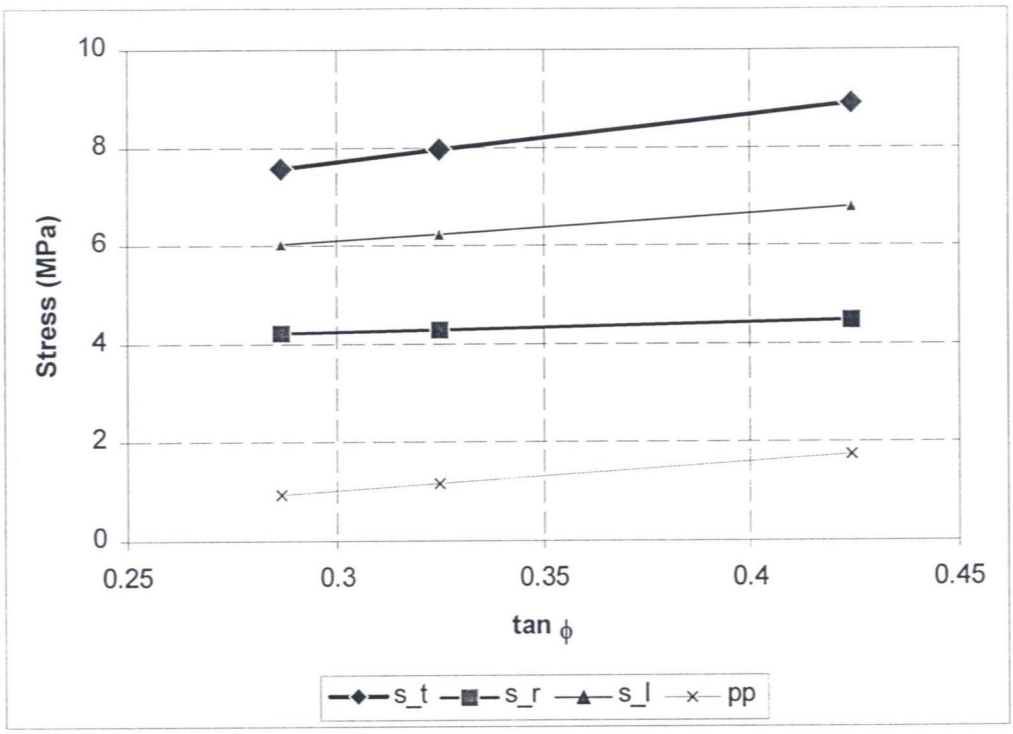

Figure B3: Influence of the friction angle on the total stress and on the pore pressure

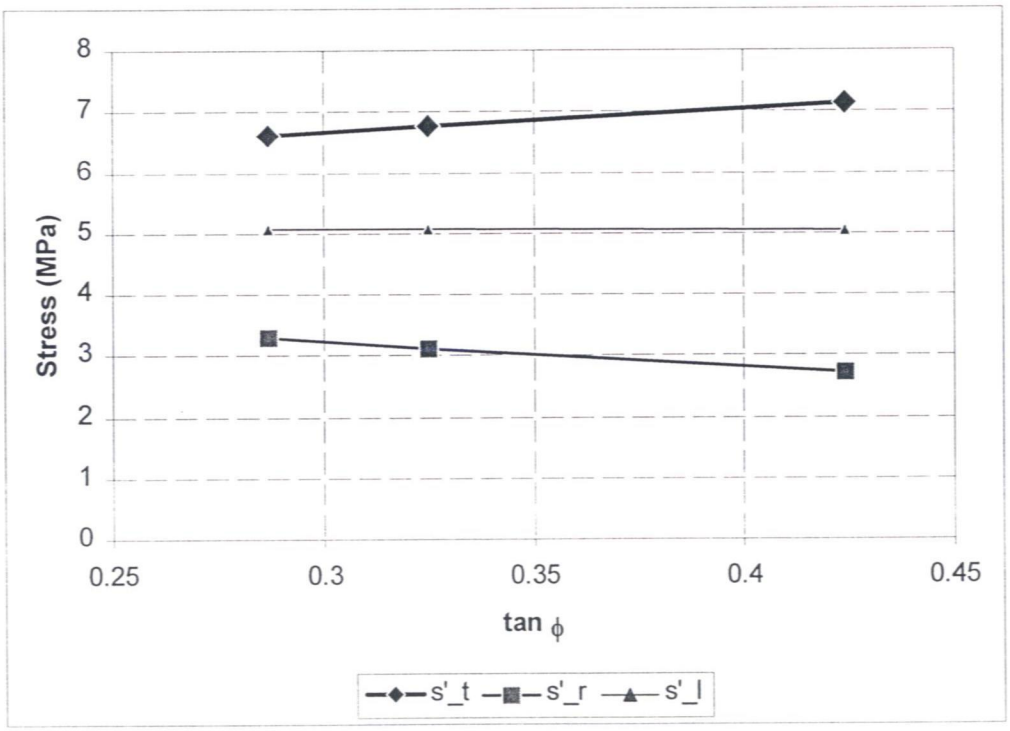

Figure B4: Influence of the friction angle on the effective stress

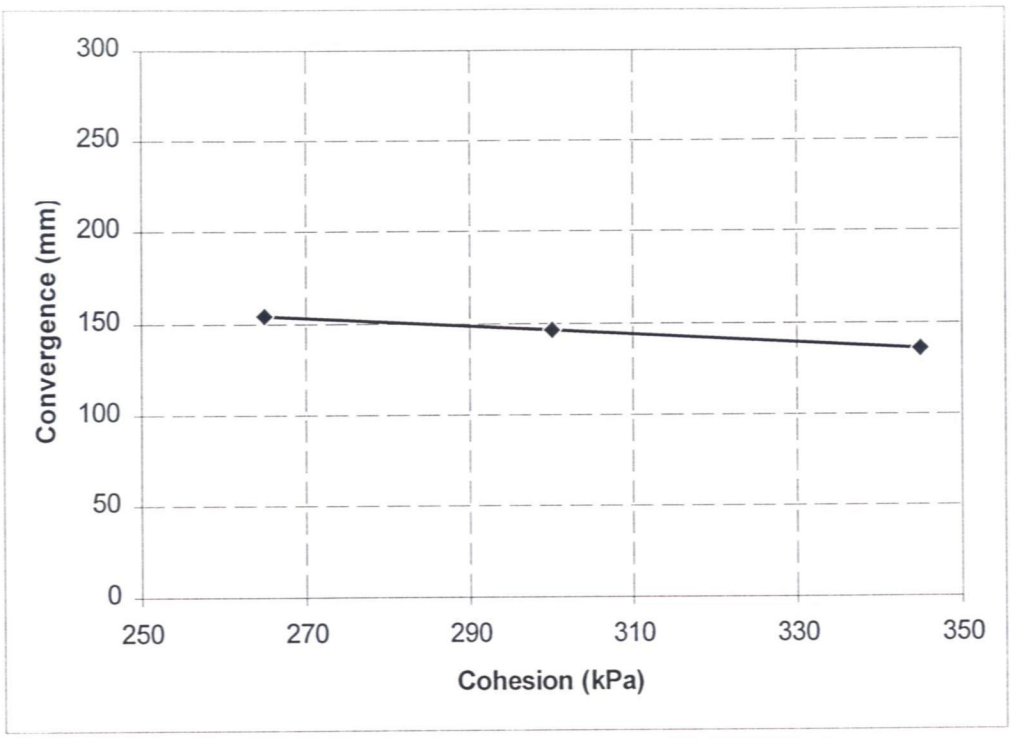

Figure B5: Influence of the cohesion on the convergence

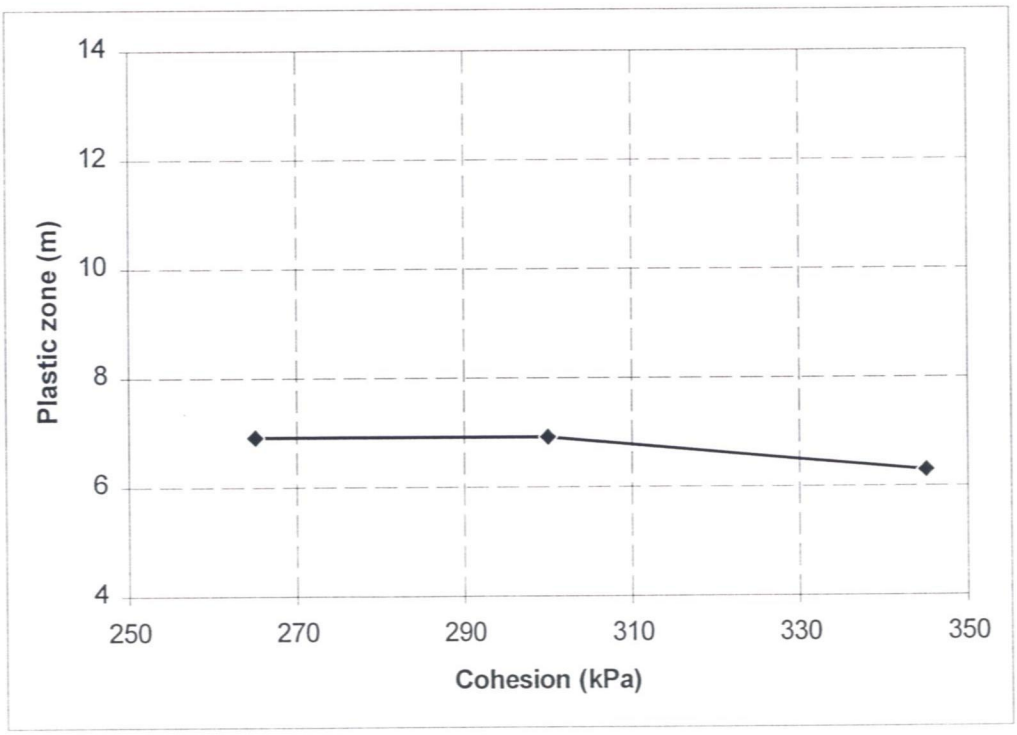

Figure B6: Influence of the cohesion on the extent of the plastic zone

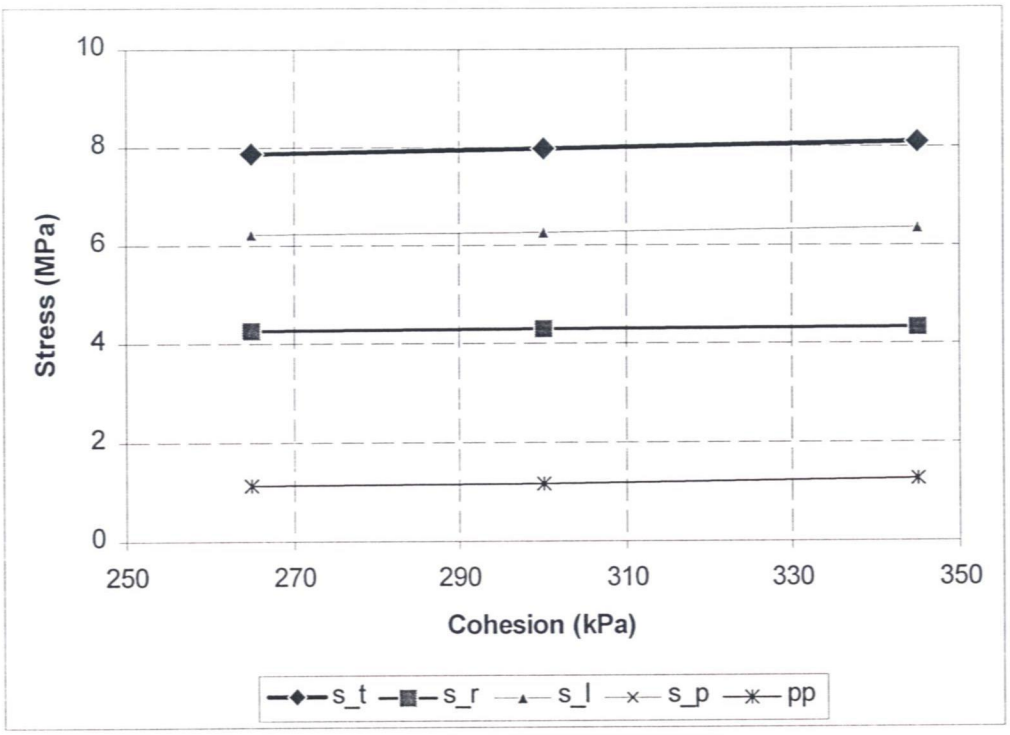

Figure B7: Influence of the cohesion on the total stess and on the pore pressure

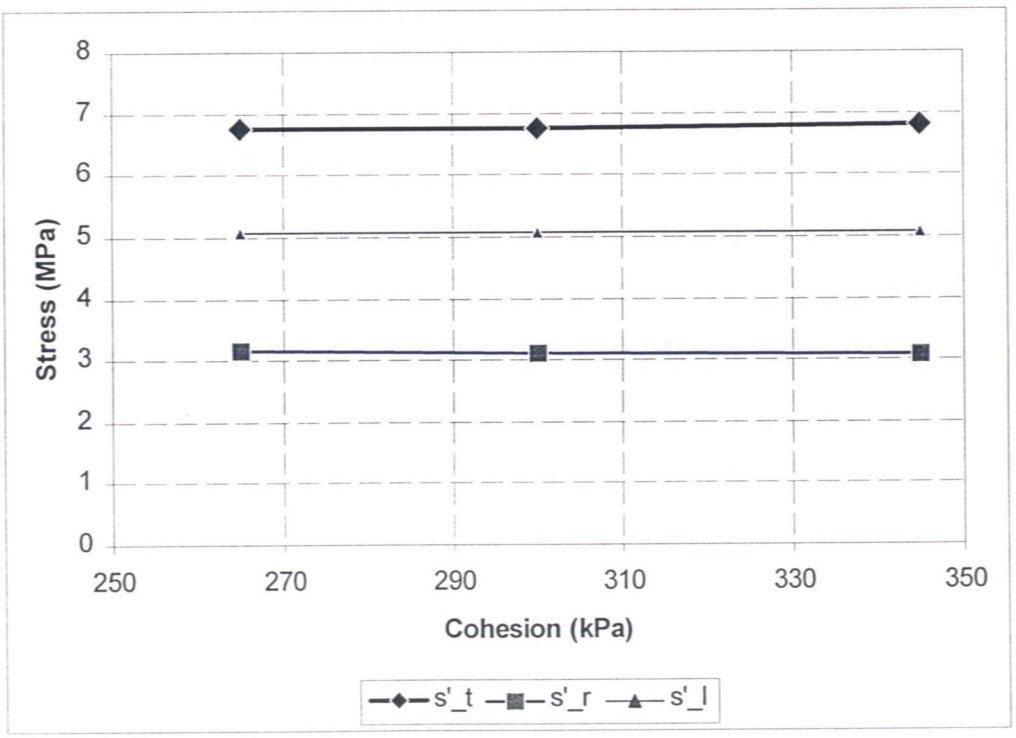

Figure B8: Influence of the cohesion on the effective stress

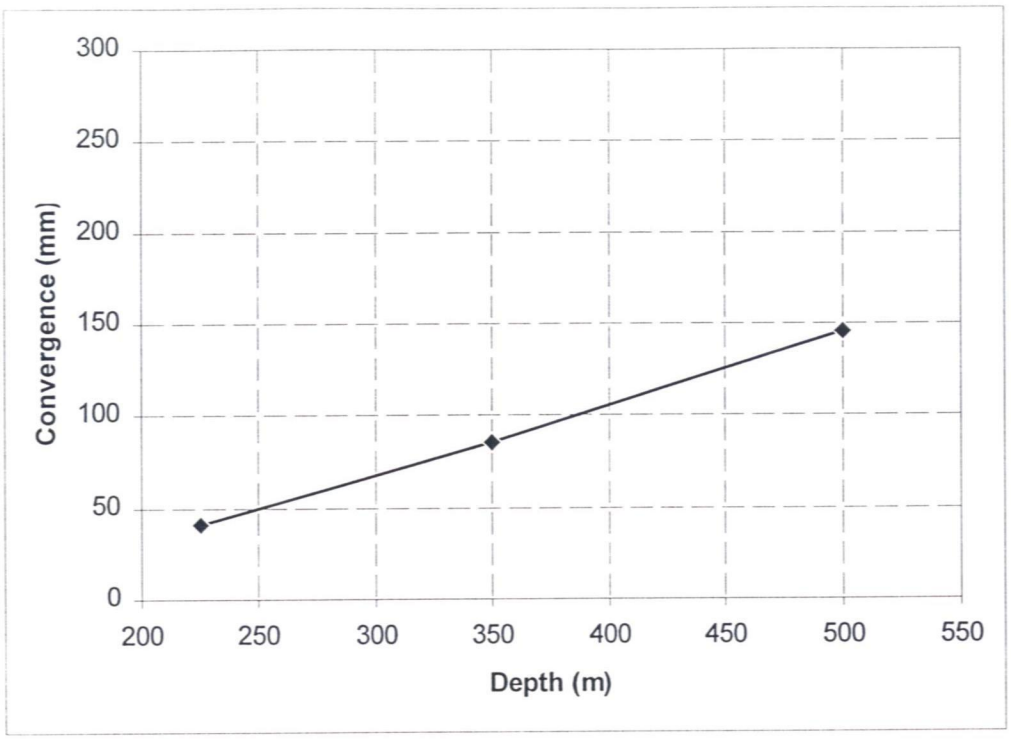

Figure B9: Influence of the depth on the convergence

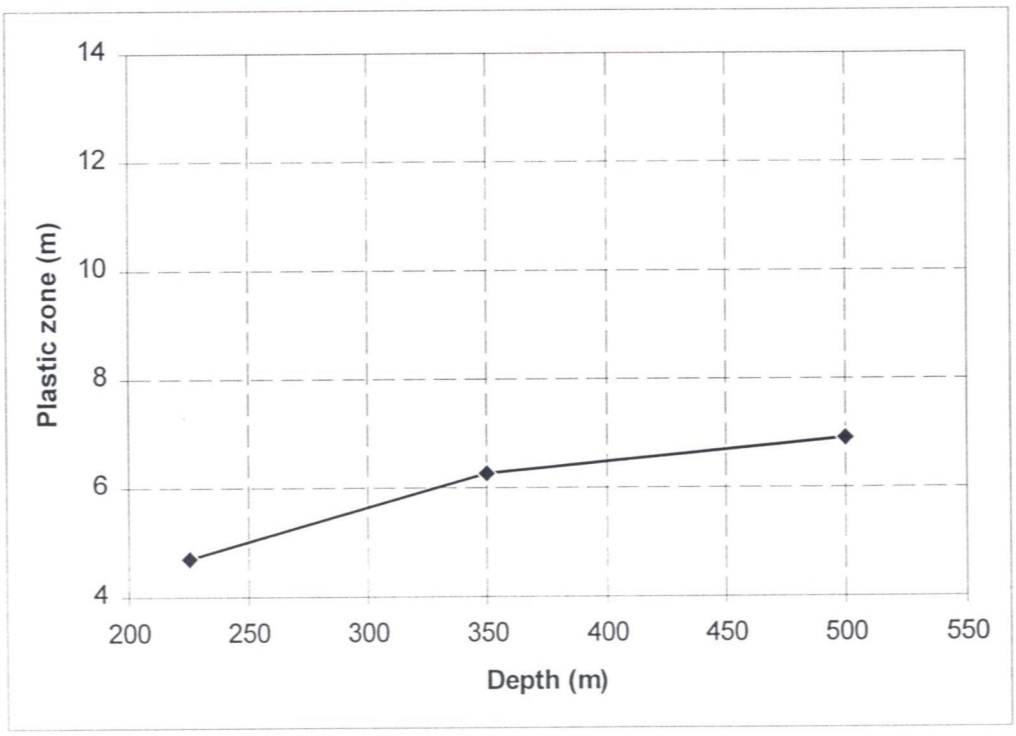

Figure B10: Influence of the depth on the extent of the plastic zone

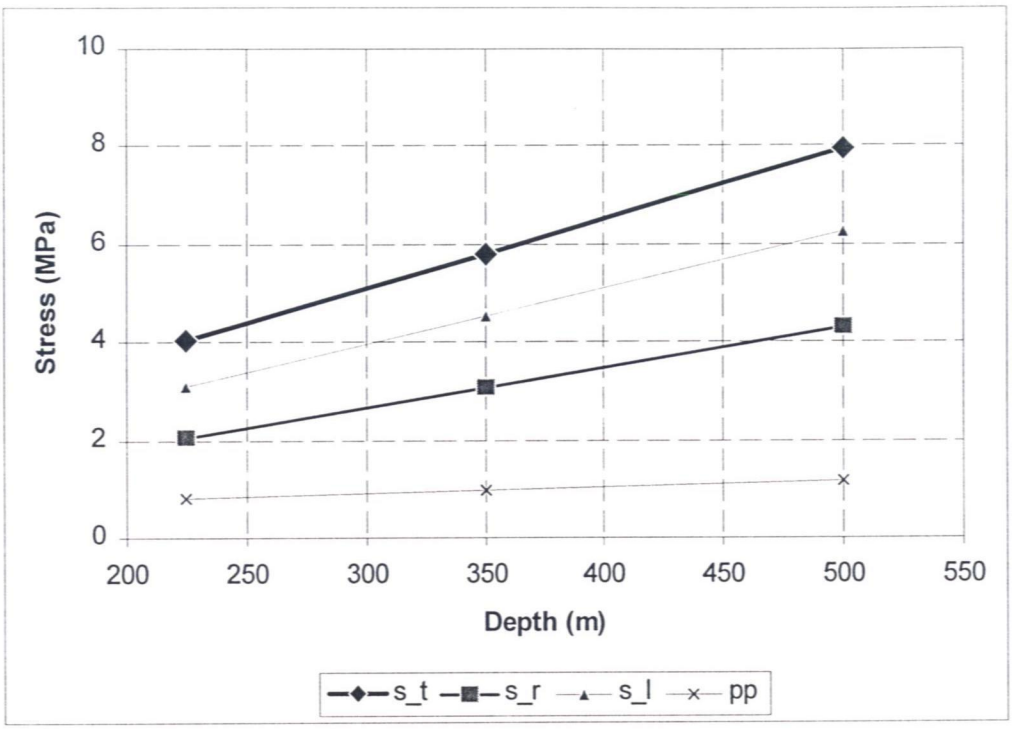

Figure B11: Influence of the depth on the total stress and on the pore pressure

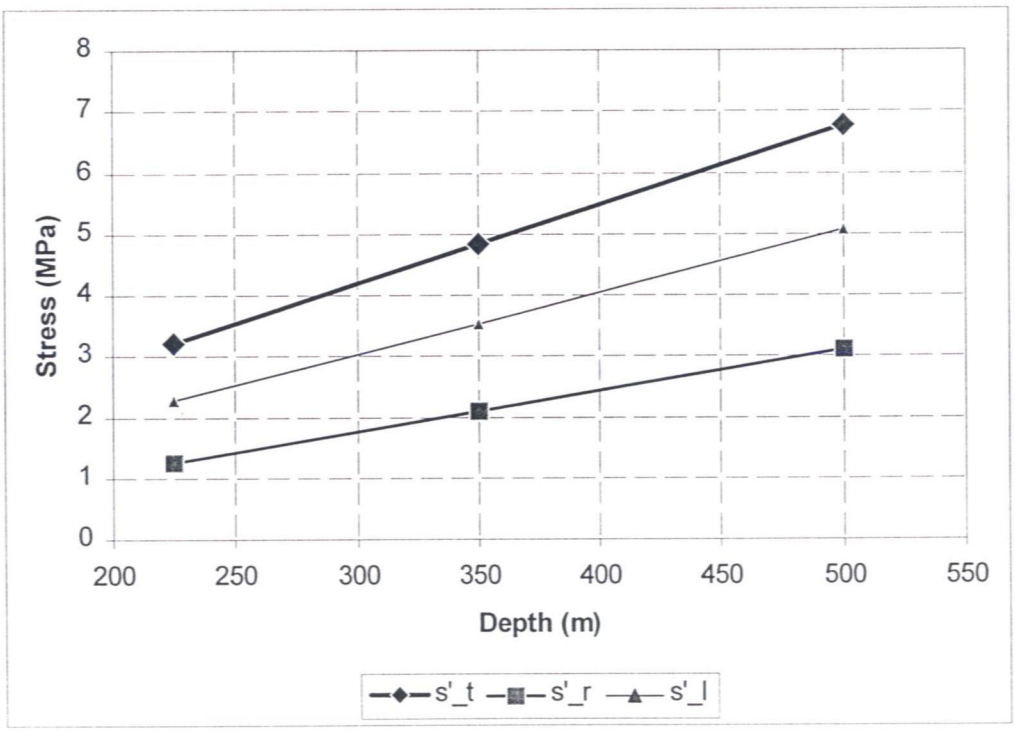

Figure B12: Influence of the depth on the effective stress

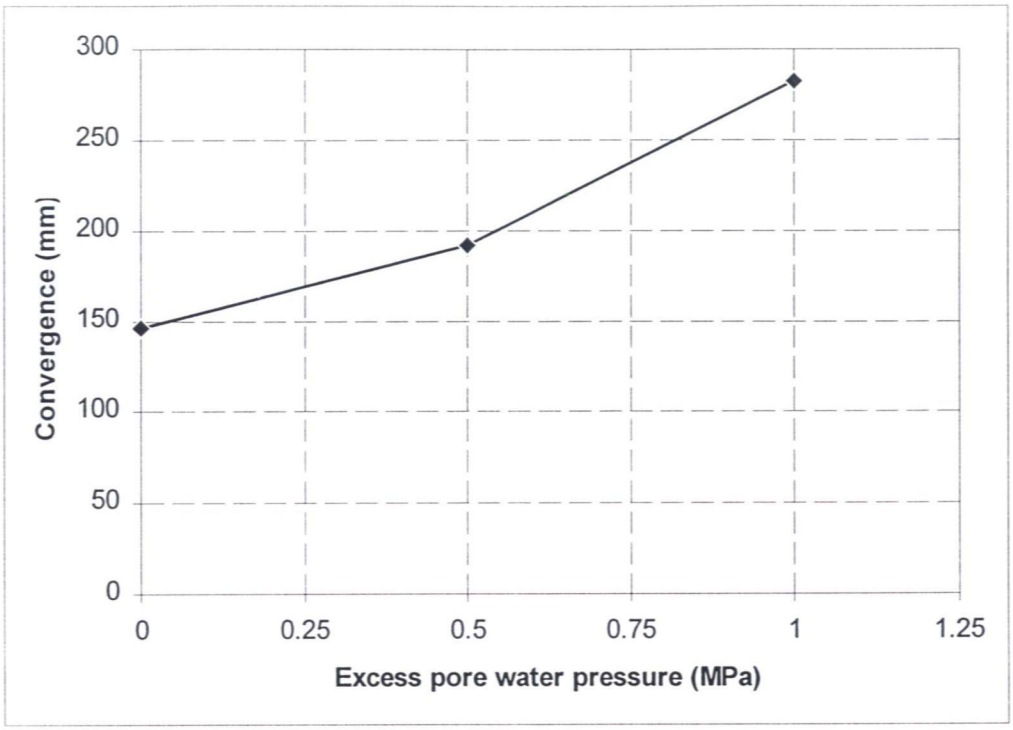

Figure B13: Influence of the excess pore water pressure on the convergence

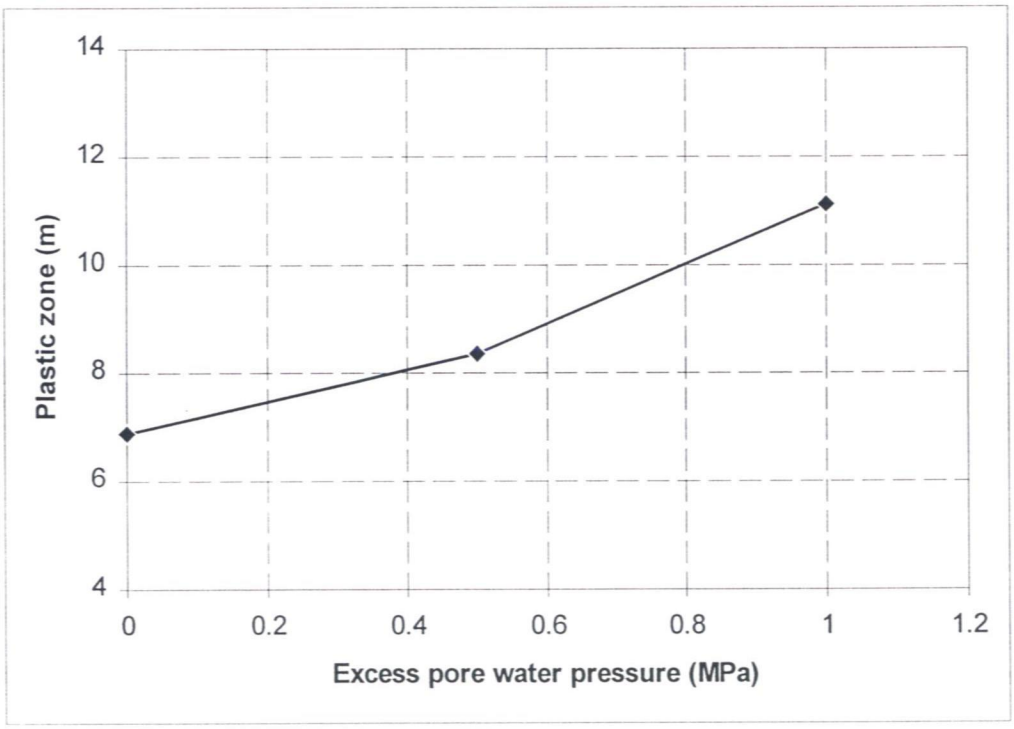

Figure B14: Influence of the excess pore water pressure on the extent of the plastic zone

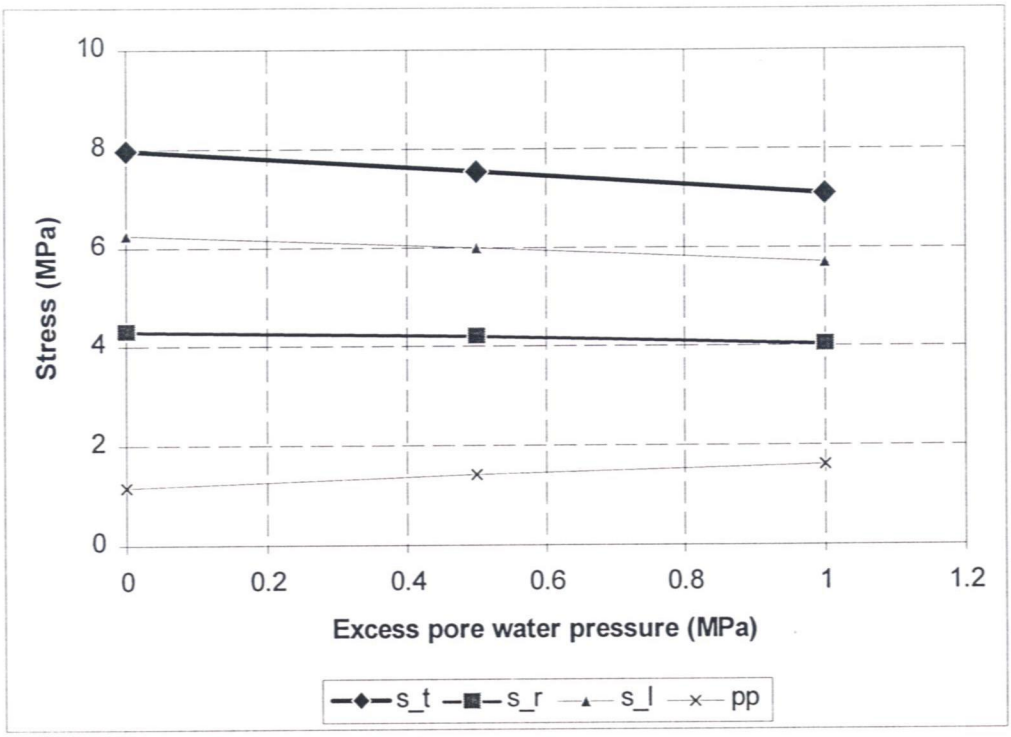

Figure B15: Influence of the excess pore water pressure on the total stress and on the pore water pressure

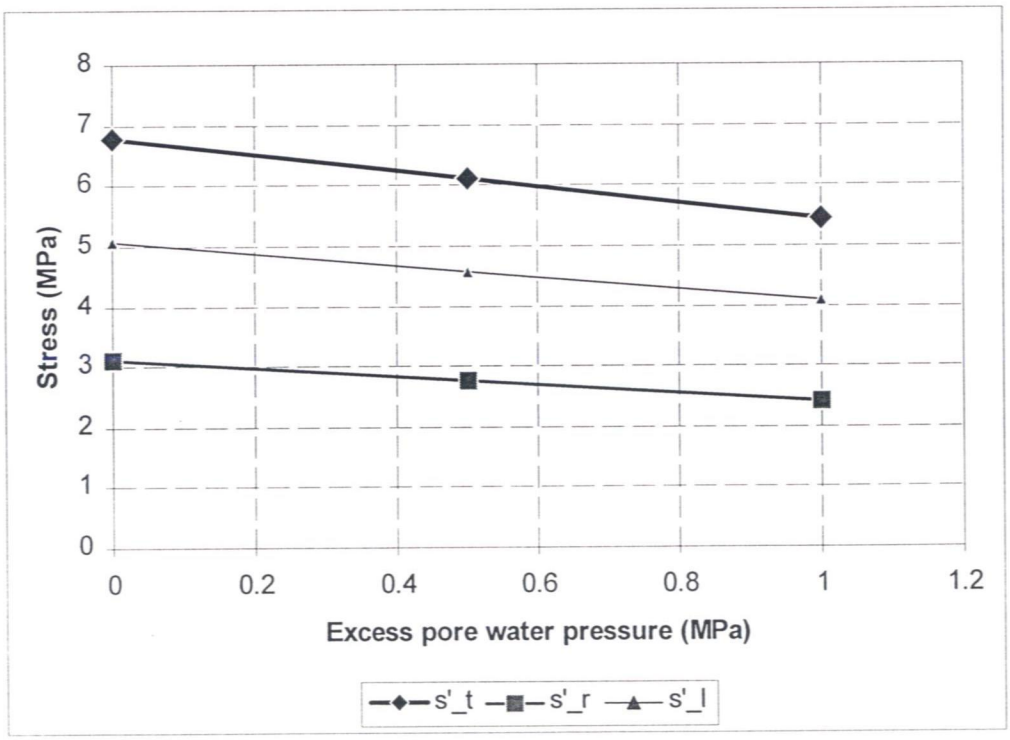

Figure B16: Influence of the excess pore water pressure on the effective stress

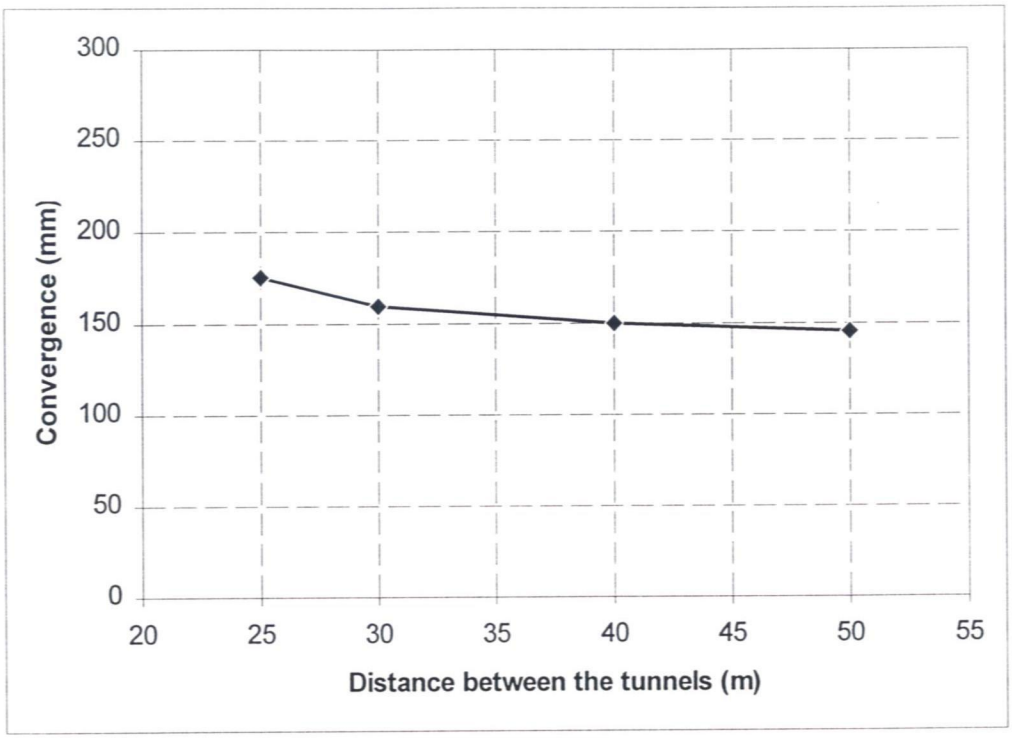

Figure B17: Influence of the distance between the tunnels on the convergence

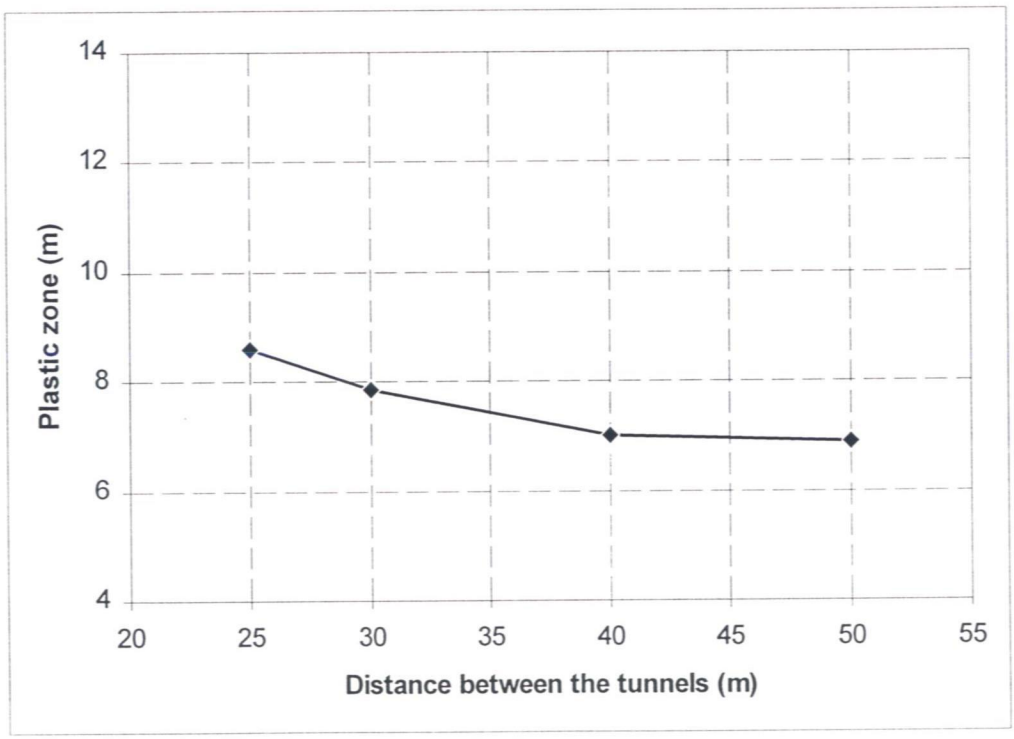

Figure B18: Influence of the distance between the tunnels on the extent of the plastic zone

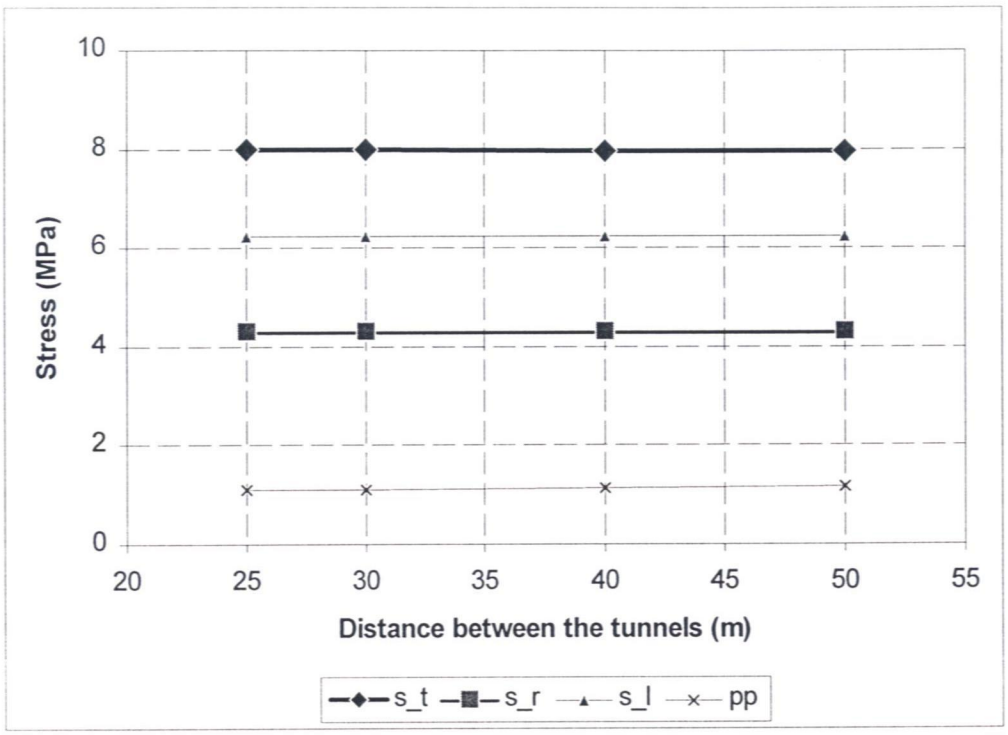

Figure B19: Influence of the distance between the tunnels on the total stress and on the pore pressure

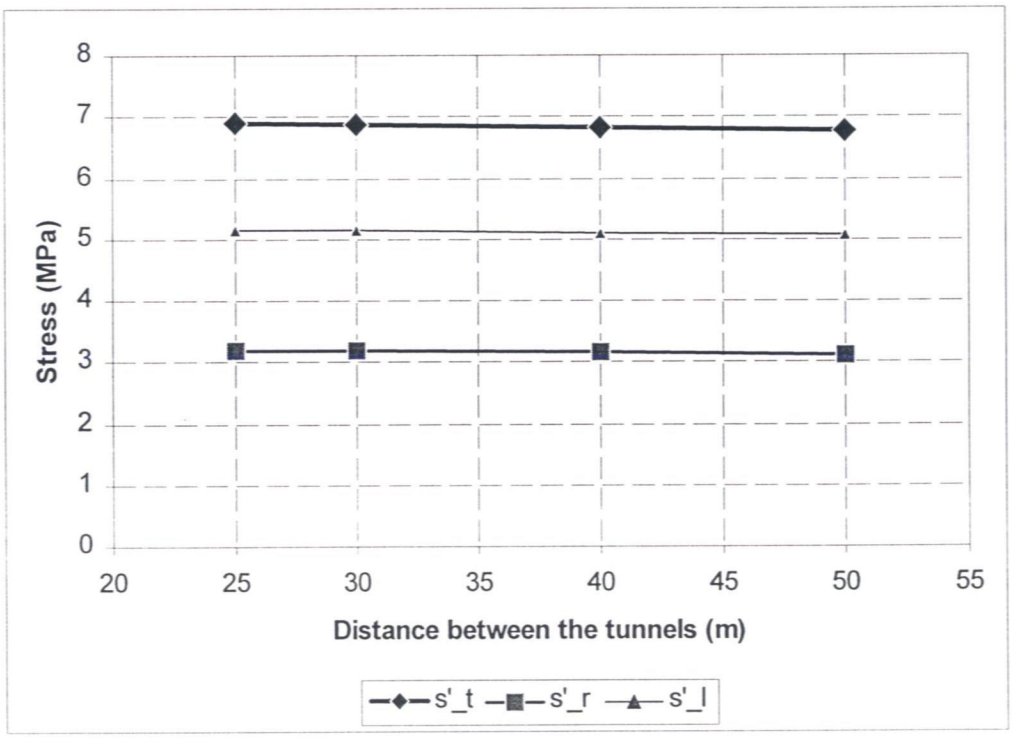

Figure B20: Influence of the distance between the tunnels on the effective stress

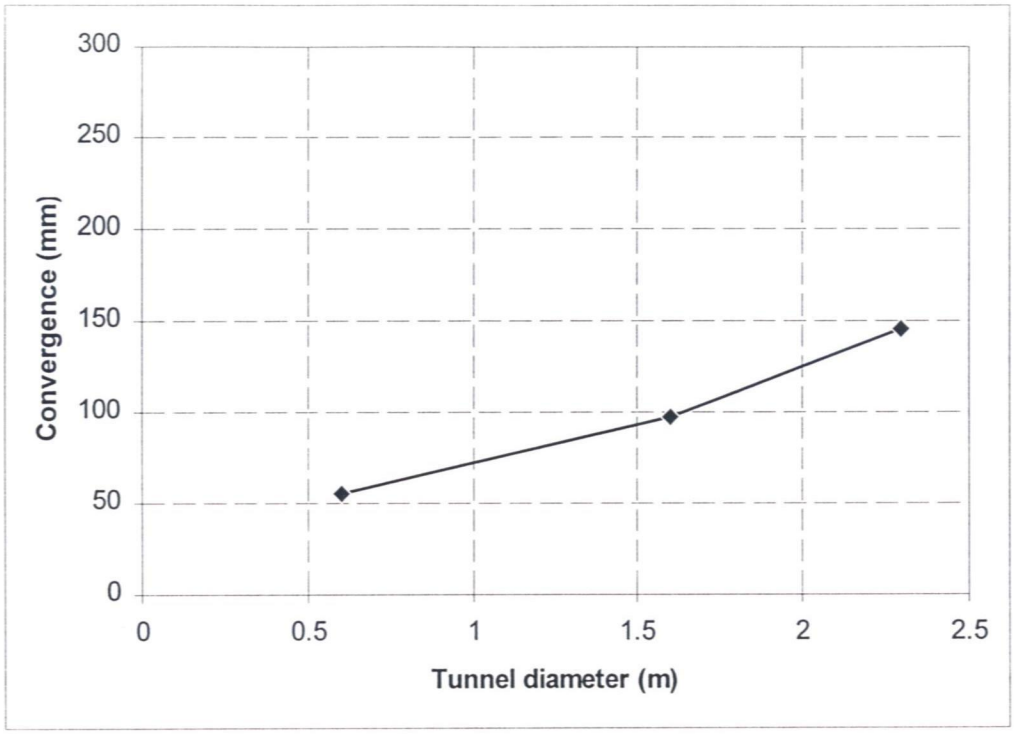

Figure B21: Influence of the tunnel diameter on the convergence

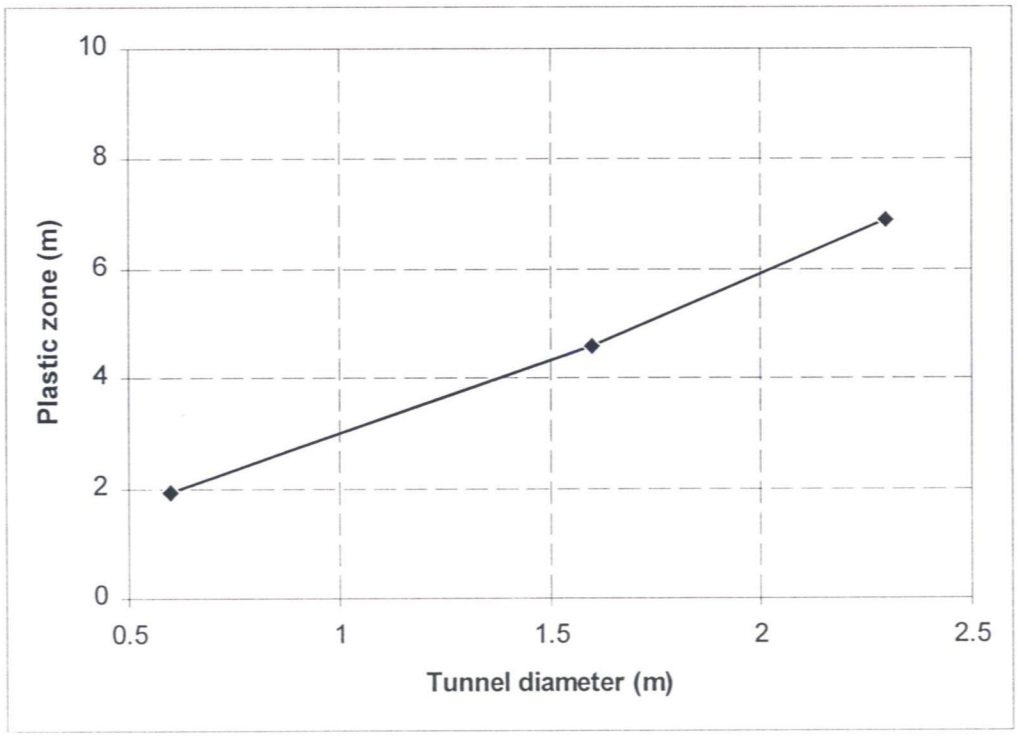

Figure B22: Influence of the tunnel diameter on the extent of the plastic zone

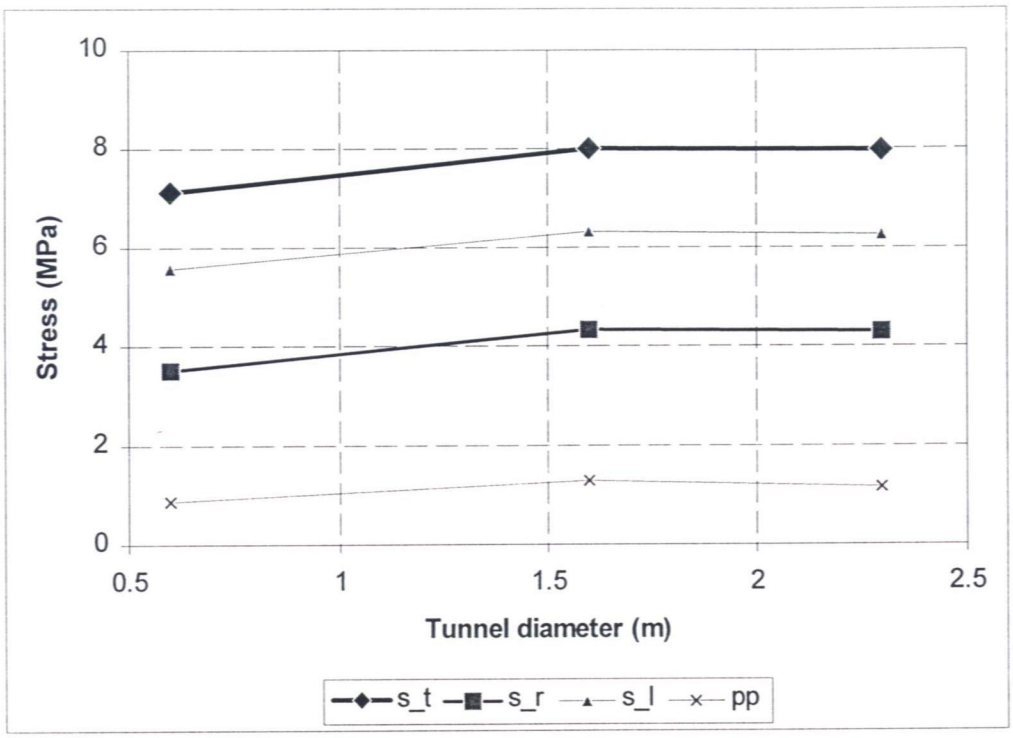

Figure B23: Influence of the tunnel diameter on the total stress and the pore pressure

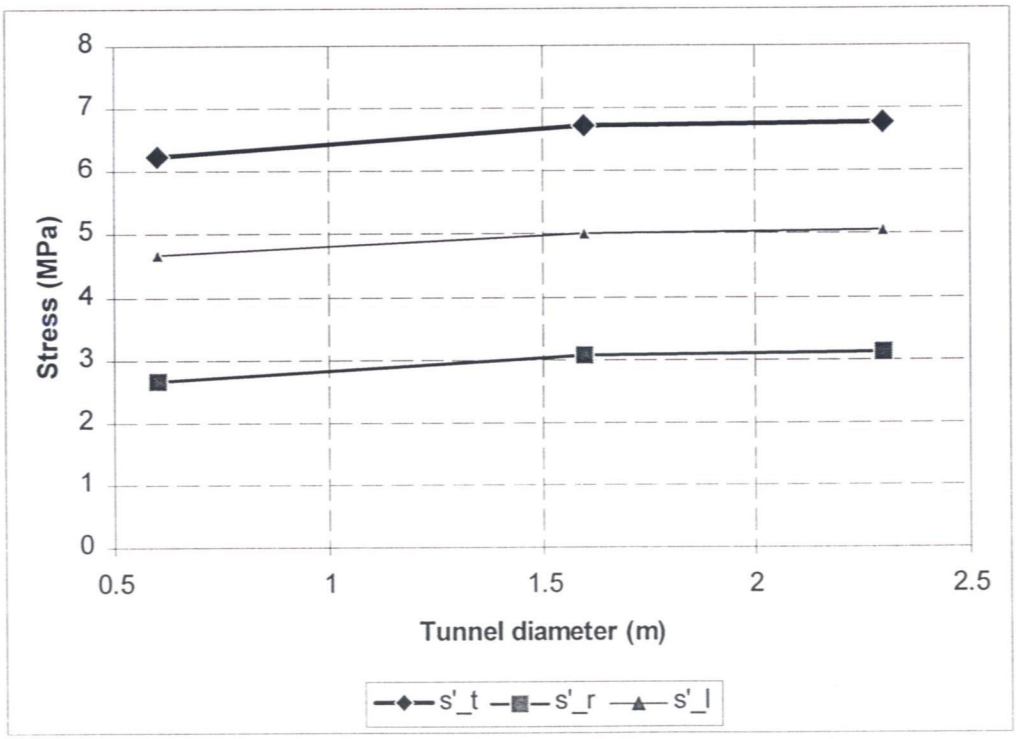

Figure B24: Influence of the tunnel diameter on the effective stress

Appendix C: Thermal modelling

C1 Modelling of the heat sources

For the thermal modelling, the three-dimensional boundary element package MAP3D is used. In the boundary element method only the surface of the rock mass to be analyzed needs to be discretized. These are for example the earth surface and the walls of an excavation. The modelled surfaces only have to be divided into smaller patches, the so-called 'surface elements'. This implies that the number of elements to be considered is significantly reduced in comparison to finite element or finite difference codes. The influence of the infinite rock mass is automatically considered in the analysis. These features make the method attractive to model the repository as a whole [G.N. Pande et al., 1990; S.L. Crouch et al., 1983].

For the temperature analysis, this means that only the parts of the tunnels kept at a fixed temperature have to be modelled; this is done as follows:

- It is assumed that the HLW canisters raise the temperature on the outside of the tunnels to a temperature of maximum 80°C. This temperature rise is modelled over a length of 4 m, corresponding to 3 times the length of the Cogema canisters. In the model, only these parts of the tunnels are modelled. Each part is approximated in the model by a rectangular prism with a height and a width equal to the tunnel diameter (i.e. 3,2 m or 1,2 m).
- The spatial distribution of the heat sources in the model corresponds to the spatial distribution of the heat sources in the repository.
- The earth surface is modelled as a plane extending at least 200 m beyond the repository.
- The number of 'surface elements', representing the earth surface and the tunnel walls, is kept to a minimum to make the modelling of the whole heat generating zone feasible. The choice of rectangular prisms as model for the tunnels, and the decision not to subdivide each side of the prism in more than one 'surface element' have to be seen in this light.
- Use is made of the existing symmetry with respect to the vertical plane parallel to the secondary and tertiary galleries. This allows to reduce the number of heat sources to be modelled by a factor 4.

The following boundary conditions are applied:

- Each 'surface element' of the modelled tunnels is kept at the same constant temperature.
- The surface plane is kept at a constant temperature of 10°C.

The following initial conditions are imposed:

- The in situ stresses are isotropic and vary linearly with the depth. The specific weight of the ground is assumed to amount to 20,5 kN/m^3.
- The thermal gradient is specified at 3°C/100 m with a temperature of 10°C at surface level.
- The analysis is carried out in total stresses, and the pore water pressure is not calculated separately. This approach was adopted as the main interest of the analysis is oriented towards the temperature distribution. The undrained material parameters are therefore used in the model ($E = 405$ MPa, $\nu = 0{,}487$, $\alpha = 4{,}19\ 10^{-5}/°C$).

C2. Analytical determination of the temperature in function of time and distance from the repository

The determination of the temperature in function of the time and space for a number of discrete heat sources out over a certain area, is only possible with software developed for this purpose, run on powerful computers. The problem requires a full three-dimensional analysis of the unsteady-state whereby the power generated by the sources decreases over time. For less complex problems, solutions can be derived by analytical expressions. As the assumptions made in deriving the analytical solution are not entirely applicable to the problem studied in this report, some artifice has to be employed to obtain a solution in agreement with the steady state solution obtained with the boundary element program.

Advantage is taken of the mathematical solution to the problem of the unsteady-state heat conduction in a semi-infinite solid. This solution can be expressed algebraically in closed form, which makes it easy to manipulate. Employing this solution implies a number of simplifications and assumptions though:

- The rock mass has a uniform temperature before the repository is built. This assumption stands in contrast with the applicable temperature gradient of 3°C and with the boundary condition imposing a temperature of 10°C on the earth surface plane. The artifice used to address the problem posed by the infinity of the analytical model, addresses these problems as well (see further).
- The temperature of the repository remains constant. The same assumption is upheld in the MAP3D simulations although the temperature depends on the time as the heat generation decreases over time. To get a feel for the influence a temperature decrease has on the temperature distribution in function of the time and in function of the height above the repository, the temperature distribution is calculated for different temperatures of the repository.
- The equation is solved for a semi-infinite solid; this implies that the repository is considered an infinite layer kept at a uniform temperature. Considering the repository as an infinite layer has two implications. It first implies that the separate heat sources are not modelled, but that the repository is modelled as a whole. This approximation is not valid just above the repository, but is acceptable at distances of 10 m and more above the plane containing the tunnel centres. The infinite layer approach secondly implies that the restricted size of the heat generating zone is not taken into account. In paragraph 2.4.3, it has been made clear that the actual size of the repository has to be taken into account to obtain acceptable results. In a model containing an infinite number of heat sources, the temperature can be expected to deviate from the temperature obtained in a model containing the actual number of heat sources as well. The way in which this problem is addressed is explained further on.
- The flow of the heat is perpendicular to the horizontal plane through the tunnel axes. This assumption can be accepted in the middle of the heat generating zone, where the temperature increases are most critical.
- The rock mass is homogeneous, having known thermal conductivity, density and specific heat.

With these simplifications and assumptions, the temperature T at a distance x above the repository is given by [H. Hens, 1992; A. Whillier, 1982]:

$$\frac{T-T_{db}}{T_v-T_{db}} = erf(X) + \exp\left(B+\frac{B^2}{4X^2}\right)\ erfc\left(X+\frac{B}{2X}\right) \qquad \text{(C1)}$$

where x = Distance above the repository (m).
T_{db} = Dry bulb temperature at which the repository is kept (°C).

T_v = Virgin temperature of the clay mass (°C).
B = Biot number.

$$X = \frac{x}{2\sqrt{at}}$$

a = Thermal diffusivity (m^2/s).
t = Time (s).

$$\text{erf}(X) = \frac{2}{\sqrt{\Pi}}\int_0^X e^{-t^2} dt$$

erfc(X) = 1- erf(X).

The Biot number can be taken as infinite, which allows to simplify the above equation to:

$$\frac{T - T_{db}}{T_v - T_{db}} = erf(X) \qquad \text{(C2)}$$

The solution for $t \rightarrow \infty$ should by definition be the steady state solution. For $t \rightarrow \infty$, $T \rightarrow T_{db}$ in (C1) and (C2), independently of the distance above the repository (x). This means that the steady state solution corresponding with (C1) and (C2) is a uniform temperature distribution equal to the temperature of the tunnel walls. The MAP3D simulations show, however, that the steady state solution is function of the height above the repository. The discrepancy between the two steady state solutions, can be brought back to two of the assumptions made in deriving the analytical solution: this solution is valid for an excavation that is equivalent to an infinite layer, and the virgin rock temperature is assumed to be uniform. The actual repository is limited in size though, and a temperature gradient together with an imposed surface temperature are modelled in the numerical model.
The following artifice is used to obtain a time-dependent temperature distribution with the analytical solution that for $t \rightarrow \infty$ corresponds to the steady state solution obtained with MAP3D. The temperatures T_v and T_{db} in (C2), are chosen in function of the height above the repository at which the temperature distribution is required. For T_v the actual in situ virgin temperature was chosen that corresponds with the height in question, and T_{db} is fixed at the temperature obtained from MAP3D at the selected height. Both the Figures 2.27 and 2.29 have been calculated in this way. In Figure 2.28, the temperature T_v is made function of the height above the repository while T_{db} is kept at a constant temperature of 80°C. The temperature distributions depicted in Figure 2.28 are therefore a slight overestimation of the temperature.

Appendix D: Excavation, ventilation, storage and backfilling schedule

D.1 Excavation

Phase 1, Shafts and shaft area

Phase 1.a, Shafts (2)

Geometry:
Length: 2 * (500 m + 20 m) = 1040 m
Diameter: 6,2 m
Total volume: 31398 m^3

Time planning:
Simultaneous excavations
Start on day +0

Preparation of sites: 3 months, or		60 working days
Excavation: 520 m @ 10 m / week results in 52 weeks or		260 working days
Installation of equipment and hauling machines: 3 months, or		60 working days
	Total:	380 working days

End on day +380

Ventilation requirements:

0,25m^3/s per square metre of cross section	
Auxiliary ventilation at shaft bottom	2 * 7,5 m^3/s
Aauxiliary ventilation at shaft top (+5% for autocompression, 0% losses)	2 * 7,9 m^3/s
Main ventilation	-
Maximum ducting length at any fan (5m from face and 25 m outside shaft)	540 m
Maximum pressure requirements	8,6 kPa

Rock material transport (during excavation period):
31398 m^3 during 260 working days, or 121 m^3/day on average

Phase 1.b, Bottom shaft areas (2) (Figure D.1)

Geometry:
Length: excavated: 2 * (25 + 50 + 50 + 50 + 25 - 6,2 m) = 2 * 193,6 m = 387,6 m
(6,2 m for the existing shafts)
scheduled: 400 m
Diameter: 5,4 m
Total volume: (400 - 2 * 6,2) * π * $2,7^2$ = 8877 m^3

Time planning:
Simultaneous excavations
Start on day +380

Preparation of site: 1 week, or		5 working days
Excavation: 200 m @ 2,5 m / day results in:		80 working days
	Total:	85 working days

End on day +465

Ventilation requirements:

0,25 m^3/s per square metre of cross sectional area	
Auxiliary ventilation at face	2 * 5,75 m^3/s
Auxiliary ventilation at shaft top (+5% for autocompression, 0% losses)	2 * 6,0 m^3/s
Main ventilation	-
Maximum ducting length for a single fan (5m from face and 25 m outside shaft)	645 m
Maximum pressure requirements	6,0 kPa

Rock material transport (during excavation period):
8877 m^3 during 80 working days, or 111 m^3/day on average

Phase 2, Basic primary layout (Excavation of three loops, one per type of waste)

Phase 2.a, Connection (1) between both shafts (Figure D.2)

Geometry:
Length: excavated: (1100 - 2 * 2,7 m) = 1094,6 m
scheduled: 1100 m
Diameter: 4,6 m
Total volume: 18191m^3

Time planning:
Single face
Start on day +465

Installation of equipment (machine 1): 1 week, or		5 working days
Excavation: 1100 m @ 10 m / day results in:		110 working days
	Total:	115 working days

End on day +580

Ventilation requirements:

0,25 m^3/s per square metre of cross sectional area	
Auxiliary ventilation at face	4,15 m^3/s
Auxiliary ventilation at shaft top (+5% for autocompression, 0% losses)	4,36 m^3/s
Main ventilation	-
Maximum ducting length for a single fan (5m from face and 25 m outside shaft)	1695 m
Maximum pressure requirements	8,2 kPa

Rock material transport (during excavation period):
18191 m^3 during 110 working days, or 165 m^3/day

Phase 2.b. Three loops (Figure D.3)

Geometry:

Length: excavated

Loop HLW-W	850 + 1100 + 850 - 2 * 2,3 m =	2795,4 m
Loop MLW	1100 - 2 * 2,3 m =	1095,4 m
Loop HLW-C	50 + 1100 + 50 -2 * 2,3 m =	1195,4 m
	Total:	5086,2 m

scheduled

Loop HLW-W	2800 m	
Loop MLW	1100 m	
Loop HLW-C	1200 m	
	Total:	5100 m

Diameter: 4,6 m

Total volume: 84528 m^3

Time planning:

Three faces (simultaneous)

Machine 1: Start on day +580

Removal and Installation: 1 week, or	5 working days
850m @ 10m/day (HLW-W)	85 working days
Repositioning: 1 week, or	5 working days
1100 m @ 10 m/day (HLW-W)	110 working days
Total:	205 working days

End on day +785

Machine 2: Start on day +580

Installation: 1 week, or	5 working days
850m @ 10m/day (HLW-W)	85 working days
Removal and installation: 1 week, or	5 working days
1100 m @ 10 m/day (MLW)	110 working days
Total:	205 working days

End on day +785

Machine 3: Start on +580

Installation: 1 week, or	5 working days
50 m @ 10 m/day (HLW-C)	5 working days
Repositioning: 1 week, or	5 working days
1100 m @ 10 m/day (HLW-C)	110 working days
Removal and installation: 1 week, or	5 working days
50 m @ 10 m/day (HLW-C)	5 working days
Total:	135 working days

End on day +715

[Remark: Machine 3 starts 70 working days earlier on Phase 3 than machines 1 and 2]

Loops	HLW-W:	Start on day +580
		End on day +785
	MLW:	Start on day +580
		End on day +785
	HLW-C	Start on day +580
		End on day +715

Ventilation requirements:

0,25 m^3/s per square metre of cross sectional area	
Auxiliary ventilation at face	3 * 4,15 m^3/s
Ventilation of connection between the shafts (air velocity of 0,25 m/s in the lined tunnel)	2,4 m^3/s
Main ventilation (air volumes at faces* 2 to prevent recirculation, losses 10 %, autocompression 5%)	31,5 m^3/s
Maximum ducting length for a single fan (5 m from face and 15 m into through ventilation)	1960 m
Maximum pressure requirements	8,6 kPa

Rock material transport (during excavation period):
Maximum per day: 499 m^3/day

Phase 3, Primary galleries and part of secondary galleries (Figure D.4) (Excavation of three secondary loops, one per type of waste)

Geometry:
Length: excavated

Loop HLW-W		400 + 1000 + 400 - 2 * 2,3 m = 1795,4 m
Loop MLW		800 + 1000 + 800 - 2 * 2,3 m = 2595,4 m
Loop HLW-C		1350 + 1000 + 1350 - 2 * 2,3 m = 2695,4 m
	Total:	7086,2 m

scheduled

Loop HLW-W		1800 m
Loop MLW		2600 m
Loop HLW-C		2700 m
	Total:	7100 m

Diameter: 4,6 m
Total volume: 117766 m^3

Time planning:
Three faces (simultaneous)

Machine 1:	Start on day +785		
	Removal and Installation: 1 week, or		5 working days
	1350 m @ 10 m/day (HLW-C)		135 working days
	Removal and Installation: 1 week, or		5 working days
	400m @ 10m/day (HLW-W)		40 working days
	Repositioning: 1 week, or		5 working days
	1000 m @ 10 m/day (HLW-W)		100 working days
		Total:	290 working days
	End on day +1075		
Machine 2:	Start on day +785		
	Removal and Installation: 1 week, or		5 working days
	400m @ 10m/day (HLW-W)		40 working days
	Removal and Installation: 1 week, or		5 working days
	800 m @ 10 m/day (MLW)		80 working days

Repositioning: 1 week, or	5 working days
1000 m @ 10 m/day (MLW)	100 working days
	Total: 235 working days

End on day +1020

Machine 3: Start on day +715

Removal and Installation: 1 week, or	5 working days
1350 m @ 10 m/day (HLW-C)	135 working days
Repositioning: 1 week, or	5 working days
1000 m @ 10 m/day (HLW-C)	100 working days
Removal and Installation: 1 week, or	5 working days
800 m @ 10 m/day (MLW)	80 working days
	Total: 330 working days

[Remark: first 70 working days of machine 3 are simultaneous to Phase 2 for machines 1 and 2]

End on day + 1045

Loops HLW-W: Start on day +785
End on day +1075
MLW: Start on day +830
End on day +1045
HLW-C Start on day +715
End on day +960

Ventilation requirements:

0,25 m^3/s per square metre of cross sectional area	
Auxiliary ventilation at face	3 * 4,15 m^3/s
Ventilation of connection between the shafts (air velocity of 0,25 m/s in the lined tunnel)	2,4 m^3/s
Main ventilation (air volumes at faces* 2 to prevent recirculation, losses 10 %, autocompression 5%)	31,5 m^3/s
Maximum ducting length for a single fan (5 m from face and 15 m into through ventilation)	2360 m
Maximum pressure requirements	10,4 kPa

Rock material transport (during excavation period):
Maximum per day: 499 m^3/day

Phase 4, Secondary galleries (Figure D.5)

Geometry:
Length: excavated

HLW-W	7 * (1000 - 2 * 2,3 m) = 6967,8 m
MLW	15 *(1000 - 2 * 2,3 m) = 14931,0 m
HLW-C	26 *(1000 - 2 * 2,3 m) = 25880,4 m
Total:	47779,2 m

scheduled

HLW-W	7000 m

MLW 15000 m
HLW-C 26000 m
Total: 48000 m

Diameter: 4,6 m
Total volume: 794044 m^3

Time planning:
Five faces (simultaneous)

Machine 1: Start on day +1075

7 * Removal and Installation: 1 week, or 1000 m @ 10 m/day (HLW-W)

7* 5 working days
7* 100 working days
Sub-total: 735 working days

2 * Removal and Installation: 1 week, or 1000 m @ 10 m/day (MLW)

2* 5 working days
2* 100 working days
Sub-total: 210 working days

Total: 945 working days

End on day +2020

Machine 2: Start on day +1020

10 * Removal and Installation: 1 week, or 1000 m @ 10 m/day (HLW-C)

10* 5 working days
10* 100 working days
Total: 1050 working days

End on day +2070

Machine 3: Start on day +1045

9 * Removal and Installation: 1 week, or 1000 m @ 10 m/day (MLW)

9* 5 working days
9* 100 working days
Total: 945 working days

End on day +1990

Machine 4: Start on day +960

10 * Removal and Installation: 1 week, or 1000 m @ 10 m/day (HLW-C)

10* 5 working days
10* 100 working days
Total: 1050 working days

End on day +2010

Machine 5: Start on day +960

6 * Removal and Installation: 1 week, or 1000 m @ 10 m/day (HLW-C)

6* 5 working days
6* 100 working days
Sub-total: 630 working days

4 * Removal and Installation: 1 week, or 1000 m @ 10 m/day (MLW)

4* 5 working days
4* 100 working days
Sub-total: 420 working days

Total: 1050 working days

End on day +2010

Zones HLW-W: Start on day +1075
End on day +1810

MLW: Start on day +1045
End on day +2075
HLW-C Start on day +960
End on day +2020

Ventilation requirements:
0,25 m^3/s per square metre of cross sectional area
Auxiliary ventilation at face 5 * 4,15 m^3/s
Ventilation of connection between the shafts (air velocity of 0,25 m/s in the lined tunnel) 2,4 m^3/s
Main ventilation (air volumes at faces* 2 to prevent recirculation, losses 10 %, autocompression 5%) 50,7 m^3/s
Maximum ducting length for a single fan 1510 m
(5 m from face and 15 m into through ventilation)
Maximum pressure requirements 6,7 kPa

Rock material transport (during excavation period):
Maximum per day: 831 m^3/day

Phase 5, Tertiary galleries

Phase 5.a and 5.b are carried out simultaneously. The rock material transport and the ventilation requirements are therefore summarized at the end of phase 5.b, and cover the whole of phase 5.

Phase 5.a, MLW zone

Geometry:
Length: excavated 24 * (800-32*2,3 m) = 17433,6 m
scheduled 24 * 800 m = 19200 m
Diameter: 3,2 m
Total volume: 140209 m^3

Time planning:
Three faces (simultaneous)
Machine 1: Start on day +0
8 * Removal and Installation: 1 week, or 8* 5 working days
800 m @ 10 m/day 8* 80 working days
Total: 680 working days
End on day +680

Machine 2: Start on day +0
8 * Removal and Installation: 1 week, or 8* 5 working days
800 m @ 10 m/day 8* 80 working days
Total: 680 working days
End on day +680

Machine 3: Start on day +0

8 *	Removal and Installation: 1 week, or		8* 5 working days
	800 m @ 10 m/day		8* 80 working days
		Total:	680 working days

End on day +680

Phase 5.b , HLW-W and HLW-C zones

Geometry:

Length: excavated

HLW-W 19 * (15 - 2,3 m + 7 * (15 - 2,3 m + 15 - 2,3 m) + 15 - 2,3 m) = 3860,8 m

HLW-C 24 * (15 - 2,3 m + 26 *(15 - 2,3 m + 15 - 2,3 m) + 15 - 2,3 m) = 16459,2 m

Total: 20320 m

scheduled

HLW-W 4560 m

HLW-C 19440 m

Total: 24000 m

Diameter: 3,2 m

Total volume: 163423 m^3

Time planning:

Five faces (simultaneous)

Machine 4: Start on day +0

2 *	Removal and Installation: 1 week, or			2* 5 working days
19 *	Repositioning and excavation of 15 m	(HLW-W)		2*19*3 working days
			Sub-total:	124 working days
3 *	Removal and Installation: 1 week, or			3* 5 working days
19 *	Repositioning and excavation of 2*15 m	(HLW-W)		3*19*5 working days
			Sub-total:	300 working days
1 *	Removal and Installation: 1 week, or			1* 5 working days
24 *	Repositioning and excavation of 15 m	(HLW-C)		1*24*3 working days
			Sub-total:	77 working days
2 *	Removal and Installation: 1 week, or			2* 5 working days
24 *	Repositioning and excavation of 2*15m	(HLW-C)		2*24*5 working days
			Sub-total:	250 working days
			Total:	751 working days

End on day +751

Machine 5: Start on day +0

4 *	Removal and Installation: 1 week, or			4* 5 working days
19 *	Repositioning and excavation of 2*15m	(HLW-W)		4*19*5 working days
			Sub-total:	400 working days
1 *	Removal and Installation: 1 week, or			1* 5 working days
24 *	Repositioning and excavation of 15 m	(HLW-C)		1*24*3 working days
			Sub-total:	77 working days

	3 *	Removal and Installation: 1 week, or		3* 5 working days
	24 *	Repositioning and excavation of 2*15m	(HLW-C)	3*24*5 working days
			Sub-total:	375 working days
			Total:	852 working days

End on day +852

Machine 6: Start on day +0

	7 *	Removal and Installation: 1 week, or		7* 5 working days
	24 *	Repositioning and excavation of 2*15m	(HLW-C)	7*24*5 working days
			Total:	875 working days

End on day +875

Machine 7: Start on day +0

	7 *	Removal and Installation: 1 week, or		7* 5 working days
	24 *	Repositioning and excavation of 2*15m	(HLW-C)	7*24*5 working days
			Total:	875 working days

End on day +875

Machine 8: Start on day +0

	7 *	Removal and Installation: 1 week, or		7* 5 working days
	24 *	Repositioning and excavation of 2*15m	(HLW-C)	7*24*5 working days
			Total:	875 working days

End on day +875

Ventilation requirements:

0,25 m^3/s per square metre of cross sectional area	
Auxiliary ventilation at face	8 * 2,01 m^3/s
Ventilation of connection between the shafts (air velocity of 0,25 m/s in the lined tunnel)	2,4 m^3/s
Main ventilation (air volumes at faces* 2 to prevent recirculation, losses 20 %, autocompression 5%)	43,5 m^3/s
Maximum ducting length for a single fan (570 mm ducts) (5 m from face and 15 m into through ventilation)	60 m
Maximum pressure requirements	0,3 kPa

Rock material transport (during excavation period):

643 m^3/day

D.2 Storage of Waste

Phase 6, Storage of waste and filling of storage galleries

Phase 6.a, HLW-W zone

Geometry:

Total number of drums:	300
Volume per drum (including shroud):	0,31 m^3
Volume of storage gallery (length to be filled12,2 m, diameter 2,2 m):	46,38m^3
Filling material required per drum:	46,07 m^3

Filling material required for entire section:
13821 m^3

Time planning:

300*	Preparation of storage gallery:	1 working day
	Transport and storage of 1 drum:	1 working day
	Filling of storage gallery:	1 working day

If one assumes that the three actions can take place simultaneously, 302 working days are required.

Filling material transport:
46 m^3 per day

Phase 6.b, HLW-C zone

Geometry:

Total number of drums:	20 with volume of 0,175 m^3 1040 with volume of 0,21 m^3 200 with volume of 1,46 m^3	
Total volume of drums:		513,9 m^3
Volume of storage gallery (length to be filled12,2 m, diameter 2,2 m):		46,38m^3
Total volume of 1260 storage galleries:		58439 m^3

Filling material required for entire section:
57925 m^3

Time planning:

1260/2*	Preparation of 2 storage galleries:	1 working day
	Transport and storage of 2 drums:	1 working day
	Filling of 2 storage galleries:	1 working day

If one assumes that the three actions can take place simultaneously, 632 working days are required.

Filling material transport:
92 m^3 per day

Phase 6.c, MLW zone

Geometry:

Total number of drums:	52508 with volume of 0,20 m^3 400 with volume of 1,18 m^3

3380 with volume of 2,43 m^3
Total: 56288
Total volume of drums: 19173 m^3

Filling material required for entire zone:
--

Time planning:
56288 drums @ 50 drums/day: 1126 days

Filling material transport: not applicable

D.3 Filling of access galleries

Phase 7, Filling of secondary tunnels

Phase 7.a, HLW-W zone

Geometry:
Number of tunnels: 9
Volume of 1 tunnel (length 996,5 m, diameter 3,5 m): 9587 m^3

Filling material required for entire zone:
86287 m^3

Time planning:
500 m^3/day: 172 working days

Filling material transport:
500 m^3/day

Phase 7.b, HLW-C zone

Geometry:
Number of tunnels: 28
Volume of 1 tunnel (length 996,5 m, diameter 3,5 m): 9587 m^3

Filling material required for entire zone:
268436 m^3

Time planning:
500 m^3/day: 537 working days

Filling material transport:
500 m^3/day

Phase 8, Filling of primary galleries

Phase 8.a, HLW-W zone

Geometry:
Length of tunnels: 2 * (400 + 850 m + 50 m) = 2600 m
Diameter of tunnels: 3,5 m

Filling material required for entire section:
25015 m^3

Time planning:
500 m^3/day: 50 working days

Filling material transport:
500 m^3/day

Phase 8.b, HLW-C zone

Geometry:
Length of tunnels: 2 * (50 + 50 + 1350) = 2900 m
Diameter of tunnels: 3,5 m

Filling material required for entire zone:
27901 m^3

Time planning:
500 m^3/day: 56 working days

Filling material transport:
500 m^3/day

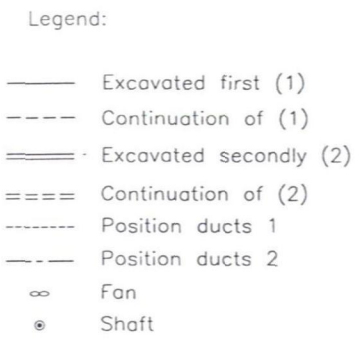

Legend Figures appendix D

Excavated first (1):	the tunnels excavated at the start of each phase.
Continuation of (1):	continuation of the trajectory of (1) up to a major move.
Excavated secondly(2):	the tunnels excavated after a major move.
Continuation of (2):	continuation of the trajectory of (2) up to the end of the phase.
Position ducts 1:	position of the ducts corresponding to (1).
Position ducts (2):	position of the ducts corresponding to (2).
Fan:	Position of the auxiliary fans.
Shaft:	Vertical shafts providing access to the workings.

The sketches in appendix D are not drawn to scale.

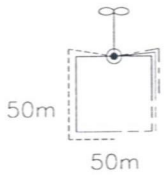

Figure D1: Phase 1.b. Shaft bottom area

Figure D2: Phase 2.a. Connection between both shafts

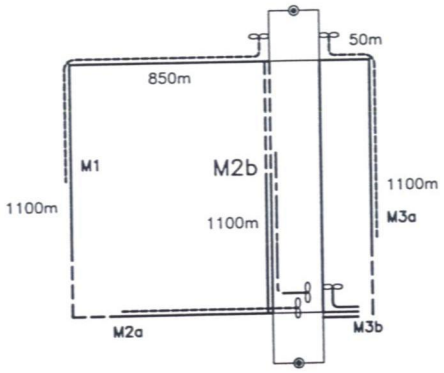

Figure D3: Phase 2.b. Three main loops

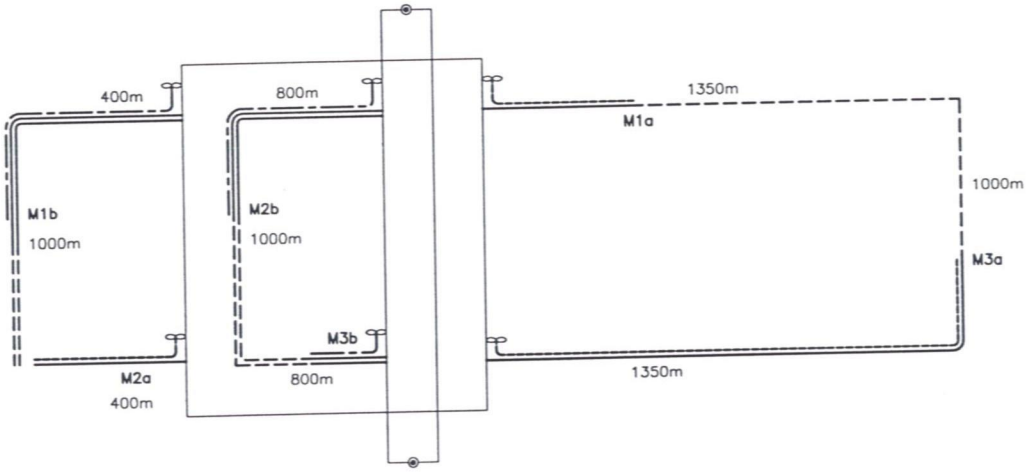

Figure D4: Phase 3. Primary galleries and connection between primary galleries

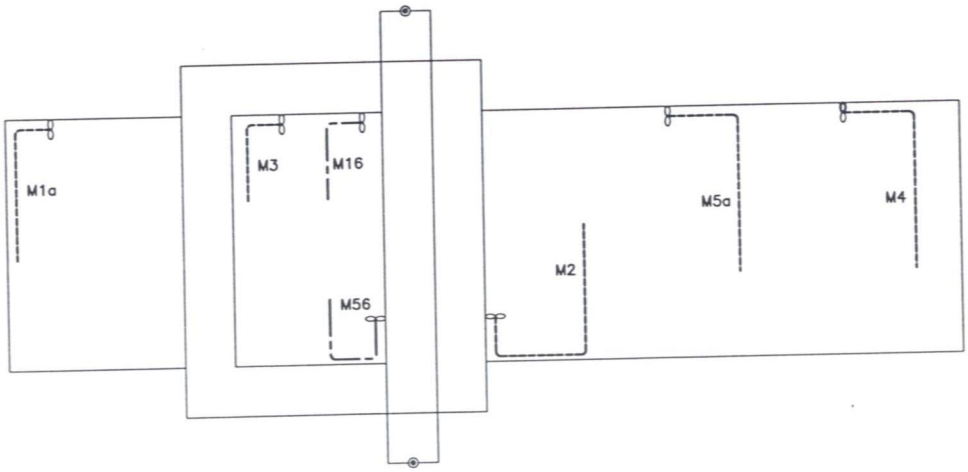

Figure D5: Phase 4. Secondary galleries

Appendix E: Autocompression and heat removal

The method and the formula used to derive some of the figures mentioned in chapter 4 will be explained in this appendix. The paragraph E.1 treating autocompression does not only provide a better understanding of the autocompression itself, but it also provides the necessary background and formulas to explain the figures mentioned about the volume increase because of a rise in temperature (see paragraph E.2).

E.1 Autocompression

When ventilation air flows down a mine shaft, its pressure, temperature and density increase. This process is known as autocompression.

For the calculations relating to autocompression, it is assumed in this study that:

- no heat is exchanged between the air and the surrounding ground,
- the moisture content of the air does not undergo any changes,
- the air velocity remains constant,
- no external work is done on the air.

With these assumptions, the steady flow energy equation

$$dQ + dW = M[dH + d(V^2/2) + gdz] \quad \text{(E.1)}$$

becomes:

$$dH = -gdz \quad \text{(E.2)}$$

Assuming the air to be a perfect gas

$$dH = c_p\, dT \quad \text{(E.3)}$$

and

$$pv = RT \quad \text{(E.4)}$$

yields

$$c_p\, dT = -gdz \quad \text{(E.5)}$$

where

Q : heat exchanged with the environment (J)
W : work done on the air by the environment (J)
M : mass flow rate of the air (kg/s)
H : enthalpy of the air (J/kg)
V : velocity of the air (m/s)
g : gravitational acceleration (m/s^2) [9,81 m/s^2]
z : elevation (m)
c_p : specific heat (J/kg °C) [1014 J/kg °C for ambient air]
T : temperature (°C)

R : gas constant (J/kg °C) [289 J/kg °C for ambient air]
v : specific volume (m^3/kg)
ρ : density (kg/m^3)

Note that although all temperatures are given in degrees Celsius, but the absolute temperatures have to be used in the formulas quoted here.

For a 500 m deep shaft, (E.5) yields a temperature increase of 4,84 °C.

The rise in pressure can be calculated, if the flow is frictionless:

$$dp = gdz/v \tag{E.6}$$

If the flow is frictionless and if no heat is transferred, the change in entropy dS = 0 J/kg °C.
For this situation:

$$dH = vdp + TdS \tag{E.7}$$

becomes

$$dH=vdp \tag{E.8}$$

with E.3 and E.4

$$c_p\, dT = vdp = RT\, dp/p \tag{E.9}$$

$$dT/T = (R/c_p)\,(dp/p) \tag{E.10}$$

$$\frac{T_2}{T_1}=\left(\frac{p_2}{p_1}\right)^{\frac{R}{c_p}} \tag{E.11}$$

$$p_1 v_1^{\frac{c_p}{c_p-R}} = p_2 v_2^{\frac{c_p}{c_p-R}} \tag{E.12}$$

or

$$\frac{v_2}{v_1}=\left(\frac{p_1}{p_2}\right)^{\frac{c_p-R}{c_p}} \tag{E.13}$$

The influence autocompression has on pressures, temperatures, specific volumes and densities for some possible inlet air temperatures is given in Table E.1. The formula (E.4) has been used in deriving the volume changes due to a variation of the air temperature.
In table E.1, the ratio of the specific volumes and the ratio of the densities have been included as well.

The variation in density (or in specific volume) amounts to approximately 4% to 5%. The downcast flow rates in appendix D have therefore been increased with 5% in comparison to the required flow rates underground.

T_1 (°C)	-10	0	10	20	30
v_1 (m^3/kg)	0,760	0,789	0,818	0,847	0,876
ρ_1 (kg/m^3)	1,316	1,286	1,223	1,181	1,142
p_2 (kPa)	106,61	106,36	106,13	105,92	105,72
T_2 (°C)	-5,16	4,84	14,84	24,84	34,84
v_2 (m^3/kg)	0,726	0,755	0,784	0,813	0,842
ρ_2 (kg/m^3)	1,377	1,325	1,276	1,231	1,188
v_2 / v_1	0,955	0,957	0,958	0,960	0,961
ρ_2 / ρ_1	1,047	1,045	1,043	1,042	1,041

Table E.1: The influence of the autocompression on the barometric pressure, the temperature, the specific volume, and the density of the air. The subscript 1 refers to the air at the top of the downcast shaft, while the subscript 2 refers to the situation at a depth of 500 m. The barometric pressure was assumed constant at 100 kPa.

E.2 Heat to be removed in the section in which the heat generating canisters are stored

In this paragraph, some details are given on how the heat to be removed is calculated, and on the relation between the temperature increase of the ventilation air and the heat to be removed.

The problem being posed is the following: which flow rate is required through the secondary galleries of the HLW heat generating section if the maximum temperature increase is fixed at 2,5°C as an example.

The air entering the heat generating section is assumed to have the same temperature as the clay mass at a depth of 500 m. The dry and the wet bulb air temperatures are assumed to be the same (= fully saturated). A temperature increase of 2,5°C is assumed whereby moisture content of the air remains constant (this implies that the relative humidity decreases from 100% to 85%).

This very modest temperature increase, and the assumption that the water content of the air remains constant, mean that the example is a lower boundary to the capacity of the air to remove heat. If besides these assumptions the air velocity remains constant, no external work is done on the air, and the galleries can be considered horizontal, equation (E.1), with (E.2) become:

$$dQ = Mc_p dT$$

with ρ_{air} at 25°C = 1,161 kg/m^3,

$$\Delta T = 0{,}85\,°C \text{ per kJ heat exchanged and per } m^3 \text{ air.} \qquad (E.14)$$

To calculate the heat to be removed by the ventilation, the heat sources are considered point sources situated at 12,8 m from the centre line of the secondary galleries (= the distance from the centre of the canister to the centre of the secondary gallery). Around each source a sphere is considered which intersects the (lined) neighbouring secondary gallery at the crown and at the lowermost point (Figure E.1). The arc α defined by the two intersection points is used to define a strip along the circumference of the sphere (Figure E.2). The ratio of the area of this strip to the area of the whole sphere is taken to be equal to the ratio of the heat generated that has to be removed by the ventilation.

From Figure E.1 one obtains $\alpha/2 = 0{,}1359$. The area of the strip is given by $4R^2 \pi \sin 0{,}1359$, where $R = 12{,}8$ m. The ratio of the strip to the area of the sphere is then $\sin 0{,}1359 = 0{,}135$. This implies that 13,5% of the heat being generated has to be removed by the ventilation.
The power generated by each canister is at its maximum at the time the canisters are stored, and is equal to 0,696 kW. A total of 38 heat generating canisters is stored per secondary gallery; this results in a total "installed" power of 26,45 kW. The heat to be removed per secondary gallery is therefore equal to 3,57 kW.

A heat source of 3,57 kW causes a temperature increase of 3°C with a flow rate of 1 m^3/s. A flow rate of 1,2 m^3/s is therefore required to limit the temperature increase to 2,5°C.

If the moisture content is allowed to evolve as well, and if a fully saturated condition would be considered at 27,5°C, about 13,3 kJ could be absorbed per m^3 of air, reducing the required flow rate to 0,27 m^3/s per secondary gallery.

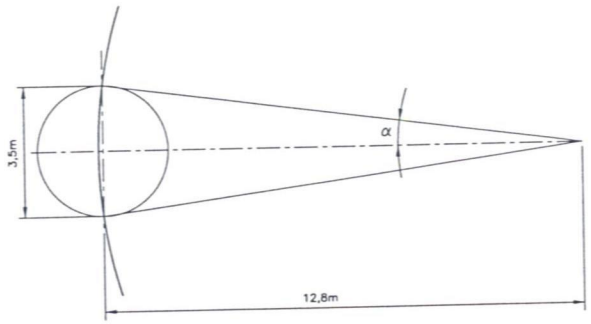

Figure E1: Sphere intersecting the tunnel at the crown, with the heat source at the centre of the sphere

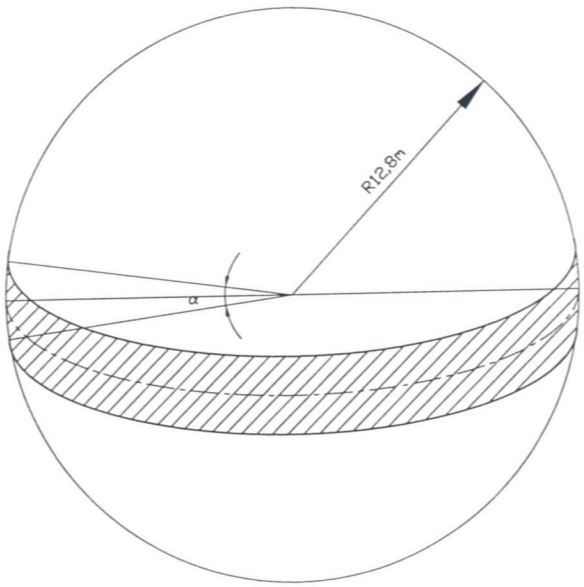

Figure E2: Strip on sphere, defining the area to be taken into account in the calculation of the heat to be removed by the ventilation